

The Geometry of Dissipative Mechanical Systems

Using Jacobi Manifolds and the Split-Quaternion Algebra

E. B. Legrand

The Geometry of Dissipative Mechanical Systems

Using Jacobi Manifolds and the Split-Quaternion Algebra

MASTER OF SCIENCE THESIS

For the degree of Master of Science in Systems and Control at Delft
University of Technology

E. B. Legrand

September 16, 2022



Copyright © Delft Center for Systems and Control (DCSC)
All rights reserved.

DELFT UNIVERSITY OF TECHNOLOGY
DEPARTMENT OF
DELFT CENTER FOR SYSTEMS AND CONTROL (DCSC)

The undersigned hereby certify that they have read and recommend to the Faculty of Mechanical, Maritime and Materials Engineering for acceptance a thesis entitled

THE GEOMETRY OF DISSIPATIVE MECHANICAL SYSTEMS

by

E. B. LEGRAND

in partial fulfillment of the requirements for the degree of

MASTER OF SCIENCE SYSTEMS AND CONTROL

Dated: September 16, 2022

Supervisor(s):

prof.em.dr.ir. M. B. Mendel

Reader(s):

prof.dr.ir. T. Keviczky

dr. D. Boskos

dr. R. Swierstra

ir. C. Hutters

Abstract

Conservative mechanical systems admit a symplectic structure. However, since real systems typically exhibit energy dissipation, this symplectic structure is often too restrictive for engineering purposes. Also in economic systems, dissipative phenomena are ubiquitous in the form of consumption and depreciation.

In this thesis, we develop an extension of the symplectic structure that does incorporate dissipation in an intrinsic manner. This geometric structure is presented in a way that makes it usable for engineering applications, which is done in two steps.

We first construct a contact Hamiltonian system for the damped harmonic oscillator by combining the symplectic structure of conservative mechanics and the contact-geometric description of thermodynamics. This system is then modified for the harmonic oscillator with both a parallel and serial damper. We show how the widely adopted Caldirola-Kanai Hamiltonian for the damped harmonic oscillator emerges from the symplectification of the contact Hamiltonian system.

In order to deal with general, multi-degree of freedom systems, the contact structure is then extended to a Jacobi structure. In contrast to the contact structure, the Jacobi structure encodes the pairing of conjugate variables and the dissipation as two separate entities. We argue that this makes it possible to construct a Hamiltonian system for any mechanical system and illustrate the practicality of this formalism by applying it to a multi-degree of freedom system.

Second, we propose split-quaternions as an alternative to the traditional matrix representation of two-dimensional linear mechanical systems. We demonstrate how the properties of the dynamical system are directly reflected in its split-quaternion representation. As a result, the split-quaternion representation offers several advantages for practical applications, e.g., for the classification of fixed points or when computing the system solution. We use models of the hyperbolic plane to find a relation between the solution geometry of underdamped systems and their split-quaternion representation.

Table of Contents

Preface	xi
1 Introduction	1
2 A Geometric Perspective of Economic Engineering	5
2-1 Symplectic manifolds in economic engineering	6
2-2 Lagrangian mechanics in economic engineering	7
2-2-1 Kinetic energy	8
2-2-2 Potential energy	9
2-2-3 Symplectic geometry in Lagrangian mechanics	9
2-3 Hamiltonian mechanics in economic engineering	11
2-3-1 The Legendre transform	11
2-3-2 Hamilton's equations	12
2-3-3 The role of dissipation	13
3 Geometric Structures in Dissipative Mechanics	15
3-1 Symplectic mechanical systems	16
3-1-1 Symplectic manifolds	16
3-1-2 Hamiltonian mechanics	17
3-2 Contact mechanical systems	20
3-2-1 Contact manifolds	21
3-2-2 Contact Hamiltonian systems	22
3-2-3 Contact geometry in dissipative mechanics	25
3-2-4 Symplectification of contact Hamiltonian systems	33
3-2-5 The harmonic oscillator with serial damping	43
3-3 Jacobi structures for general systems	46
3-3-1 Jacobi structures	48
3-3-2 Jacobi structure of mechanical systems	50

4 Split-Quaternion Representations of Dynamical Systems	55
4-1 The algebra of split-quaternions	55
4-1-1 Basic properties of split-quaternions	56
4-1-2 Relation with two-dimensional matrix algebra	60
4-2 Dynamical systems as split-quaternions	63
4-2-1 The Lie algebra of vector fields	64
4-2-2 System classification with split-quaternions	67
4-2-3 The exponential function of split-quaternions	70
4-3 Application to mechanical systems	74
4-3-1 Equations of motion	74
4-3-2 Physical interpretation of the split-quaternion representation	76
4-3-3 Geometric analysis of underdamped systems	80
5 Conclusions and Recommendations	93
A Geometry of Lagrangian Mechanics	97
A-1 The double tangent bundle	97
A-2 The Euler-Lagrange equations	99
B Contact Geometry	101
B-1 Contact structures	101
B-2 The manifold of contact elements	102
B-3 Contact Hamiltonian systems	104
Bibliography	109
Glossary	115

List of Figures

2-1	The difference between kinetic energy and co-energy. Kinetic energy is a function of momentum, and kinetic co-energy is a function of velocity. The two are numerically equivalent for this particular relation between momentum and velocity. Figure courtesy of B. Krabbenborg [16].	8
2-2	Geometric illustration of the Legendre transform of a function. The Legendre transform of the function $L = L(q, \dot{q})$ is a function of p and q , defined as the difference $p\dot{q} - L_q$, where this difference must be maximal with respect to \dot{q} . If L is a convex function in \dot{q} , this is achieved where the partial derivative $\partial L / \partial \dot{q}$ evaluated at \dot{q} is equal to p , which is equivalent to being locally parallel to $p\dot{q}$. Because the Legendre transform is supposed to be a function of p , one can consider p as 'given'. L_q denotes L as a function of \dot{q} , for some given q	12
3-1	On the left, a schematic of the mechanical harmonic oscillator is shown as a mass-spring system with mass m and spring constant k . On the right, the equivalent bond graph representation is shown. It consists of an inductive I-element (mass) and capacitive C-element (spring) connected through a 1-junction, indicating that the 'flow' (i.e. velocity) is constant across the connection, which is to say that both are connected to the same mass.	19
3-2	Splitting of the tangent and cotangent bundle using the structure provided by the contact form, with $\dim(M) = 3$. The left figure shows the cotangent space to M at some point x , where the blue plane contains the semi-basic forms. The other subbundle is of rank 1 and consists of all the scalar multiples of the contact form α . On the right, the tangent space to M at x is depicted, with the red plane containing the horizontal vector fields. The blue line is spanned by the vertical vector fields.	23
3-3	The left figure shows a schematic of the mechanical damped harmonic oscillator with mass m , spring constant k , and damping constant b . The bond graph representation is shown on the right. In addition to the I- and R-element in Figure 3-1, there is now an R-element as well.	27
3-4	System boundaries of the damper-oscillator system. The mechanical subsystem stores mechanical energy E in the form of kinetic and potential energy, while the heat bath stores internal energy in the form of heat. The damper forms an interface between them.	28

3-5	Integral curves of X_K for $b = 0.3 \frac{\text{kg}}{\text{s}}$, $m = 1 \text{ kg}$ and $k = 10 \frac{\text{kg}}{\text{s}^2}$. The left plot shows the physical trajectory ($K = 0$) in black, together with some neighboring non-physical trajectories that approach the black trajectory with increasing time. The trajectories on the right are all unphysical but show the case where we would choose a zero initial value for U (also with some perturbations). The ‘wobble’ is caused by the exponentially decaying value of the Hamiltonian being counterbalanced by the nonuniform decrease of the mechanical energy in the system. In this case, U clearly does <i>not</i> represent the internal energy of the heat bath or any other physical variable.	32
3-6	A contact element on the manifold Q_e is a line through the origin in the tangent space. The manifold of contact elements of Q_e is the space of all contact elements at every tangent space to Q_e	34
3-7	Illustration of the principal \mathbb{R}_x -bundle $\dot{T}^*M \xrightarrow{\pi} \mathbb{P}T^*M$. x is a point in the extended configuration space Q_e , where we attach fibers $\dot{T}_x^*Q_e$ and $\mathbb{P}T_x^*Q_e$. The orbits of the group action $\blacktriangleleft \mathbb{R}_x$ on \dot{T}^*Q_e are identified by σ and mapped to the orbit space $\mathbb{P}T^*M$	37
3-8	Schematic of the harmonic oscillator with two dampers: one in series and one in parallel. The corresponding bond graph representation is shown on the right.	44
3-9	Multi-degree of freedom mechanical system with two masses, two dampers, and three springs. The corresponding bond graph representation is shown below.	47
4-1	The dihedral group D_4 is the symmetry group of a square. This group is isomorphic to the group formed by $1, \hat{i}, \hat{j}$ and \hat{k} under multiplication.	57
4-2	The cycle graph of the dihedral group D_4 . There are five cycles: one of order four which represents the rotations (or the element \hat{i}) of the square, and four order-2 cycles, which are all the possible reflections. The colored element represents the identity.	57
4-3	Basis vector fields corresponding to the basis elements of the split-quaternions.	65
4-4	The split-quaternion Poincaré diagram is based on the regime combinations defined in Table 4-2. The determinant axis coincides with the squared norm of the split quaternion being 0. The parabolic double stroke line corresponds to the split-quaternions with zero vector norm. A further distinction is made with the scalar part of the split-quaternion, which, for each of the regimes, determines (asymptotic) (in)stability.	68
4-5	A generalized version of a root locus plot in terms of hypercomplex numbers. The traditional root locus is set in the complex s -plane (shown in blue), but we added a third axis for the hyperbolic part of the eigenvalue. When the gain is increased, the initially complex pole pair ventures towards the real axis. If the pole pair is critically damped, both poles are separated from the real axis by an infinitesimal distance of ε . Increasing the gain even more pushes the pole pair into the hyperbolic regime (the associated split-quaternion vector is now spacelike). Observe that in this picture, the symmetry with respect to the real axis is preserved. In the traditional root locus, these points are projected onto the real axis, indicated by the dashed lines.	73
4-6	Comparison between the influence of the \hat{j} -component (left) and \hat{k} -component on the integral curves of $X_{\hat{i}}$. The \hat{j} component stretches the elliptic trajectory along the horizontal axis and squeezes it by the same amount in the vertical direction, while the \hat{k} component does the same but along axes that are rotated by 45 degrees. As shown by the figures, this is a consequence of the constructive or destructive interference of those vector fields in these particular directions.	79

4-7	The disconnected ‘unit sphere’ in the Lorentzian 3-space. The red surface is the one-sheet hyperboloid, containing all the spacelike unit vectors, or overdamped systems. The gray sheet is the light cone, that contains all the lightlike ‘null’ vectors with zero norm, or critically damped systems. Finally, the two blue surfaces constitute the two-sheet hyperboloid, or underdamped systems.	81
4-8	Solution trajectories and vector field of an exemplary underdamped system. The green trajectories are the actual solution of the system, while the blue trajectories are the conservative version, i.e. with the real part of the split-quaternion removed.	81
4-9	Geometric parameters of the ellipse. Its shape is characterized by two lengths: the semi-major axis r_+ and the semi-minor axis r_- . The various measures of the aspect ratio of the ellipse given in Table 4-8 express the relative size of r_+ with respect to r_- in various ways. The (first) eccentricity e parameter locates the focal points F_1, F_2 as a proportion of the semi-major axis. The angle ϑ by which the semi-major axis is rotated with respect to the horizontal is called the <i>tilt</i>	83
4-10	Illustration of the projection on the Poincaré disk and the Cayley-Klein disk. The Lorentzian 3-space is intersected along the \hat{i} - \hat{j} -plane; both disks therefore appear as a line segment with radius 1.	86
4-11	The Cayley-Klein disk and the hyperboloid model are related through gnomonic projection. A geodesic on the hyperboloid model is shown as well, its projected image in the Cayley-Klein disk (also a geodesic) is a straight line. Illustration adapted from Balazs and Voros [78].	87
4-12	The Poincaré disk and the hyperboloid model are related through stereographic projection. A geodesic on the hyperboloid model is shown as well, its projected image in the Poincaré disk (also a geodesic) is part of a circle that intersects the boundary of the disk at right angles. Illustration adapted from Balazs and Voros [78].	88
4-13	Vector field generated by the Lorentzian cross product by a on the vectors in the plane that is Lorentz-orthogonal to a . The vectors s_+ and s_- are the principal axes of (one of the) elliptic trajectories. The positive sheet of the hyperboloid is shown as well.	90
B-1	The standard contact structure on \mathbb{R}^3 , given by the contact form $dq^0 - p_1 dq^1$; the hyperplanes tilt more in the increasing y -direction.	102
B-2	A point in the manifold of contact elements on $Q = \mathbb{R}^2$. A coordinate system for CQ consists of $q = (q^0, q^1)$ to indicate a point on Q , and projective coordinates $[p_0 : p_1]$, which denote the contact element at that point. Without loss of generalization, one can choose $p_0 = 1$, and the remaining coordinate p_1 covers all but one points in the projective space. A potential confusion rests in this two-dimensional example, since both the ‘hyperplane’ and the equivalence class of 1-forms are both lines in the tangent and cotangent space respectively. This is not the case for higher-dimensions, for which $n - 1 \neq 1$	104
B-3	Intuitive picture of the canonical contact on the manifold of contact elements. In this case, let $(t, q) \in Q$, and let v be a coordinate for the contact (line) element. The standard contact form is then $dq - v dt$. On the left, the curve corresponding to a falling object is shown in Q . When this curve is ‘lifted’ to CQ , the contact structure imposes that it be locally tangent to the contact structure, or that $v = \frac{dq}{dt}$. If the vertical direction is projected down onto the $(q - t)$ -plane ($C(Q) \rightarrow Q$), the hyperplanes defined by the contact structure are line elements tangent to the trajectory, making v the actual velocity of the curve.	105

List of Tables

2-1	Overview of some important analogies between economic engineering and mechanics.	14
4-1	Multiplication table for the split-quaternion algebra.	56
4-2	All the possible combinations of the regime of the split-quaternion and the regime of its vector part. Spacelike split-quaternions can only have a spacelike vector, while lightlike split-quaternions can only have lightlike or spacelike vector parts. The numbering of these cases coincides with the classification of dynamical systems in Section 4-2-2.	59
4-3	Overview of the split-quaternion properties that are often used in this chapter.	60
4-4	Regime transition under the action of split-quaternion multiplication. The timelike split-quaternions form a group under multiplication, the lightlike and spacelike split-quaternions do not: lightlike split-quaternions do not have an inverse and the spacelike split-quaternions are not closed.	62
4-5	Overview of the correspondence between the algebra of split-quaternions and the algebra of 2×2 matrices, given that $A = \phi(a)$ and $B = \phi(b)$. In the top section, we compare matrices to split-quaternions, which means that they are related by the isomorphism ϕ . The bottom section compares scalar properties: these are numerically equal.	63
4-6	Vector field representation of the split-quaternion basis elements. The Hamiltonian is the function that generates the associated vector field through Hamilton's equations: $\dot{x} = \frac{\partial H}{\partial y}$ and $\dot{y} = -\frac{\partial H}{\partial x}$	66
4-7	Overview of the classification of fixed points based on the regime of the associated split-quaternion and its vector part.	70
4-8	Commonly used parameters to measure the eccentricity (or alternatively, the flattening) of an ellipse in terms of its semi-major axis r_+ and semi-minor axis r_- [74].	84

Preface

Man must sit in chair with open mouth for very long time before roast duck fly in.

— *Chinese proverb*

Chapter 1

Introduction

Symplectic manifolds are widely recognized as the appropriate geometric setting for classical mechanics. The reason is that the symplectic structure facilitates the mechanism of both Hamiltonian and Lagrangian mechanics. However, autonomous mechanical systems with a symplectic structure are necessarily conservative. By its very nature, the symplectic structure leaves no room for dissipative phenomena in the system. For the physicists that use analytical mechanics, this does not usually cause significant trouble, for the systems they are concerned with are so small or idealized that the effects of dissipation are benign or nonexistent altogether.

In contrast, energy dissipation is ubiquitous in many engineering applications, whether mechanical, electrical, or economic. This is because there are virtually always resistive or frictional elements present whose influence on the system cannot be ignored. Consequently, engineers typically revert to Newtonian (or vectorial) mechanics rather than Hamiltonian or Lagrangian (or analytical) mechanics.

Despite this shortcoming, we believe that analytical mechanics does offer substantial advantages in engineering applications over the Newtonian framework. We give two reasons to support this claim:

The first reason originates in the discipline of *economic engineering*, which is the field of study of the research group for which this thesis is written. In economic engineering, analogies are used between the mechanical, electrical, and economic domains to produce *causal* models for economic systems. In opposition to ‘classic’ *black box* models used by econometrists, economic engineering models are *gray box*, which is to say that the latter is based on first principles instead of pure statistics.

The economic engineer can barely go without analytical mechanics. This is because, perhaps contrary to classical mechanics, the Hamiltonian and Lagrangian formalisms are the most intuitive from an economic perspective compared to Newtonian mechanics. The role of Lagrangian and Hamiltonian mechanics in economic engineering is explained in Chapter 2. Because dissipative phenomena are as common in practical economic systems as in mechanical

systems, we feel that there is a need to reconcile analytical mechanics with energy dissipation or the economic analog thereof.

A second reason is that Hamiltonian and Lagrangian mechanics are based on the *energy description* of a mechanical system, in contrast to using forces, as is done in Newtonian mechanics. The energy description is often much more economical and easily constructed based on physical observation, even for complicated systems. In addition, the sophistication of these methods allows one to use mathematically powerful concepts such as symmetry to gain insights into the system, e.g., using Noether's theorem.

Some solutions have been proposed in the past to include dissipation into the symplectic framework of Hamiltonian and Langrangian mechanics nonetheless. The first is using a time-dependent formulation, which specifies explicitly how the energy in the system is changing, thereby making the system nonautonomous, e.g., the methods proposed by Caldriola [1] and Kanai [2]. However, in engineering, time dependence is usually reserved for exogenous inputs, which are either controlled inputs or uncontrolled disturbance or noise inputs into the system. A second solution is to use a complex formulation of the system states. A drawback of these methods is that they require a modification of the underlying complex structure, see for example Hutters and Mendel [3], Dedene [4] and Rajeev [5].

In contrast to these approaches, we will not use a symplectic structure for dissipative systems. Instead, we draw inspiration from the mathematical theory of thermodynamics to develop a different geometric structure for the mechanical system.

For simple systems, this geometric structure is a *contact structure*. However, for more general multi-degree of freedom mechanical systems, the contact structures are insufficient: it has to be modified into a specific instance of the overarching class of *Jacobi structures*.

Some authors have already recognized the applicability of contact and Jacobi structures in the past; see respectively Bravetti et al. [6] and Ciaglia et al. [7]. However, the arguments made in the existing literature are mainly mathematical in nature, and the contact structure does not translate to the physical aspects of the mechanical system. As Vladimir Arnold's once wrote¹

“Every mathematician knows that it is impossible to understand any elementary course in thermodynamics. The reason is that thermodynamics is based [...] on a rather complicated type of geometry, called contact geometry.”

We prefer to turn this issue the other way around, for thermodynamics comes entirely natural to the engineer, but contact geometry certainly does not. Therefore, we propose a formulation of the geometric structures that has a direct physical interpretation rooted in both thermodynamics and classical mechanics.

In Chapter 3, we use the thermodynamic insights to progressively build our way from contact Hamiltonian systems to simple mechanical systems, ultimately leading to Hamiltonian systems based on Jacobi structure that apply to any mechanical system.

Whereas Chapter 3 exclusively considers the domain of mechanical systems, Chapter 2 explains the associated economic analogies. Using these analogies, the findings in Chapter 3

¹See *Contact Geometry: the Geometrical Method of Gibbs' Thermodynamics* as a part of the 1989 *Proceedings of the Gibbs Symposium* [8, p. 163].

can be readily translated to the domain of economic engineering. The contents of Chapter 2 can be viewed as separate and are not prerequisites for the rest of the thesis.

In addition to the differential geometric structure underlying the mechanical systems, we also propose a new representation of mechanical systems (and dynamical systems in general) in the form of split-quaternions² in Chapter 4.

We make the case in this thesis that the split-quaternions provide a powerful alternative to the traditional state-space form of linear dynamical systems. This is because the natural properties of the split-quaternions coincide with the properties of the associated dynamical system. As a result, the classification of dynamical systems follows almost immediately from the corresponding split-quaternion. Furthermore, we also show how the geometry of the solution trajectories can be obtained directly from the split-quaternion representation.

To the author's knowledge, the relation between split-quaternions and dynamical (or mechanical) systems has never been studied in this way. As a result, the findings in this thesis about this relation are all new.

Notation

²Also colloquially known as *coquaternions*.

Chapter 2

A Geometric Perspective of Economic Engineering

The discipline of economic engineering is a very new one. The theoretical foundations have been developed over the past few years at the Delft Center of Systems and Control, primarily by prof. em. Mendel, in combination with the contributions of several theses that have been recently written about the subject [3, 9, 10, 11]. Economic engineering aims to use tools from various engineering disciplines and physics to improve the predictive power of (macro)economic models.

In economic engineering, *domain-neutral* modeling techniques such as bond graph modeling are used to construct models for economic systems. This is done based on analogies between economics and mechanical and/or electrical engineering. This results in dynamic gray-box models that rely on past data only for the identification of their parameters but not for the dynamics of the model itself. These gray box models are what sets economic engineering apart from other disciplines that produce economic models, such as econometrics.

In this chapter, we focus on the theoretical foundations of economic engineering, particularly its relation to symplectic manifolds and Hamiltonian and Lagrangian mechanics. The theoretical contributions in Chapter 3 are formulated exclusively in terms of concepts from classical mechanics, but the analogies provided in this chapter allow to extend the results in Chapter 3 to the economic domain as well.

The structure of this chapter is as follows. First, in Section 2-1, we explain the relevance of symplectic manifolds in economic engineering. Second, we first provide the economic engineering analogies for Lagrangian mechanics in Section 2-2. Although Chapter 3 is written from the Hamiltonian perspective, the Lagrangian formalism provides a more intuitive introduction to the economic engineering analogies, which is why it is treated first. Then, in Section 2-3 we make the transition from the Lagrangian formalism to the Hamiltonian formalism in economic engineering, and motivate why dissipative elements are an essential part of economic systems that must properly be dealt with.

2-1 Symplectic manifolds in economic engineering

A collection of goods forms the basis of any economic system. These goods can be physical (e.g., bushels of wheat) but also more abstract notions such as capital in the financial analogy [9]. The *economic configuration space* Q is analogous to the configuration space of mechanics and consists of all the possible combinations of goods in the economy. Hence, in economic engineering, the goods are analogous to the (*generalized*) *positions* in classical mechanics.

The natural coordinates for this space are the number of each of the goods in the economic system, denoted by $q = (q^1, q^2, \dots, q^n)$, also called *stock levels*. We say that each of these coordinates is measured in units of *quantity*, denoted by ‘[#]’.

In many cases, the economic configuration manifold is simply a vector space containing all the goods, subject to a total constraint on the total *endowment* for each of the goods (i.e., the total number of goods available). This is also referred to as an *Edgeworth box* in the two-dimensional case. However, we will not assume in general that Q is a vector space, for it may be constructed from holonomic constraints imposed on a larger space.

The tangent space $T_x Q$ to a point x in Q is the vector space of differential changes in goods, also called the *flow of goods*. A vector in the tangent space is denoted by $\dot{q} = (\dot{q}^1, \dot{q}^2, \dots, \dot{q}^n)$. It is important to distinguish between a flow of goods and an absolute amount of goods. From a mathematical perspective, the former is a vector in the tangent space, and the latter is a point in the economic configuration manifold. This distinction is often not given much attention in economics but is fundamental in economic engineering.

The *dual space* of $T_x Q$ is the cotangent space $T_x^* Q$ containing all the linear functions that map vectors in the tangent space to a real number. This is the natural setting of the *prices* in the economy: as a function, they assign a *value to a change in goods*. These prices are measured in units of currency per quantity, i.e. $\left[\frac{\text{€}}{\#}\right]$. A covector in the cotangent space is denoted by $p = (p_1, p_2, \dots, p_n)$. The action of a price covector on a vector measuring the change in goods is (observing the summation convention):

$$p(\dot{q}) = p_i \dot{q}^i, \quad (2-1)$$

i.e., it produces the total value associated with this change in goods.

The *cotangent bundle* $T^* Q$ of the economic configuration manifold is the space of prices and quantities: we call it the *economic phase space*. Like in mechanics, a point in this space determines the state of the economic system: points in this space specify the amount of each of the goods in the system and their associated price.

The economic phase space has a natural structure that pairs each price coordinate to the associated stock level coordinate. From a mathematical perspective, this is equivalent to the fact that the cotangent bundle of any manifold has a 1-form canonically defined on it: the Liouville form (also called tautological 1-form or canonical 1-form), defined as

$$\vartheta := p_i dq^i. \quad (2-2)$$

Even more so than in mechanics, this Liouville 1-form has a very intuitive interpretation in economic engineering: it relates the goods and their prices. When integrated over a curve in $T^* Q$, it measures the total accumulation of value along that curve.

The (negative of) the exterior derivative of the Liouville form is a *symplectic 2-form* ω :

$$\omega := -d\vartheta = dq^i \wedge dp_i. \quad (2-3)$$

When integrated over, this form measures the *oriented area* in the economic phase space, with units of currency [€]. This quantity is analogous to *action* in classical mechanics. The symplectic 2-form relates every price to the associated stock level and thereby encodes the fundamental structure of the economic phase space.

The link between symplectic geometry and economics has been recognized by (more mathematically inclined) researchers outside the field of economic engineering as well, most notably Russell [12] and Swierstra [13].

The role of symplectic geometry in economics begs the question of whether the concepts of Hamiltonian mechanics can also be applied to economic dynamical systems. In the field of economic engineering, we argue that this is indeed the case. To explain how this works, we start from Lagrangian mechanics, after which we transition to Hamiltonian mechanics.

2-2 Lagrangian mechanics in economic engineering

The *Lagrangian* is a function on the tangent bundle of the configuration manifold:

$$L : TQ \rightarrow \mathbb{R}. \quad (2-4)$$

Lagrangian mechanics is based on *Hamilton's principle* which states that the physical motion $\gamma : [t_0, t_1] \rightarrow TM$ is the one for which the *action functional* \mathcal{A} .

$$\mathcal{A}[\gamma] := \int_{t_0}^{t_1} (L \circ \gamma) dt \quad (2-5)$$

is stationary¹ [14].

A necessary and sufficient condition for a curve to satisfy Hamilton's principle is given by the set of n *Euler-Lagrange equations*:

$$\frac{d}{dt} \left(\frac{\partial L}{\partial \dot{q}^i} \right) - \frac{\partial L}{\partial q^i} = 0. \quad (2-6)$$

In economic engineering, Hamilton's principle is interpreted as an economic agent minimizing his or her *disutility*, in practice often considered to be the *cost*. The interpretation of the Lagrangian function is then the *running cost* or *running disutility*. This Lagrangian therefore has units of currency per time, e.g. $\left[\frac{\text{€}}{\text{yr}} \right]$.

As mentioned, the Lagrangian is a function of the flow of goods \dot{q} and the stock levels q . The partial derivative of the Lagrangian with respect to the flow of goods is equal to the *price vector*:

$$p_i := \frac{\partial L}{\partial \dot{q}^i}. \quad (2-7)$$

This means that prices and flows of goods are *conjugate variables*. Intuitively, the prices are the marginal increase in cost with respect to a marginal change in the flow (say, demand) of goods.

¹Although often referred to as the 'Principle of *minimum* action', this is inaccurate: Hamilton's principle only asserts that the first variation of the functional vanishes, which does not necessarily imply a minimum.

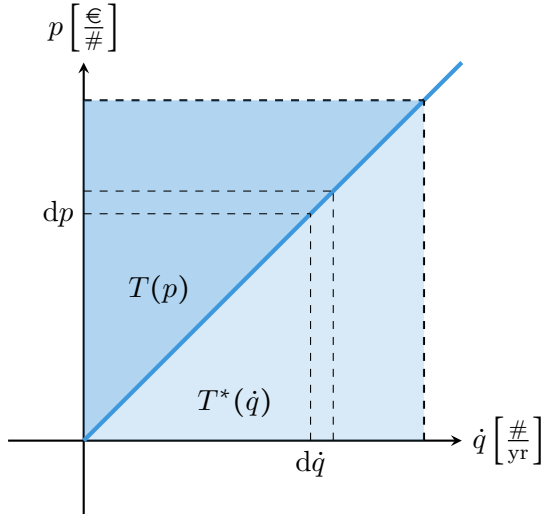


Figure 2-1: The difference between kinetic energy and co-energy. Kinetic energy is a function of momentum, and kinetic co-energy is a function of velocity. The two are numerically equivalent for this particular relation between momentum and velocity. Figure courtesy of B. Krabbenborg [16].

2-2-1 Kinetic energy

When the Lagrangian depends quadratically on the flow of goods (analogous to kinetic energy), the price and the flow of goods are linearly related by an *elasticity*: this is the typical picture of a supply and demand curve. We have:

$$p_i = m_{ij}\dot{q}^j, \quad (2-8)$$

where the m_{ij} are referred to as *price elasticities*. In the simplest of cases, the m_{ij} form a diagonal matrix, and every good has its price. However, any cross-terms appearing in the elasticity matrix represent the marginal elasticity of one good relative to another. These cross terms encode the effect of *substitution* of one good for another. The matrix of price elasticities is analogous to the (inverse) mass matrix in classical mechanics.

In mechanics, the part of the Lagrangian that depends on \dot{q} is called the *kinetic co-energy*² T^* :

$$T^* = \frac{1}{2}m_{ij}\dot{q}^i\dot{q}^j. \quad (2-9)$$

The kinetic co-energy is equivalent to the *cost* associated with a flow of goods: the factor of one-half is there to subtract the market surplus from the total expenditure (which is equal to $\mathbf{p}(\dot{\mathbf{q}})$).

Traditionally, microeconomics makes the distinction between *firm theory* and *consumer theory*. In economic engineering, we dispense with this explicit distinction, for we argue that they are fundamentally based on the same mathematical principles. However, it is important

²We make the distinction between the kinetic energy T and co-energy T^* : they are dual representations related through the Legendre transform. Because work is the integral of force over distance, kinetic energy is naturally represented in terms of *momentum*, rather than velocity, for which we need to apply the Legendre transform first [15]. The difference between the kinetic energy and kinetic co-energy is illustrated by Figure 2-1.

to keep in mind that the situation for firms and consumers is typically mirrored: the cost of one represents the surplus of the other, and vice versa. Also, a flow of goods that a consumer buys from a firm has an opposite direction depending on the perspective of the firm or the consumer: this is the reason why a demand curve typically slopes downwards and the supply curve upwards, because their associated surplus is flipped around. In the grand scheme of things, both perspectives are two sides of the same coin. The ‘minimization principle’ can therefore just as well be considered to be a ‘maximization principle’ if the signs flip due to a change in perspective.

If the matrix of elasticities is positive definite, the kinetic energy expression forms a *Riemannian metric* on the economic configuration manifold. Level lines of the metric are *indifference curves*: they represent a constant level of (dis)utility or cost for different combinations of flows of goods. Furthermore, in more complicated situations, the price elasticities are allowed to vary with the stock levels, i.e. $m = m(q^1, q^2, \dots, q^n)$, which would (under appropriate conditions) imply that the configuration manifold exhibits *Riemannian curvature*.

In the language of bond graphs, we say that the kinetic energy (or market surplus) is stored in an I-element. As such, in economic engineering, I-elements represent a local ‘piece’ of demand or a ‘market’ where an exchange of goods can occur.

2-2-2 Potential energy

In mechanics, the part of the Lagrangian that does not depend on \dot{q} is called the *potential energy* $V = V(q^1, q^2, \dots, q^n)$. In economic engineering, we say that potential energy either represents the *benefits* of holding a good, also called *convenience yield*. It gives rise to a restoring force that provides an incentive *against* exchanging goods on the market.

When the potential energy is quadratic in q , we have something similar to a spring force acting on the system. In a bond graph, this is called a C-element: it measures or stores³ the number of goods in the system.

2-2-3 Symplectic geometry in Lagrangian mechanics

We will now give a brief description of the differential geometric infrastructure underpinning Lagrangian mechanics and its economic interpretation. This section is slightly more technical, and the reader may want to revisit it after reading Chapter 3. Furthermore, a detailed account of the geometry of Lagrangian mechanics is given in Appendix A.

The geometry of Lagrangian mechanics is based on the geometry of the so-called *double tangent bundle* TTQ . This is because we consider the amount of goods q and the flow of goods \dot{q}^i to be separate coordinates, but of course, the flow of goods \dot{q}^i should *also* be the time rate of change of the associated amount of goods⁴. This extra constraint pairing the q^i 's with their associated \dot{q}^i is embedded in the canonical structure of the double tangent

³With ‘measuring’ we mean that this element makes a particular quantity part of the dynamics of the system, which is to say that they are measurable. For example, if there are no C-elements, one can still conceptualize the stock level, but they do not influence the system and can therefore not be measured.

⁴In this context, the ‘dot’ simply distinguishes the coordinates, but does not intrinsically imply that one is the time derivative of the other.

bundle. Said otherwise, the significance of this structure is equivalent to Newton's law being second-order.

The pairing of flows and amounts of goods is specified by the *vertical isomorphism*, which is a tensor of valence (1, 1) on TQ : [17]

$$S = \frac{\partial}{\partial \dot{q}^i} \otimes dq^i. \quad (2-10)$$

Using the vertical isomorphism, the *Lagrange 1-form* is defined as

$$\vartheta_L := dL \circ S = \frac{\partial L}{\partial \dot{q}^i} dq^i. \quad (2-11)$$

The Lagrange 1-form has an interpretation similar to the Liouville form in the previous section. Recall that $\frac{\partial L}{\partial \dot{q}^i}$ are equal to the prices, so ϑ_L computes the ‘valuation’ of a flow of goods based on the price levels dictated by the Lagrangian.

Similarly, the negative of the exterior derivative of ϑ_L yields the *Lagrange 2-form* ω_L :

$$\omega_L := -d\vartheta_L = \frac{\partial^2 L}{\partial v^i \partial v^j} dq^j \wedge dv^i + \frac{\partial^2 L}{\partial q^i \partial v^j} dq^j \wedge dq^i. \quad (2-12)$$

This 2-form has a compelling economic interpretation: the first term contains the *price elasticities* associated with each of the goods in the economy. The second term contains the dependency of the price elasticities on the amounts of goods. We propose here that the Lagrange 2-form can be seen as the mechanical analog of the *Slutsky matrix* in microeconomics, which relates the total elasticity to two factors: [18]

- (i) the elasticity due to *substitution* (i.e., the local elasticities), represented by the first term of the above equation,
- (ii) the *wealth effects*: these are the changes in the elasticities due to the changing state of the economic system (i.e., the accumulation of goods).

We will, however, not go into the implications of this (potential) relation and reserve them as a recommendation for future research in the theory of economic engineering.

The Lagrange 2-form can be used to state the Euler-Lagrange equations in a geometric language. Define the *energy function* E as⁵

$$E : TQ \rightarrow \mathbb{R} : E := \frac{\partial L}{\partial \dot{q}^i} \dot{q}^i - L. \quad (2-13)$$

From the perspective of the firm, the energy function is analogous to *profit* since it is equal to the Lagrangian (being the cost function) subtracted from the total revenue of the firm $\frac{\partial L}{\partial \dot{q}^i} \dot{q}^i$.

The dynamics of the mechanical system are then given by the *Lagrangian vector field* X_L , which is defined

$$X_L \lrcorner \omega_L = dE, \quad (2-14)$$

or alternatively denoted as $X_L = \omega_L^\sharp(dE)$ ⁶.

⁵There is also a coordinate-free definition involving the Liouville vector field, which is given in Appendix A.

⁶This notation is further explained in Chapter 3

The Lagrange 2-form is a symplectic form *if* the matrix of price elasticities is regular. In an economic context, this means that there are no ‘zero price directions’; i.e. there every change in the amounts of goods is associated with some change in value. Usually, an even stronger condition is assumed on L , namely that it is *convex* in the flows of products, which is sometimes known as the *Legendre condition*. In economics, this means that the prices increase in the same direction as the flow of goods⁷. If this is indeed the case, the *Legendre transform* can be used to pass from the Lagrangian representation to the Hamiltonian representation and back; this is the subject of the next section.

Finally, we want to emphasize an important subtlety in the Lagrangian formalism. Since the price vectors live in the cotangent space, the notion of price is *not* canonically defined in Lagrangian mechanics: Lagrangian function is needed to obtain it from a flow of goods. In contrast, the Hamiltonian formalism discussed in the next section, is defined in terms directly in terms of prices. This gives the Hamiltonian mechanics an advantage, since prices are arguably a more fundamental notion in economics than the associated flow of goods (although there are probably good arguments for the contrary).

2-3 Hamiltonian mechanics in economic engineering

In this section, we first use the Legendre transform to pass from the perspective of Lagrangian mechanics (i.e. TQ) to Hamiltonian mechanics (defined on T^*Q). We then discuss the economic interpretations of Hamilton’s equations and the significance of dissipation in economic systems.

2-3-1 The Legendre transform

When the economic Lagrangian function is convex in \dot{q} , we can use the *Legendre transform* to pass to the Hamiltonian formalism as follows [19]

$$H : T^*Q \rightarrow \mathbb{R} : \quad H = E \circ (\mathcal{F}L)^{-1}, \quad (2-15)$$

where E is the previously defined energy function and $\mathcal{F}L$ is the *fiber derivative* of L : [20]

$$\mathcal{F}L : TQ \rightarrow T^*Q : \quad [\mathcal{F}L(\mathbf{v})](\mathbf{w}) = \frac{d}{ds} \Big|_{s=0} L(\mathbf{v} + s\mathbf{w}), \quad (2-16)$$

where \mathbf{v}, \mathbf{w} are vectors in $T_q Q$. The fiber derivative maps a flow of goods to the associated price vector. As a result, the Hamiltonian function is simply equal to the energy function E but expressed in terms of the price coordinates p_i rather than \dot{q}^i . The fiber derivative is a local diffeomorphism only if the Lagrangian is regular.

Since the energy function and the Hamiltonian are numerically equal, the economic interpretation of the Hamiltonian is also *profit* (from the perspective of the firm). This fact has been recognized by economists as well, in the so-called *duality theory*. The duality theory states that *profit function* and *cost function* are dual representations of the same firm (in literature, this is called a *technology*) [18, 21].

⁷This makes intuitive sense, although there are exceptions; for example, the negative yield on some government bonds in recent years.

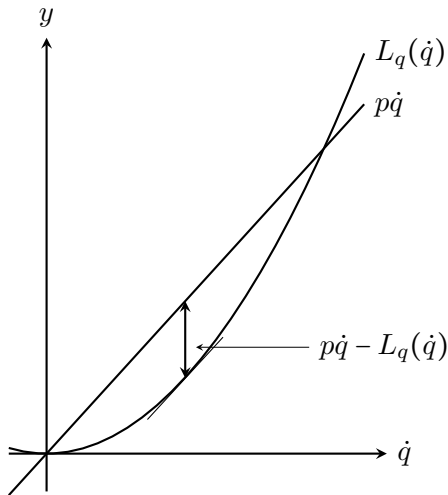


Figure 2-2: Geometric illustration of the Legendre transform of a function. The Legendre transform of the function $L = L(q, \dot{q})$ is a function of p and q , defined as the difference $p\dot{q} - L(q, \dot{q})$, where this difference must be maximal with respect to \dot{q} . If L is a convex function in \dot{q} , this is achieved where the partial derivative $\partial L / \partial \dot{q}$ evaluated at \dot{q} is equal to p , which is equivalent to being locally parallel to $p\dot{q}$. Because the Legendre transform is supposed to be a function of p , one can consider p as 'given'. L_q denotes L as a function of \dot{q} , for some given q .

The economic interpretation of the Legendre transform may be better understood geometrically. The Legendre transform of a function $L = L(q, \dot{q})$ with respect to \dot{q} is alternatively defined as

$$\max_{\dot{q}} \{p\dot{q} - L(q, \dot{q})\}. \quad (2-17)$$

If L is convex in \dot{q} , this is achieved at the point where the function L is locally parallel to the function $p\dot{q}$, which is to say that

$$\left. \frac{\partial L}{\partial \dot{q}} \right|_{\dot{q}} = p. \quad (2-18)$$

In the Lagrangian formalism, this is the very *definition* of p : if L is convex, the maximization is satisfied by default and is often disregarded.

For the economic interpretation, it is important to keep in mind the underlying maximization in the definition: it states that firms or consumers automatically operate at the optimal price point, given their cost (or utility) function.

2-3-2 Hamilton's equations

Hamilton's equations are derived by applying the symplectic isomorphism to the gradient of the Hamiltonian function, which is defined by the relation

$$dH = X_H \lrcorner \omega, \quad (2-19)$$

or in alternative notation $X_H = \omega^\sharp(dH)$. Here, ω is the symplectic 2-form on T^*Q (cf. Section 2-1). The symplectic isomorphism (and Hamilton's equations) are covered in greater detail in Chapter 3.

Conventionally, the symplectic 2-form is equal to $dq^i \wedge dp_i$, and Hamilton's equations are:

$$\dot{q}^i = \frac{\partial H}{\partial p_i}, \quad \dot{p}_i = -\frac{\partial H}{\partial q^i}. \quad (2-20)$$

It is easy to see that these equations of motion are equivalent to the Euler-Lagrange equations, given that $p_i = \partial L / \partial \dot{q}^i$. We will go a lot more into detail on the (geometric) nature of Hamilton's equations in Chapter 3; the discussion here is limited to their interpretation in economic engineering.

The first Hamilton equation is equivalent to *Hotelling's lemma*, which states that the demand for a particular good is that the supply (i.e. \dot{q}^i) of a good i is equal to the derivative of the profit function with respect to the price p_i . It is usually emphasized that this is only the case when the price is the *optimal* price for profit, but this is built into the definition of p_i . As given by Equation (2-20), the price value $p_i = \partial L / \partial \dot{q}^i$ is exactly the one for which the profit function

$$p_i \dot{q}^i - L, \quad (2-21)$$

is maximized, provided L is convex in \dot{q}^i .

The second Hamilton equation provides the change in momentum or *force*. In economic engineering, these forces are analogous to *economic wants*, i.e. what drives a price up or down. The equation can be interpreted as the *law of scarcity*, i.e. economic wants arise as a consequence of the stock levels/amount of goods in the system, pushing the price of the goods up or down.

2-3-3 The role of dissipation

Traditional Hamiltonian and Lagrangian mechanics deal with conservative systems only; which are those that conserve the value of the Hamiltonian, being equal to the energy in the system. In economics, these would be systems that would, without external sources, always maintain the same level of profit. These types of conservative economic systems are just as hypothetical as their mechanical counterpart since there are *always* elements present that limit the 'efficiency' of an economic system, such as the depreciation of goods, consumption of goods, and transaction costs.

Given the prominent role that the Hamiltonian and Lagrangian formalism play in the field of economic engineering, it is therefore essential to find a suitable way to include dissipative effects in the Hamiltonian and Lagrangian formalism (or an extension thereof), while still maintaining their economic interpretation. This is the subject of Chapter 3, and although it is formulated in terms of classical mechanics, the analogies described in this chapter may be readily used to substitute the mechanical quantities for their economic engineering counterparts. To that end, Table 2-1 provides an overview of the most important analogies used in economic engineering.

Table 2-1: Overview of some important analogies between economic engineering and mechanics.

Symbol	Mechanical variable	Units	Economic variable	Units
q	Displacement	[m]	Quantity of goods	[#]
\dot{q}	Velocity	[$\frac{m}{s}$]	Flow of goods	[$\frac{\#}{yr}$]
p	Momentum	[$\frac{kg\ m}{s}$]	Quantity of goods	[$\frac{\$}{\#}$]
F	Force	[$\frac{kg\ m}{s^2}$]	Economic want	[$\frac{\$}{\#\ yr}$]
m	Mass	[kg]	Price elasticity	[$\frac{\$}{\#^2}$]
H	Hamiltonian / total energy	[J]	Profit	[$\frac{\$}{yr}$]
L	Lagrangian	[J]	Running cost / disutility	[$\frac{\$}{yr}$]

Chapter 3

Geometric Structures in Dissipative Mechanics

In this chapter, we develop a geometric structure that can be used to construct Hamiltonian formalism for mechanical systems with dissipative elements. This formalism may also be applied to economic engineering systems using the analogies outlined in Chapter 2.

Throughout this chapter, we progressively extend the conventional Hamiltonian formalism to more ‘advanced’ types of manifolds.

First, in Section 3-1, the conventional Hamiltonian theory based on symplectic manifolds is explained. This section serves as a technical introduction to the rest of the chapter and does not contain new contributions.

Second, in Section 3-2, we look at *contact Hamiltonian systems* defined on contact manifolds. These have been proposed by some authors for dissipative mechanical systems (in particular, the damped harmonic oscillator) in the past, see e.g. Bravetti et al. [22]. However, we propose a different formulation of the contact structure based on physical reasoning instead of a purely mathematical one. Moreover, we show how the Caldirola-Kanai model is directly equivalent to the symplectification of the contact Hamiltonian system.

Third, in Section 3-3, we point out by means of an example why contact Hamiltonian systems are not able to describe general (multi-degree of freedom) mechanical systems. A (slight) generalization of contact manifolds is required instead. These manifolds belong to the general class *Jacobi manifolds* that also includes symplectic and contact manifolds as particular instances.

The extension towards Jacobi manifolds has been proposed by Ciaglia et al. [7], but it has received little to no additional attention in literature — at least, not regarding their application to mechanical systems. We formulate the Jacobi structure using the same physical reasoning as for the contact Hamiltonian systems.

3-1 Symplectic mechanical systems

First, symplectic manifolds are defined in Section 3-1-1, after which symplectic Hamiltonian systems are covered in Section 3-1-2.

3-1-1 Symplectic manifolds

In their traditional sense, Hamiltonian systems are defined on *symplectic manifolds*. A symplectic manifold (M, ω) is a smooth manifold M equipped with a *closed, nondegenerate* 2-form ω . Because ω must be nondegenerate, symplectic manifolds are necessarily even-dimensional.

The celebrated Darboux theorem asserts that locally, all symplectic manifolds of the same dimension (say $2n$) are all symplectomorphic¹ to each other. As a result, we define the prototypical symplectic 2-form that serves as a representative for *all* symplectic structures of that dimension as

$$\omega = \sum_{i=1}^n dq^i \wedge dp_i, \quad (3-1)$$

where p_i and q^i are coordinates for the manifold M . A coordinate chart in which the symplectic 2-form has the above form is called a *Darboux chart*, and the associated coordinates *Darboux coordinates* [14, 23].

In mechanics, the *configuration manifold* Q is the manifold specified by all the possible generalized positions q^i (or configurations) of the mechanical system. The *generalized momenta* associated with each of the generalized positions live in the collection of cotangent spaces to the configuration manifold. The momenta are cotangent variables because, from the Lagrangian viewpoint, the generalized momenta are defined by

$$p_i = \frac{\partial L}{\partial \dot{q}^i}, \quad (3-2)$$

which indicates that the vector of p_i 's is a cotangent (covariant) vector to Q . Hence, the *cotangent bundle* of the configuration manifold contains all the possible position and momentum pairs; it is colloquially referred to as the *phase space* [14, 19, 24].

The structure that associates each position with its corresponding momentum is given by the *Liouville 1-form*² ϑ on T^*Q . The Liouville form is defined at every point

$$(q^1, \dots, q^n, p_1, \dots, p_n) \in T^*M$$

as³

$$\vartheta = \sum_{i=1}^n p_i dq^i. \quad (3-4)$$

¹Symplectomorphisms are diffeomorphisms that preserve the symplectic structure; they are the isomorphisms of symplectic manifolds.

²The Liouville 1-form makes its appearance in literature under a myriad of names, such as the canonical 1-form, tautological 1-form, Poincaré 1-form, or the symplectic potential.

³In coordinate-free language, the Liouville 1-form is defined pointwise as follows. Given $q \in Q$, $p \in T_q^*Q$, we call $x = (q, p) \in T^*Q$. Let π be the bundle projection map of $T^*Q \xrightarrow{\pi} Q$. For every x , The Liouville 1-form $\vartheta|_x$ is defined as

$$\vartheta|_x := p \circ (\pi^*|_x), \quad (3-3)$$

where p is interpreted as a map on the tangent space to q [23].

Hence, the Liouville form tells us which momentum coordinate corresponds to a given position coordinate and vice versa. This turns out to be an essential piece of the geometric structure that underpins classical mechanics.

Every cotangent bundle is canonically endowed with a Liouville form. The exterior derivative of the Liouville form produces a *symplectic* 2-form. By convention, we define this symplectic form as follows:⁴

$$\omega = -d\vartheta = \sum_{i=1}^n dq^i \wedge dp_i. \quad (3-5)$$

Hence, the space of generalized positions and momenta (i.e. the cotangent bundle of the configuration manifold Q) is canonically symplectic. The symplectic structure pairs the corresponding position and momentum coordinates in a skew-symmetric fashion.

In the context of bond graphs, the symplectic form represents the dual nature of a bond. That is to say, a bond represents an exchange of both an effort and a flow, and they are inherently tied to each other. The flow is a change in position, and the effort is a change in momentum. The effort and flow associated with a bond are conjugate: the symplectic form provides precisely the structure that is visually present in a bond graph (e.g. Figure 3-1).

3-1-2 Hamiltonian mechanics

In Hamiltonian mechanics, the equations of motion are given by *Hamilton's equations*

$$\dot{q}^i = \frac{\partial H}{\partial p_i} \quad \dot{p}_i = -\frac{\partial H}{\partial q^i} \quad (3-6)$$

provided with the Hamiltonian function H , which is equal to the mechanical energy in the system. Observe that the above equation assumes that the pairing between the positions and momenta is known a priori.

In the language of differential geometry, Hamilton's equations are specified by a symplectic structure on T^*Q and an appropriate Hamiltonian function on that manifold: the pairing between the positions and momenta is therefore built in. A generic Hamiltonian system is a triple (M, ω, H) , where (M, ω) is a symplectic manifold. In mechanics, we have that $M = T^*Q$. The symplectic structure allows one to formulate Hamilton's equations in a coordinate-free manner.

The Hamiltonian isomorphism for symplectic manifolds

To produce the equations of motion, the symplectic structure provides a mapping between the smooth functions on the manifold and the vector fields on the manifold.

$$\omega^\flat : TM \rightarrow T^*M : X \mapsto X \lrcorner \omega. \quad (3-7)$$

Because ω is nondegenerate by definition, the mapping ω^\flat is an isomorphism. Thus, the inverse mapping is well-defined and is denoted by ω^\sharp [24].

⁴In this text, the ‘ q -first’ sign convention used by Abraham and Marsden [19] and Cannas da Silva [23] is observed and maintained when we extend towards contact and Jacobi manifolds.

For the notation used here, the difference between the manifolds Q and M is crucial. In the context of mechanics, we have that the symplectic manifold M is the cotangent bundle of Q . Hence, since the Hamiltonian is a function on $M = T^*Q$, dH and X_H are sections of T^*T^*Q and TT^*Q respectively. This is illustrated by the diagram below (the projection arrows from T^*T^*Q and TT^*Q indicate the bundle structure but are left unnamed).

$$\begin{array}{ccc} T^*T^*Q & \xrightleftharpoons[\omega^\flat]{\omega^\sharp} & TT^*Q \\ & \searrow & \swarrow \\ & T^*Q & \\ & \downarrow \pi & \\ & Q & \end{array}$$

This isomorphism specified by ω allows us to find the corresponding Hamiltonian vector field X_H to a Hamiltonian function H as follows:

$$X_H = \omega^\sharp(dH). \quad (3-8)$$

In Darboux coordinates, the action of ω^\sharp on the basis 1-forms is

$$dp_i \mapsto \frac{\partial}{\partial q^i} \quad dq^i \mapsto -\frac{\partial}{\partial p_i}. \quad (3-9)$$

The minus sign arises as a consequence of the anticommutativity of the wedge product appearing in ω . From these expressions, we can observe that the traditional form of Hamilton's equations (cf. Equation (3-6)) is recovered when Darboux coordinates are used.

A classical example of this formalism is the harmonic oscillator (undamped) shown in Figure 3-1. The Hamiltonian function is the sum of the potential and kinetic energy in the system

$$H = \frac{p^2}{2m} + \frac{1}{2}kq^2, \quad (3-10)$$

where m is the mass and k is the spring constant. The Hamiltonian vector field is then

$$X_H = \omega^\sharp(dH) = \omega^\sharp\left(\frac{p}{m}dp + kqdq\right) = \frac{p}{m}\frac{\partial}{\partial q} - kq\frac{\partial}{\partial p}, \quad (3-11)$$

or stated as a system of differential equations

$$\dot{q} = \frac{p}{m}, \quad \dot{p} = -kq. \quad (3-12)$$

Poisson brackets

The symplectic form endows the manifold M also with a *Poisson structure*, i.e. a Lie algebra structure on the vector space of functions on M . The commutator of this algebra structure



Figure 3-1: On the left, a schematic of the mechanical harmonic oscillator is shown as a mass-spring system with mass m and spring constant k . On the right, the equivalent bond graph representation is shown. It consists of an inductive I-element (mass) and capacitive C-element (spring) connected through a 1-junction, indicating that the ‘flow’ (i.e. velocity) is constant across the connection, which is to say that both are connected to the same mass.

is the *Poisson bracket*,

$$\begin{aligned} \{ , \} : C^\infty(M) \times C^\infty(M) &\rightarrow C^\infty(M) : \quad \{f, g\} = \omega(\omega^\sharp df, \omega^\sharp dg) \\ &= \omega(X_f, X_g) \\ &= \mathcal{X}_{X_f} g \end{aligned} \tag{3-13}$$

$$(\text{Darboux coordinates}) \quad = \sum_{i=1}^n \left(\frac{\partial f}{\partial q^i} \frac{\partial g}{\partial p_i} - \frac{\partial f}{\partial p_i} \frac{\partial g}{\partial q^i} \right).$$

Poisson brackets are anticommutative, bilinear, and satisfy the Jacobi identity. Additionally, they also satisfy the *Leibniz property*,

$$\{f, gh\} = \{f, g\}h + \{f, h\}g. \tag{3-14}$$

The Poisson brackets defined in terms of the symplectic structure make symplectic manifolds to be also Poisson manifolds. In Sections 3-2 and 3-3 the notion of Poisson manifolds is generalized to *Jacobi manifolds* to cover more general mechanical systems. In contrast to the Poisson structure, a Jacobi structure does *not* satisfy the Leibniz property [14, 24].

The usefulness of Poisson brackets is due to the fact that they provide a convenient way to calculate the time rate of change of an observable f :

$$\frac{df}{dt} = \{f, H\} + \frac{\partial f}{\partial t}. \tag{3-15}$$

If the Hamiltonian does not depend on time, it is conserved under its own Hamiltonian vector field. This is easily seen from the anticommutativity of Poisson brackets ($\{H, H\} = 0$). Therefore, Hamiltonian systems conserve energy; they do not allow for dissipative (friction) forces in a straightforward manner, unless included in the form of an explicit time dependence. This is a direct consequence of the symplectic structure: because X_H is generated by the symplectic 2-form, the Hamiltonian vector field conserves its own generating function. The fact that the system is conservative should therefore be seen as something that is built into

the structure of the symplectic Hamiltonian system itself, and not as an emergent fact⁵.

To conclude, the overall structure that constitutes a conservative mechanical system is three-fold: first, there is the configuration manifold and its cotangent bundle. Secondly, the symplectic structure on that manifold, and thirdly, we have the Hamiltonian function. In principle, the symplectic structure is a canonical consequence of the cotangent bundle structure, but we wish to emphasize that the system dynamics are also symplectic. That is to say, the Hamiltonian vector field is a symplectic vector field: it leaves ω invariant.

The symplectic nature of the dynamics does not persist to the extension for systems with dissipation. This is in contrast to the fact that even for the most general systems, we still require the pairing of conjugate variables to be encoded into the geometric structure of the system. Hence, we expect the symplectic structure to remain important even in the upcoming generalizations.

In the next section, we will extend the Hamiltonian formalism to *contact manifolds* to incorporate dissipation in the Hamiltonian system.

3-2 Contact mechanical systems

In this section, the thermodynamic principles and their relation with contact geometry are used to establish a contact Hamiltonian system for i.a. the damped harmonic oscillator. The dissipation in this system precludes it from being modeled by a symplectic Hamiltonian system that is not explicitly time-dependent.

An explicit time dependence is typically reserved to model either external control inputs or disturbance inputs. What both disturbances and control inputs have in common, is that they are inherently *exogenous*: they are not part of the system itself. In contrast, the dissipative element in the form of the damper *is* part of the system (*endogenous*). From both a conceptual and practical standpoint, modeling dissipation as a time-dependence, and therefore as an exogenous phenomenon, is not desirable. This is why we aim to use contact geometry to include dissipation as an intrinsic component of the overall system.

First, in Section 3-2-1 we give a very brief introduction to contact geometry.

Second, in Section 3-2-2 we extend the notion of Hamiltonian systems to contact manifolds, resulting in *contact Hamiltonian systems*. Both Section 3-2-1 and Section 3-2-2 contain no new contributions, they are there to present the theoretical infrastructure required for the remaining sections.

Third, in Section 3-2-3, we develop a systematic procedure to construct a contact Hamiltonian system for the damped harmonic oscillator using thermodynamic principles.

Fourth, in Section 3-2-4, we use a technique called *symplectification* to lift the contact Hamiltonian system to a symplectic manifold with one more dimension to show its equivalence to the Caldirola-Kanai Hamiltonian.

⁵This is especially clear from the explicit coordinate expressions of the dynamics. The mapping from H to X_H takes the partial derivatives, and switches them around between the associated q 's and p 's, while one of them picks up a minus sign. As such, it is very clear that $\mathcal{L}_{X_H} H = X_H(H) = 0$, given that H is not explicitly time-dependent.

Finally, in Section 3-2-5, the procedure developed in Section 3-2-3 is applied on the harmonic oscillator with a parallel and serial damper.

3-2-1 Contact manifolds

In contrast to symplectic manifolds, contact manifolds are odd-dimensional. A contact manifold (M, ξ) is a smooth manifold M of dimension $2n + 1$ equipped with a maximally non-integrable hyperplane distribution ξ . At every point $x \in M$ the contact structure specifies a $2n$ -dimensional linear subspace (i.e. a hyperplane) of TM . Locally⁶, the hyperplane distribution is specified as the kernel of a 1-form on M , which must be nondegenerate:⁷ [14, 23, 25]

$$\xi|_x = \ker \alpha|_x. \quad (3-16)$$

It is worth pointing out that the correspondence between a hyperplane and the kernel of a 1-form is not one-to-one. Indeed, multiplying α by any nonzero function yields a different 1-form with the same kernel. The contact forms are different, but they give rise to the same contact structure. This ambiguity is essential, and will play a vital role in the process of symplectification discussed in Section 3-2-4.

For the hyperplane distribution to be maximally nonintegrable, it means that one cannot find codimension-1 foliations that are everywhere tangent to the distribution of hyperplanes [25]. This is analogous to a nonholonomic constraint on a mechanical system: these constraints cannot be integrated to obtain a submanifold of the configuration space that contains all the allowable positions. Indeed, the condition for nonholonomicity applies here as well: for ξ to be nonintegrable, the associated contact form α must satisfy the Frobenius condition

$$\alpha \wedge d\alpha \neq 0, \quad (3-17)$$

or equivalently, that $\alpha \wedge (d\alpha)^n$ is a volume form on M .

Contact geometry is closely related to symplectic geometry, for the nonintegrability condition implies that $d\alpha|_{\xi}$ is a symplectic form.

There is also an extension of the Darboux theorem to contact manifold, which says that locally, every contact form can be written as

$$dq^0 - \sum_i p_i dq^i, \quad (3-18)$$

the coordinates $(q^0, q^1, \dots, q^n, p_1, \dots, p_n)$ are then called *Darboux coordinates*.

For a slightly more comprehensive introduction to contact geometry, the reader is referred to Appendix B. More extensive resources are, among others, the works of Geiges [25], Libermann and Marle [24], Arnol'd [14, 26] and Godbillon [27].

⁶Contact structures which are globally defined by a 1-form are called *exact* or *strictly* contact structures. This is the case when the quotient line bundle TM/ξ is orientable.

⁷Equations of the form $\alpha = 0$, where α is a 1-form, determine so-called *Pfaffian equations* [24].

3-2-2 Contact Hamiltonian systems

Similar to symplectic Hamiltonian systems, *contact Hamiltonian systems* need three ingredients: a smooth manifold M , a contact form α on that manifold, and a Hamiltonian function K on the manifold. The contact structure then provides a mapping between the smooth functions on the manifold and the contact Hamiltonian vector fields on the manifold. As such, the contact structure generates the contact version of Hamilton's equations.

The mapping Ψ_α that relates the smooth functions and contact Hamiltonian vector fields, given a contact 1-form α , is defined as follows:

$$\Psi_\alpha : \mathfrak{X}_c(M) \rightarrow C^\infty(M) : X_K \mapsto K = -X_K \lrcorner \alpha, \quad (3-19)$$

where $\mathfrak{X}_c(M)$ is the collection of infinitesimal strict contactomorphisms⁸. These are vector fields that preserve the strictly contact structure specified by α , and are subject to the following condition:

$$\mathcal{L}_{X_K} \alpha = s\alpha, \quad (3-20)$$

where s is an arbitrary smooth function on M . This condition is based on the fact any nonzero multiple of a given contact form determines the same contact structure.

Horizontal and vertical vector fields

To obtain the vector field from a Hamiltonian function, we are interested in the inverse mapping Ψ_α^{-1} . This mapping is not quite straightforward, for it has to map the general class of smooth functions back to a very specific subclass of vector fields. The trick is to use a splitting of the (co)tangent bundle, decomposing the vector field into two components: horizontal and vertical.

The nonintegrability condition imposed on the contact structure ensures that $\alpha \wedge d\alpha \neq 0$. As such, we have at any $x \in M$:

$$\ker \alpha|_x \cap \ker d\alpha|_x = \{\mathbf{0}\}, \quad (3-21)$$

i.e. they can only intersect at the origin. Consequently, we can define the following splitting of the tangent bundle:

$$TM = \ker \alpha \oplus \ker d\alpha, \quad (3-22)$$

where \oplus denotes the Whitney sum⁹. Vector fields that are in the kernel of α are called *horizontal*; they form a subbundle of rank $2n$, which coincides with the hyperplane distribution specified by the contact structure. In contrast, *vertical* vector fields are in the kernel of $d\alpha$, which is a subbundle of rank 1 [24].

The *Reeb vector field* R_α associated with α is a ‘unit’ vertical vector field, defined by the conditions¹⁰

$$R_\alpha \lrcorner \alpha = 1 \quad R_\alpha \lrcorner d\alpha = 0. \quad (3-23)$$

⁸Contactomorphisms are diffeomorphisms that preserve the contact structure, they are the isomorphisms of contact manifolds. ‘Strict’ refers to a subclass that is defined in terms of the contact *form*, which need not be defined globally.

⁹The Whitney sum applies to vector bundles, and is roughly speaking, a ‘fibered’ version of the direct sum for vector spaces. The Whitney sum of two vector bundles (over the same base space) is a vector bundle over that base space, where every fiber is equal to the direct sum of the fibers of the original vector bundles.

¹⁰The Reeb vector field is not uniquely associated with a contact structure and depends on the particular choice of contact form.

In the Darboux coordinates as given in Equation (3-18), the Reeb vector field is

$$R_\alpha = \frac{\partial}{\partial q^0}. \quad (3-24)$$

Because the space of vertical vector fields is of rank 1, every vertical vector field is colinear with the Reeb vector field.

An arbitrary vector field $X \in \mathfrak{X}(M)$ can be canonically decomposed into a horizontal and a vertical component as follows:

$$X = \underbrace{(X \lrcorner \alpha) R_\alpha}_{\text{vertical}} + \underbrace{X - (X \lrcorner \alpha) R_\alpha}_{\text{horizontal}}. \quad (3-25)$$

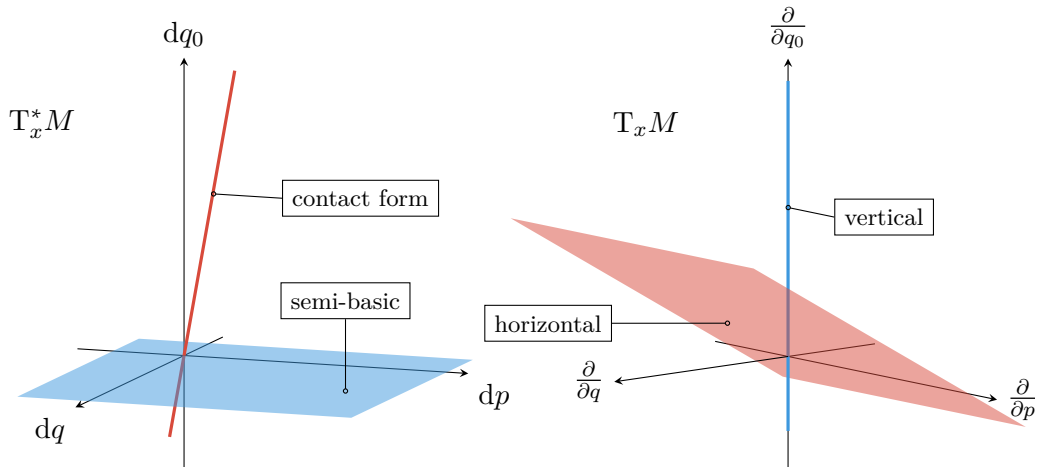


Figure 3-2: Splitting of the tangent and cotangent bundle using the structure provided by the contact form, with $\dim(M) = 3$. The left figure shows the cotangent space to M at some point x , where the blue plane contains the semi-basic forms. The other subbundle is of rank 1 and consists of all the scalar multiples of the contact form α . On the right, the tangent space to M at x is depicted, with the red plane containing the horizontal vector fields. The blue line is spanned by the vertical vector fields.

Semi-basic forms

Similar to the splitting of the tangent bundle, the cotangent bundle may be decomposed into two subbundles as well. The first subbundle consists of the annihilators of the horizontal vector fields. This is a subbundle of rank 1 that contains all the multiples of the contact form; they generate the contact structure. The other subbundle contains the *semi-basic forms*, which annihilate the vertical vector fields [24].

Any 1-form $\zeta \in \Gamma(T^*M)$ can be canonically decomposed into a semi-basic component and a multiple of α as follows:

$$\zeta = \underbrace{(R_\alpha \lrcorner \zeta) \alpha}_{\text{contact struct.}} + \underbrace{\zeta - (R_\alpha \lrcorner \zeta) \alpha}_{\text{semi-basic}}. \quad (3-26)$$

In Darboux coordinates, semi-basic forms are forms that have no component in dq^0 .

The decompositions of T^*M and TM for the three-dimensional case are shown in Figure 3-2, they also play an important role in Section 3-3.

The Hamiltonian isomorphism for contact manifolds

To find the Hamiltonian vector field X_K associated with a Hamiltonian K , we decompose X_K into a horizontal and a vertical component:

$$X_K = X_K^{\text{hor}} + X_K^{\text{ver}}. \quad (3-27)$$

The vertical component of X_K is easily obtained from the definition of Ψ_α :

$$X_K^{\text{ver}} = -KR_\alpha, \quad (3-28)$$

where R_α is the *Reeb vector field*¹¹ associated to the contact form α .

Finding the horizontal component is more involved; a detailed account of the required technicalities is given in Appendix B. In short, we again need a mapping similar to the one defined in Equation (3-7), but now defined in terms of $d\alpha$ instead:

$$d\alpha^\flat(X) := X \lrcorner d\alpha. \quad (3-31)$$

However, this is not an isomorphism between TM and T^*M , for it will annihilate any vertical component X . However, it *is* an isomorphism from the horizontal vector fields to the semi-basic forms (respectively the red and blue planes in Figure 3-2). Likewise, the inverse mapping $d\alpha^\sharp$ takes a semi-basic form as an argument and produces a horizontal vector field.

The horizontal component of the Hamiltonian vector field is equal to this mapping applied to dK , canonically projected to the space of semi-basic forms (cf. Equation (3-26)):

$$X_K^{\text{hor}} = d\alpha^\sharp(dK - (R_\alpha \lrcorner dK)\alpha). \quad (3-32)$$

Hence, the Hamiltonian vector field is equal to

$$X_K = \Psi_\alpha^{-1}(K) = -KR_\alpha + d\alpha^\sharp(dK - (R_\alpha \lrcorner dK)\alpha). \quad (3-33)$$

In Darboux coordinates, we have:

$$X_K = \left(\sum_{i=1}^n p_i \frac{\partial K}{\partial p_i} - K \right) \frac{\partial}{\partial q^0} - \sum_{i=1}^n \left(\frac{\partial K}{\partial q^i} + p_i \frac{\partial K}{\partial q^0} \right) \frac{\partial}{\partial p_i} + \sum_{i=1}^n \frac{\partial K}{\partial p_i} \frac{\partial}{\partial q^i}. \quad (3-34)$$

To apply the contact Hamiltonian formalism to dissipative mechanical systems, we first require a manifold with a suitable contact structure. This contact structure is derived from the principles of thermodynamics in the next section. Subsequently, the contact Hamiltonian system and the equations of motion are constructed.

¹¹The Reeb vector field is defined by two conditions: [24]

$$R_\alpha \lrcorner \alpha = 1 \quad R_\alpha \lrcorner d\alpha = 0. \quad (3-29)$$

In the Darboux coordinates as given in Equation (3-18), the Reeb vector field has the form

$$R_\alpha = \frac{\partial}{\partial q^0}. \quad (3-30)$$

3-2-3 Contact geometry in dissipative mechanics

In order to motivate the thermodynamic underpinning of the contact structure, the next section first discusses the traditional role of contact geometry in thermodynamics. Subsequently, these thermodynamic principles are exploited to establish a contact structure for dissipative mechanical systems.

Contact geometry in classical thermodynamics

It has been argued in the past by several authors that contact geometry is the natural framework for thermodynamics by i.a. Arnol'd [8, 14, 26, 28], Bamberg and Sternberg [29], Burke [30] and Hermann [31], ultimately leading back to the seminal work of Gibbs [32]. It is commonly seen as a testament to the brilliance of Gibbs' work that he managed to recognize and describe the correct geometric framework well before the required mathematical infrastructure was invented [33]. In recent years, the contact Hamiltonian formalism has been successfully applied to thermodynamic theory by e.g. Mrugała et al. [34], Mrugała [35, 36, 37, 38, 39], Balian and Valentin [40], van der Schaft [41], van der Schaft and Maschke [42], Maschke and van der Schaft [43], Bravetti et al. [22], and Simoes et al. [44].

Contact geometry arises in thermodynamics as a consequence of the first law, which asserts that the change in internal energy of the system is equal to the difference between the heat added *to* the system and the work performed *by* the system.

The first law of thermodynamics To state the first law in the language of exterior forms, define the 1-forms η and β as the differential amounts of heat and work (in respective order) added to the system. η and β are 1-forms that are generally *not* closed [29, 45]. However, the first law states that the difference between them *is* a closed form. Locally, this closed form can be written as the gradient of a function called the *internal energy* U . Hence, we state the first law as¹²:

$$dU = \eta - \beta. \quad (3-35)$$

This equation can be equivalently expressed as the fact that the 1-form

$$\alpha = dU - \eta + \beta \quad (3-36)$$

should pull back to zero over the physical trajectories of the systems.

The Gibbs 1-form For the purposes of illustration, we now apply this concept to what is arguably the most simple thermodynamic system: the ideal gas in a piston.

The ideal gas is characterized by five thermodynamic properties: the temperature T , entropy S , volume V , pressure P , and the internal energy U . We call the five-dimensional space containing all the possible states the *thermodynamic phase space*.

For the ideal gas, we have that the work done by the system is equal to the pressure multiplied by the change in volume, i.e. $\beta = P dV$. Furthermore, heat added to the system is given by the

¹²By using differential forms, the inexactness of the heat and work differentials need not be explicitly emphasized using additional notation such as δ or d .

temperature multiplied by the change of energy: $\eta = T dS$ [8, 29, 33]. Therefore, Equation (3-36) becomes

$$\alpha_G := dU - T dS + P dV, \quad (3-37)$$

which is called the *Gibbs form* (hence the subscript). It is clear that the Gibbs form defines a contact structure on the thermodynamic phase space (these are Darboux coordinates). Along the physically allowable trajectories, the Gibbs form must pull back to zero.

Legendre submanifolds In contact geometry, submanifolds on which the contact form vanishes everywhere are called *Legendre submanifolds*. As such, these submanifolds are vital in thermodynamics, because they contain the allowable states (Balian and Valentin [40] call them thermodynamic manifolds). Due to the nonintegrability condition on the contact structure, Legendre submanifolds have at most dimension n , if the overall contact manifold is of dimension $2n+1$.

For the ideal gas, the Legendre submanifolds are two-dimensional. They can be computed explicitly by integrating the Gibbs form. To do so, we need two additional *equations of state*,

$$U = c n_s R_g T \quad PV = n_s R_g T, \quad (3-38)$$

where n_s is the amount of substance, $R_g = 8.314 \frac{\text{J}}{\text{mol K}}$ is the ideal gas constant and c is another constant dependent on the molecular nature of the gas¹³.

In addition, the internal energy is, by definition, a function of the extensive state properties: in this case, the entropy and the volume. We can therefore integrate the Gibbs form by rearranging the equations of state to express T and P in terms of S and V as well. Integrating Equation (3-37) yields

$$U = \log(C_0) e^{\frac{S}{cn_s R_g}} V^{\frac{-1}{c}}, \quad (3-39)$$

where C_0 is an integration constant. Since $U = U(S, V)$, we have that

$$dU = \frac{\partial U}{\partial S} dS + \frac{\partial U}{\partial V} dV. \quad (3-40)$$

Hence, we can fully specify a Legendre submanifold by the integrated equation and the following conditions

$$T = \frac{\partial U}{\partial S} \quad P = -\frac{\partial U}{\partial V}. \quad (3-41)$$

Contact geometry of the damped harmonic oscillator

The damped harmonic oscillator is shown in Figure 3-3, together with its bond graph representation. We assume here that this system is completely isolated: there is no exchange of energy or matter with the environment.

¹³For a monatomic gas, $c = \frac{3}{2}$.

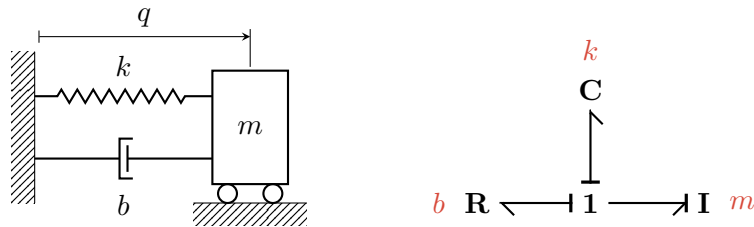


Figure 3-3: The left figure shows a schematic of the mechanical damped harmonic oscillator with mass m , spring constant k , and damping constant b . The bond graph representation is shown on the right. In addition to the I- and R-element in Figure 3-1, there is now an R-element as well.

Energy balance of the damped oscillator We distinguish two types of energy that can be stored in the damped oscillator system: microscopic and macroscopic energy.

Microscopic energy consists of the kinetic energy of particles that do not result in an overall observable motion of the system. This energy is called internal energy U and manifests itself as temperature.

Internal energy is stored in a ‘heat bath’. This is to be interpreted loosely: it can be the damper fluid, but also the surrounding air (although a heterogeneous medium will not allow for an unambiguous notion of temperature). We will not be concerned with all these possibilities and consider a single heat bath with a single temperature: generalizations to more complex thermodynamic systems are immediate.

In contrast, macroscopic energy *is* observable, either due to an observable motion of the system (kinetic energy) or the energy resulting from external force potentials (potential energy). Their sum is called the mechanical energy E : in the damped harmonic oscillator, it is the sum of the kinetic energy stored in the mass (I-element) and the potential energy stored in the spring (C-element).

Since the system is isolated, the first law states that

$$d(E + U) = 0. \quad (3-42)$$

Let us now decompose the system into two subsystems, one containing the mass and the spring and one the heat bath, as illustrated in Figure 3-4.

Through the dissipative action of the damper, energy flows from the mechanical subsystem to the heat bath. We can apply the first law to the subsystems separately, too: the first subsystem performs work on the damper, which manifests itself as the heat added to the heat bath. We therefore have

$$\begin{aligned} dE &= -\beta, \\ dU &= \eta, \end{aligned} \quad (3-43)$$

where β is the (differential) work done *by* the mechanical subsystem on the damper and η is the (differential) heat added *to* the second subsystem as a result of this.

As a consequence of Equation (3-42), we have that $\beta = \eta$; i.e. all the work done by the damper enters the fluid as heat. For a linearly damped system, the work form is by definition equal



Figure 3-4: System boundaries of the damper-oscillator system. The mechanical subsystem stores mechanical energy E in the form of kinetic and potential energy, while the heat bath stores internal energy in the form of heat. The damper forms an interface between them.

to

$$\beta := \gamma p \, dq, \quad (3-44)$$

with $\gamma := b/m$ being the damping coefficient of the damped oscillator.

Contact structure for the damped oscillator We now define the phase space of the system to be equal to $M = \mathbb{R} \times T^*Q$, where Q is the configuration space considered in Section 3-1. For the damped harmonic oscillator, $Q = \mathbb{R}$. With coordinates for M being U, q and p , we can define a *contact form* on this space by combining Equation (3-43) and Equation (3-44):

$$\alpha = dU - \gamma p \, dq. \quad (3-45)$$

This contact form specifies precisely how energy is dissipated in the system and enters the ‘reservoir’ that is the heat bath, characterized by its internal energy U .

Observe from Equation (3-45) that $d\alpha = \gamma dq \wedge dp$, i.e. a multiple of the symplectic form used in Section 3-1. As such, the contact form contains *both* information about the rate of dissipation present in the system, and about the pairing of the conjugate variables p and q . We get the latter ‘for free’ in this particular instance, since the pairing in this simple three-dimensional system is rather trivial.

It is important to note that, in the general case, a 1-form that describes the dissipation in the system is *under no obligation* to be of this very specific form (that is, one that pairs the conjugate variables). As such, we cannot expect this situation to occur in general: this is the subject of Section 3-3.

Contact Hamiltonian system for the damped harmonic oscillator

With the contact structure defined, we can now establish the contact Hamiltonian system for the damped harmonic oscillator using Equations (3-28), (3-32) and (3-33).

Recall that the Hamiltonian vector field is split into a horizontal and vertical component, which belong respectively to the kernel of α and $d\alpha$.

Vertical component of the Hamiltonian vector field The Reeb vector field R_α associated with the contact form given in Equation (3-45) is

$$R_\alpha = \frac{\partial}{\partial U}. \quad (3-46)$$

As such, the vertical component of the Hamiltonian vector field is, in accordance with Equation (3-28):

$$X_K^{\text{ver}} = -K \frac{\partial}{\partial U}. \quad (3-47)$$

However, we can only guess what the Hamiltonian function might be. Indeed, its definition is rather circular, since the vertical part of the vector field is *defined* in terms of the vertical part and vice versa.

Horizontal component of the Hamiltonian vector field The horizontal part is obtained by projecting dK (an arbitrary exact form) to a *semi-basic* form, and mapping it to a vector field using the isomorphism $d\alpha^\sharp$ like so:

$$X_K^{\text{hor}} = d\alpha^\sharp(dK - (R_\alpha \lrcorner dK)\alpha). \quad (3-48)$$

The Hamiltonian is a function on the contact manifold M , i.e. $K = K(U, q, p)$. In coordinates, the projected form is

$$\frac{\partial K}{\partial q} dq + \frac{\partial K}{\partial p} dp + \frac{\partial K}{\partial U} \gamma p dq. \quad (3-49)$$

The projection thus removes any term in dU (which makes it semi-basic).

Recall that $d\alpha = \gamma\omega$. Therefore, we can compare the above equation to the purely symplectic case without dissipation, where the isomorphism is provided by ω (cf. Equation (3-8)). The difference here is (apart from the factor γ) that we have to project dK by means of the term $(R_\alpha \lrcorner dK)\alpha$. In the conservative case, the symplectic Hamiltonian H is simply equal to the mechanical energy E :

$$H(p, q) = E(p, q) = \frac{p^2}{2m} + \frac{1}{2}kq^2. \quad (3-50)$$

It is, therefore, reasonable to expect that the form in Equation (3-49) contains the differential of E (representing the conservative side, or the I- and C-element) plus an extra term that enforces the dissipation (R-element).

Clearly, the rightmost term in Equation (3-49) is the work form of the damper, i.e. the amount of energy escaping from E . We can thus conjecture that the first two terms in Equation (3-49) amount to dE .

However, there is one complication: $d\alpha$ contains the factor γ . To cancel this factor out, we include γ in the Hamiltonian as well. That is

$$\frac{\partial K}{\partial q} dq + \frac{\partial K}{\partial p} dp = \gamma \left(\frac{\partial E}{\partial q} dq + \frac{\partial E}{\partial p} dp \right) \quad (3-51)$$

and

$$\frac{\partial K}{\partial U} = \gamma. \quad (3-52)$$

As a result, the gradient of the Hamiltonian is equal to

$$dK = \gamma(dE + dU), \quad (3-53)$$

and we obtain the correct Hamiltonian up to a closed form

$$K(p, q, U) = \gamma[E(p, q) + U] = \gamma \left(\frac{p^2}{2m} + \frac{1}{2}kq^2 + U \right). \quad (3-54)$$

Hence, the Hamiltonian function is equal to the total amount of energy in the system, both mechanical and internal, multiplied by the damping coefficient.

Now to derive the horizontal component of the vector field. The interior product of $d\alpha$ with the basis vectors yields:

$$\frac{\partial}{\partial q} \lrcorner d\alpha = \gamma dp \quad \frac{\partial}{\partial p} \lrcorner d\alpha = -\gamma dq \quad (3-55)$$

Clearly, the image of this mapping for any vector field is a semi-basic form. The inverse mapping must, to qualify as an isomorphism, map a semi-basic form back to a horizontal vector field (i.e. one that is in the kernel of α). Hence, we have that

$$d\alpha^\sharp(dq) = -\frac{1}{\gamma} \frac{\partial}{\partial p}, \quad d\alpha^\sharp(dp) = \frac{1}{\gamma} \frac{\partial}{\partial q} + p \frac{\partial}{\partial U}. \quad (3-56)$$

The term in dU ensures that the vector field is horizontal. Using this mapping, and the expression for the Hamiltonian in Equation (3-54), we obtain the horizontal component of the Hamiltonian vector field:

$$X_K^{\text{hor}} = \frac{p}{m} \frac{\partial}{\partial q} - (\gamma p + kq) \frac{\partial}{\partial p} + \gamma \frac{p^2}{m} \frac{\partial}{\partial U}. \quad (3-57)$$

Equations of motion Combining Equation (3-47) and Equation (3-57), the Hamiltonian vector field is

$$X_K = \frac{p}{m} \frac{\partial}{\partial q} - (\gamma p + kq) \frac{\partial}{\partial p} + \left(\gamma \frac{p^2}{m} - K \right) \frac{\partial}{\partial U}. \quad (3-58)$$

The corresponding equations of motion are

$$\begin{aligned} \dot{q} &= \frac{p}{m} \\ \dot{p} &= -kq - \gamma p \\ \dot{U} &= \gamma \frac{p^2}{m} - K(q, p, U) = \gamma p \dot{q} - K(q, p, U). \end{aligned} \quad (3-59)$$

The correct dynamics are certainly obtained for p and q . However, from a physical standpoint, we expect \dot{U} to be the rate of energy (i.e. the power) dissipated by the damper, i.e. equal to $\gamma p\dot{q}$. However, the additional term $-K(q, p, U)$ (a result of the vertical component of the vector field) contributes to the rate of change of U as well, ‘spoiling’ the physical dynamics.

If we wish to impose that U indeed be the internal energy of the heat bath, the *vertical vector field must vanish*. This is the case only if the Hamiltonian is numerically equal to zero, $K = 0$. This equation is a so-called *weak equality*, as opposed to a *strong* or *identical* equality. In the former case, the Hamiltonian is numerically equal to zero, but its partial derivatives do not vanish. That is to say, there is a specific submanifold of M on which K vanishes, but we are allowed to make variations that are not necessarily tangent to this submanifold (see Dirac [46] for further details). On this submanifold, the equations of motion read

$$\begin{aligned}\dot{q} &= \frac{p}{m} \\ \dot{p} &= -kq - \gamma p \\ \dot{U} &= \gamma p\dot{q},\end{aligned}\tag{3-60}$$

which indeed represent the damped harmonic oscillator with U being the dissipated energy.

From a thermodynamic standpoint, energy is only determined up to an additive constant, so this assertion would be admissible conceptually. Additionally, a value of 0 for the total energy is a common convention in literature, see for example Fermi [47].

Here, our result differs again from the existing literature on this subject. The applicability of contact Hamiltonian systems has already been recognized from a mathematical standpoint by Bravetti et al. [6], resulting in the equations of motion *including* the vertical vector field. However, when the variables are given a physical interpretation (in particular, the ‘extra dimension’ represented by the internal energy U) as we do here, the vanishing of the Hamiltonian is crucial. Leaving the vertical vector field in leads to extra ‘parasitic’ dynamics that are unphysical and delude us from the intended meaning of the variable U .

Why the Hamiltonian must vanish The assumption that the contact Hamiltonian should be equal to zero is rather striking, and the preceding arguments do not provide a sound mathematical basis for it. Indeed, we could (and should) be quite leery of canceling terms using zero factors, for it often leads to unanticipated consequences or even downright contradictions. This is why we provide some more mathematically oriented arguments to show that this is indeed allowed.

Recall from Equation (3-19) that, by definition, $K = -X_K \lrcorner \alpha$. In the previous section, we defined Legendre submanifolds as manifolds on which the contact form pulls back to zero: in other words, tangent vectors to a Legendre manifold produce zero when contracted with the contact form. So, K measures in essence how ‘non-Legendrian’ an integral manifold of X_K is. We have stipulated earlier that Legendre submanifolds contain physically meaningful trajectories. That is, the dynamics must take place on a Legendre submanifold to be physical, which is why $K = 0$.

As an additional argument, we can show that

$$\mathcal{L}_{X_K^{\text{hor}}} K = 0 \quad \Rightarrow \quad \frac{dK}{dt} = \mathcal{L}_{X_K^{\text{ver}}} K = -K \frac{\partial K}{\partial U}.\tag{3-61}$$

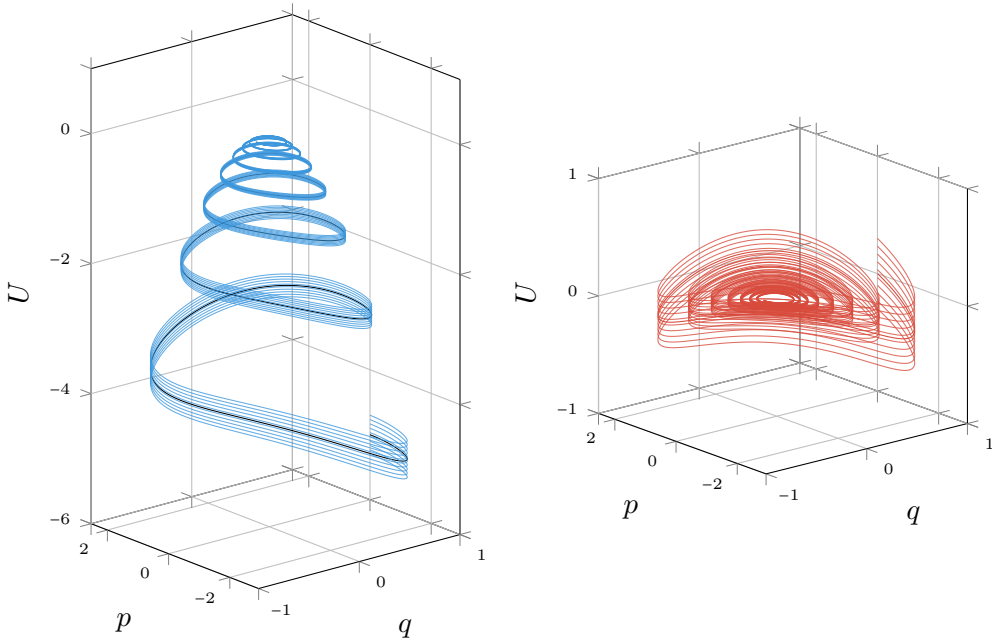


Figure 3-5: Integral curves of X_K for $b = 0.3 \frac{\text{kg}}{\text{s}}$, $m = 1 \text{ kg}$ and $k = 10 \frac{\text{kg}}{\text{s}^2}$. The left plot shows the physical trajectory ($K = 0$) in black, together with some neighboring non-physical trajectories that approach the black trajectory with increasing time. The trajectories on the right are all unphysical but show the case where we would choose a zero initial value for U (also with some perturbations). The ‘wobble’ is caused by the exponentially decaying value of the Hamiltonian being counterbalanced by the nonuniform decrease of the mechanical energy in the system. In this case, U clearly does *not* represent the internal energy of the heat bath or any other physical variable.

Hence, if the Hamiltonian does not vanish, it changes exponentially over time (for its change is proportional to its own value). If $\gamma > 0$, the Hamiltonian decays exponentially from its initial value:

$$K(t) = K_0 e^{-\gamma t}. \quad (3-62)$$

As a result, any nonphysical trajectories will approach a Legendre submanifold as time proceeds; the associated vector fields also become ever more tangent to the Legendre submanifold.

Based on the expression for K , an expression for U may also be derived:

$$U(t) = \frac{1}{\gamma} (K_0 e^{-\gamma t} - E). \quad (3-63)$$

If $K = 0$, the internal energy is equal to the negative of the mechanical energy in the system. These findings are illustrated by Figure 3-5: the left plot shows perturbations of the ‘ideal’ physical trajectory. The right plot shows the trajectories for an initial value of $U = 0$ (also with perturbations); as a result of the above equation, U ‘wobbles’ around its zero point; but it is clearly not a physical trajectory.

Finally, recall that the contact form α is not uniquely determined with respect to the associated contact structure. It can be multiplied with any nonzero function and still represent the same contact structure.

We can regard this ambiguity as a gauge transformation of the system (cf. Balian and Valentin [40]). However, the Hamiltonian is not intrinsically invariant under these transformations; if $\alpha' = f\alpha$ (f being a function without zeros), then the mapping Ψ'_α and the corresponding Hamiltonians are also different: [24, p. 321]

$$\Psi_{\alpha'}^{-1}(K) = \Psi_\alpha^{-1}\left(\frac{1}{f} K\right). \quad (3-64)$$

The vertical component *is* directly dependent on the numerical value of the Hamiltonian. As a result, the *only* way to maintain invariance under the gauge transformation (which we assert to be crucial for it to be of physical significance) is to set $K = 0$.

In the following section, we exploit the intrinsic ambiguity of the contact 1-form to *symplectify* the contact Hamiltonian system.

3-2-4 Symplectification of contact Hamiltonian systems

In this section, we use a procedure called *symplectification* to cast the contact manifold of the previous section on a symplectic manifold in a canonical fashion. The advantage of this method is that the calculations for the dynamics are considerably simplified since we can use the theory for symplectic Hamiltonian systems outlined in Section 3-1. To quote Vladimir Arnol'd, who originally came up with the concept of symplectification, [26, 41]

“One is advised to calculate symplectically but to think rather in contact geometry terms.”

In addition, we show that the resulting ‘symplectified’ Hamiltonian system explains the particular form of a widely adopted existing model for the damped harmonic oscillator: the time-dependent Caldirola-Kanai Hamiltonian.

Symplectification of contact manifolds

To make the process of symplectification mathematically precise, we first need to move to a slightly different space than the manifold M used in the previous section. M is the product manifold of the cotangent bundle of Q (the space of the position q) with the real line to accommodate for the internal energy U . In contrast, we now start with the *extended configuration manifold* $Q_e \cong \mathbb{R}^2$, equipped with an extra position coordinate q_e ¹⁴. That is,

$$(q_e, q) \in Q_e. \quad (3-65)$$

¹⁴In this case, the ‘0’ is a label for the extra position coordinate q_e — we wish not to refer to the other position as q^1 because there is only one real position of the mass. Because the other coordinates are not numbered, we do not make the notational distinction between contravariant and covariant components, and use a subscript to label the extra coordinates.

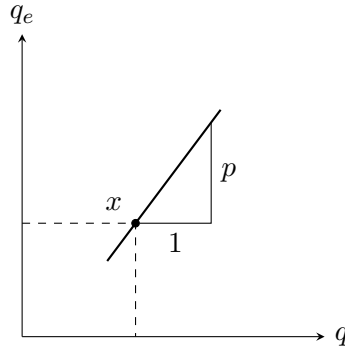


Figure 3-6: A contact element on the manifold Q_e is a line through the origin in the tangent space. The manifold of contact elements of Q_e is the space of all contact elements at every tangent space to Q_e .

The manifold of contact elements Consider now the *manifold of contact elements* of Q_e . This is a fiber bundle with base Q_e , and the fibers at each point are the space of lines (through the origin) in the tangent space to Q_e at that specific point. For more details about the manifold of contact elements, the reader is referred to Appendix B.

The fibers of this bundle are projective spaces; more specifically, they are diffeomorphic to the one-dimensional real projective line \mathbb{PR} . The fibers are therefore compact manifolds. It can be shown that the manifold of contact elements of Q_e (or any manifold) is diffeomorphic to the projectivization of its tangent bundle: we denote this by \mathbb{PT}^*Q_e [14, 23, 24].

The manifold \mathbb{PT}^*Q_e is three-dimensional. Consider a chart for \mathbb{PT}^*Q_e with coordinates (q_e, q, p) , where p represents the *slope* of the line in the tangent space, illustrated in Figure 3-6. This chart cannot cover the entire manifold, for the fiber is compactified at the point $p = \infty$ (in this specific chart).

Because p is meant to represent momentum just like in the previous section, and infinite momentum lies outside our realm of interest, this space can be thought of as *roughly* equivalent (for practical purposes) to M . That is to say, by disregarding the point $p = \infty$, we end up with a manifold that is diffeomorphic to M .

The manifold of contact elements \mathbb{PT}^*Q_e is equipped with a natural contact structure [14], represented by

$$\alpha_e = dq_e - p dq. \quad (3-66)$$

Observe the similarity with the contact form α defined in Equation (3-45):

$$\alpha_e = \frac{1}{\gamma} \alpha, \quad q_e = \frac{U}{\gamma}. \quad (3-67)$$

Because the contact forms differ simply by multiplication, they represent the same contact structure (provided that γ is nonzero).

Contact Hamiltonian system in Darboux coordinates The contact Hamiltonian system (M, α, K) of the damped harmonic oscillator can be defined on the manifold of contact elements as well, with the silent understanding that M and \mathbb{PT}^*Q_e are slightly different from a

topological perspective. Since the new contact form is scaled by $\frac{1}{\gamma}$, we can use Equation (3-64) to find the new Hamiltonian K_e :

$$K_e = \frac{1}{\gamma} K. \quad (3-68)$$

Furthermore, because $U = \gamma q_e$, the contact Hamiltonian in the new coordinates is

$$K_e(q_e, q, p) = \frac{p^2}{2m} + \frac{1}{2} kq^2 + \gamma q_e. \quad (3-69)$$

Numerically, K_e is equal to the total energy in system (the scaling factor is removed). Observe also that the units of the Hamiltonian have been changed from power to energy.

The corresponding Hamiltonian vector field is then

$$X_{K_e} = \frac{p}{m} \frac{\partial}{\partial q} - (\gamma p + kq) \frac{\partial}{\partial p} + \left[\frac{p^2}{m} - K_e(q_e, q, p) \right] \frac{\partial}{\partial q_e}. \quad (3-70)$$

If we enforce that $K = 0$ (as motivated in the previous section), then K_e vanishes as well and the vector field becomes

$$X_{K_e}|_{K_e=0} = \frac{p}{m} \frac{\partial}{\partial q} - (\gamma p + kq) \frac{\partial}{\partial p} + \frac{p^2}{m} \frac{\partial}{\partial q_e}. \quad (3-71)$$

This contact Hamiltonian system can be lifted to the symplectification of the contact manifold $\mathbb{P}\mathrm{T}^*Q_e$.

Symplectification of a contact Hamiltonian system The procedure known as symplectification of a contact manifold turns a contact manifold in a symplectic manifold, thereby raising its dimension by one. The power of this method resides in the fact that this can be done in a canonical fashion: it is uniquely determined by the contact structure of the contact manifold [14].

The symplectification procedure exploits the natural ambiguity that contact forms have, and that has been pointed out in Section 3-2-1. Multiplying the contact form α_e with any nonzero real number¹⁵ $\lambda \in \mathbb{R}_x$

$$\lambda(dq_e - p dq). \quad (3-72)$$

The above expression gives a representation of *all* the contact forms that give rise to the same contact structure as α_e . Hence, if λ is considered to be an additional coordinate in its own right, we move to a four-dimensional space with coordinates (q_e, q, p, λ) ; this is the space of all contact forms on the contact manifold.

We now adopt the coordinates ρ and ρ_e , defined as follows

$$\rho := -\lambda p \quad \rho_e := \lambda. \quad (3-73)$$

In these coordinates, Equation (3-72) becomes

$$\rho_e dq_e + \rho dq =: \vartheta_e. \quad (3-74)$$

¹⁵ \mathbb{R}_x denotes both the real multiplicative group and the underlying set, being the real line excluding zero.

Observe that this is precisely the Liouville form on the cotangent bundle T^*Q_e in Darboux coordinates, denoted by ϑ_e . From this form, we obtain the canonical symplectic structure on T^*Q_e as follows

$$\omega_e := -d\vartheta = dq_e \wedge d\rho_e + dq \wedge d\rho. \quad (3-75)$$

The coordinate λ , and therefore ρ_e and ρ , are not canonical coordinates, for they depend on the particular choice of the contact form, to begin with. Indeed, in this particular choice of α_e one point in the fiber is left out ($p = \infty$), which effectively rules all the points for which $\rho_e = 0$.

In reality, only the points for which *both* ρ and ρ_e vanish should be taken out of the manifold, because the other cases can be covered by picking a different coordinate chart (this will be made clear later). The resulting space is the cotangent bundle of Q_e without its zero section, denoted by \dot{T}^*Q_e [24, 41].

As illustrated by the point above, the former discussion relies heavily on the choice of the particular coordinate chart. Therefore, we wish to make the symplectification procedure more mathematically precise using the language of principal bundles.

Liouville geometry and principal G-bundles

A *principal G-bundle* is a smooth bundle $P \xrightarrow{\sigma} B$, where P is equipped with a *free* right G -action \blacktriangleleft , G being a Lie group [48]. Furthermore, let

$$\begin{array}{ccc} P & & P \\ \downarrow \sigma & \cong_{\text{bundle}} & \downarrow \sigma' \\ B & & P/G \end{array}$$

where σ' is the quotient map that sends each point in P to the corresponding point in the orbit space P/G . In other words, if we define the equivalence relation between two points $x_1, x_2 \in P$ as

$$x_1 \sim x_2 \iff \exists g \in G : x_2 = x_1 \blacktriangleleft g, \quad (3-76)$$

then

$$\sigma' : P \rightarrow P/G : x \mapsto [x]_\sim, \quad (3-77)$$

with $[x]_\sim$ being the equivalence class with respect to \sim and $P/G = P/\sim$.¹⁶

Principal \mathbb{R}_\times -bundles In our context of symplectification, the Lie group in question is the real multiplicative group \mathbb{R}_\times . The group acts on the cotangent bundle of Q_e without zero section¹⁷ (i.e. \dot{T}^*Q_e) through *dilation of its fibers*. In the coordinates defined above, we define the group action $\blacktriangleleft \mathbb{R}_\times$ as:

$$\blacktriangleleft : \dot{T}^*Q_e \times \mathbb{R}_\times \rightarrow \dot{T}^*Q_e : (q_e, q, \rho_e, \rho) \blacktriangleleft \lambda = (q_e, q, \lambda \rho_e, \lambda \rho) \quad \lambda \in \mathbb{R}_\times. \quad (3-78)$$

¹⁶This is the definition used in the lectures of F. P. Schuller, see [48].

¹⁷The zero section must be removed from the cotangent bundle because otherwise, the group action defined above is not free (the origin of any cotangent space is stabilized by the entire group). If the group action is free, the orbits are diffeomorphic to the group itself. If this is not the case, not all the orbits are diffeomorphic to each other, and the ‘bundle of orbits’ would not be a fiber bundle. In this case, the origin (being the orbit of the origin) is of course not diffeomorphic to the other orbits (lines with a point removed).

The orbit space of \dot{T}^*Q_e with respect to $\blacktriangleleft \mathbb{R}_x$ is precisely equal to the projectivization of the cotangent bundle $\mathbb{P}\dot{T}^*Q_e$. As a result, we have the principal \mathbb{R}_x -bundle structure given by the following diagram:

$$\begin{array}{ccc} \dot{T}^*M & & \\ \blacktriangleleft \mathbb{R}_x \uparrow & & \\ \dot{T}^*M & & \\ \downarrow \sigma & & \\ \mathbb{P}\dot{T}^*M. & & \end{array}$$

The symplectification \dot{T}^*Q_e is therefore a principal \mathbb{R}_x -bundle, with as base manifold the contact manifold $\mathbb{P}\dot{T}^*Q_e$. The projection map σ is equal to

$$\sigma : \dot{T}^*Q_e \rightarrow \mathbb{P}\dot{T}^*Q_e : (q_e, q, \rho_e, \rho) \mapsto (q_e, q, -\rho/\rho_e). \quad (3-79)$$

A geometric picture of this construction is given in Figure 3-7. Both \dot{T}^*Q_e and $\mathbb{P}\dot{T}^*Q_e$ are also bundles over the extended configuration space Q_e . The fiber $\dot{T}_x^*Q_e$ is the cotangent space to x without the origin. The group action $\blacktriangleleft \mathbb{R}_x$ manifests itself as dilations of the fiber: this is indicated by the arrows. The *orbits* of this group are lines through the origin, with the origin removed (which are diffeomorphic \mathbb{R}_x itself, since the action is free).

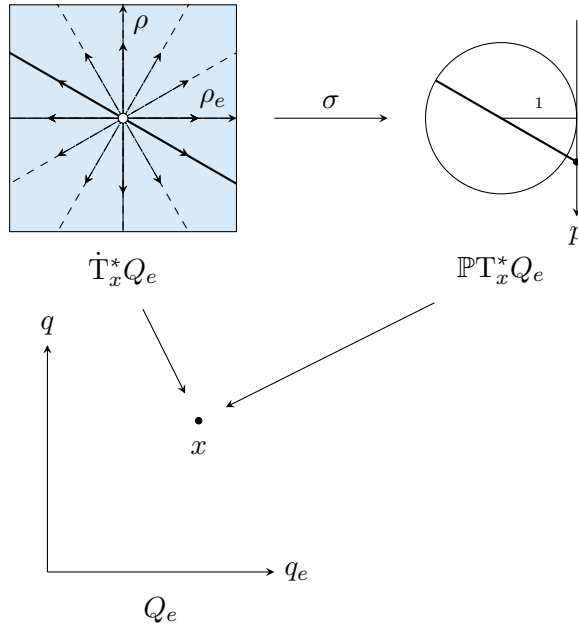


Figure 3-7: Illustration of the principal \mathbb{R}_x -bundle $\dot{T}^*M \xrightarrow{\pi} \mathbb{P}\dot{T}^*M$. x is a point in the extended configuration space Q_e , where we attach fibers $\dot{T}_x^*Q_e$ and $\mathbb{P}\dot{T}_x^*Q_e$. The orbits of the group action $\blacktriangleleft \mathbb{R}_x$ on \dot{T}^*Q_e are identified by σ and mapped to the orbit space $\mathbb{P}\dot{T}^*M$.

The space of all orbits is a circle with antipodal points identified, which is again diffeomorphic to a circle: this is the space \mathbb{PR} , and it is the fiber $\mathbb{P}\dot{T}_x^*Q_e$ of $\mathbb{P}\dot{T}^*Q_e$ at the point x . The projection map that takes a point in $\mathbb{P}\dot{T}_x^*Q_e$ to its associated point in the orbit space is σ .

In Figure 3-7, the coordinate chart used for $\mathbb{P}T^*Q_e$ is indicated as well: $p = -\rho/\rho_e$, which is as the negative of the slope of that line. This coordinate chart covers almost the entire fiber, apart from one ‘point’ (i.e. orbit): the north and south poles of the circle on the right.

From the perspective of $\mathbb{P}T^*Q_e$, ρ_e and ρ can also be seen as *homogeneous coordinates* for this space.

Principal bundles in system theory To illustrate the concept of principal bundles and their relevance, we give an instructive example of principal bundles in control theory. For more information, the reader is referred to Hermann [49].

Linear time-invariant (LTI) systems can be represented both as a collection of state-space matrices or in the frequency domain using a transfer matrix. The state-space representation is typically specified by a collection of four matrices: A, B, C, D . For an LTI system with n states, m inputs and o outputs, we have:

$$A \in \mathbb{R}^{n \times n}, \quad B \in \mathbb{R}^{n \times m}, \quad C \in \mathbb{R}^{o \times n}, \quad D \in \mathbb{R}^{o \times m}. \quad (3-80)$$

Hence, the ‘manifold of LTI systems’ with these dimensions is diffeomorphic to [50]

$$\mathbb{R}^\ell, \quad \ell = n^2 + nm + on + om. \quad (3-81)$$

This is the total space of the principal bundle.

A state space representation of a transfer matrix is not unique: any similarity transform of the state space yields different state space matrices that correspond to the same transfer matrix. Hence, the *structure group* is in this case the general linear group of dimension n , $\text{GL}(n, \mathbb{R})$, which contains all the similarity transforms. The group action $\triangleleft \text{GL}(n, \mathbb{R})$ is defined as follows:

$$(A, B, C, D) \triangleleft T = (TAT^{-1}, TB, CT^{-1}, D). \quad (3-82)$$

The orbit space $\mathbb{R}^\ell/\text{GL}(n, \mathbb{R})$ can be identified with the space of transfer matrices. The projection map that takes the state space representation to a transfer matrix is given by

$$\sigma(A, B, C, D) = C(sI - A)^{-1}B + D, \quad (3-83)$$

which is invariant with respect to the group action.

The topology of the orbit space, and therefore of the space of transfer matrices, is highly nontrivial. This makes the process of system identification very challenging, for there are usually no easy coordinate charts of this space [49, 50].

Homogeneous Hamiltonian systems

In this section, we will lift the contact Hamiltonian system defined in Section 3-2-3 to the symplectified manifold, resulting in a symplectic Hamiltonian system with a *Liouville structure*.

Liouville structures The symplectified space \dot{T}^*Q_e has a symplectic structure because the cotangent bundle (with zero section removed) is canonically equipped with one. Moreover, the group action that makes it into a principal bundle provides an additional structure: a *symplectic Liouville structure*, which requires that the symplectic 2-form is *homogeneous of degree 1* with respect to the group action $\blacktriangleleft \mathbb{R}_\times$. That is,

$$(\blacktriangleleft \lambda)^* \omega_e = \lambda \omega_e, \quad \lambda \in \mathbb{R}_\times, \quad (3-84)$$

which is indeed the case for ω_e as defined in Equation (3-75) [24]. Because the group action $\blacktriangleleft \mathbb{R}_\times$ is free, the symplectic Liouville structure is said to be *fibered* [24].

It can be shown that there is again a mapping between the smooth functions on the manifold with Liouville structure and vector fields that preserve this structure¹⁸, along the same line as for the symplectic manifolds in Section 3-1 and the contact manifolds earlier in this section.

The smooth functions, in this case, are not completely arbitrary, since they must also comply with the Liouville structure. More precisely, they must be *homogeneous* of degree 1 with respect to the group action $\blacktriangleleft \mathbb{R}_\times$. For a function \mathcal{H} on \dot{T}^*Q_e to be homogeneous means that it must satisfy the following condition:

$$(\blacktriangleleft \lambda)^* \mathcal{H} = \lambda \mathcal{H}. \quad (3-85)$$

In the coordinates defined above, this is equivalent to:

$$\mathcal{H}(q_e, q, \lambda \rho_e, \lambda \rho) = \lambda \mathcal{H}(q_e, q, \rho_e, \rho) \quad \lambda \in \mathbb{R}_\times, \quad (3-86)$$

which is to say that \mathcal{H} commutes with the group action \blacktriangleleft .

Thus, we have an isomorphism between the vector fields preserving the Liouville structure and the homogeneous functions on the manifold. Because we are dealing with a symplectic manifold, the Hamiltonian isomorphism is defined in terms of the symplectic form ω_e like so (and in an identical fashion to Equation (3-7)),

$$\omega_e^\sharp(d\mathcal{H}) = X_{\mathcal{H}}. \quad (3-87)$$

This gives rise to the notion of *homogeneous Hamiltonian systems*, consisting of a manifold with fibered symplectic Liouville structure and a homogeneous Hamiltonian function \mathcal{H} .

Equations of motion for the symplectified system The contact Hamiltonian system for the damped harmonic oscillator, as defined by Equation (3-69), can now be lifted to a homogeneous Hamiltonian system on the symplectified space. The relation between the contact Hamiltonian and the corresponding homogeneous Hamiltonian is defined as [14, 24, 41]

$$K_e(q_e, q, p) = \mathcal{H}(q_e, q, -1, \rho), \quad (3-88)$$

or equivalently

$$\mathcal{H}(q_e, q, \rho_e, \rho) := \rho_e K_e\left(q_e, q, -\frac{\rho}{\rho_e}\right). \quad (3-89)$$

¹⁸For a vector field X to preserve the Liouville structure means (i) that it preserves ω_e , i.e. $\mathcal{L}_X \omega_e = 0$, and (ii) that it is invariant under the group action: $(\blacktriangleleft \lambda)_* X = X$ ($\lambda \in \mathbb{R}_\times$).

Based on Equation (3-69), we obtain the following expression for the homogeneous Hamiltonian:

$$\mathcal{H}(q_e, q, \rho_e, \rho) = -\rho_e \left[\frac{1}{2m} \left(-\frac{\rho}{\rho_e} \right)^2 + \frac{1}{2} kq^2 + \gamma q_e \right]. \quad (3-90)$$

The Hamiltonian vector field is easily obtained, for we can use the mapping ω_e^\sharp . As already mentioned this is a major advantage of performing calculations in the symplectified space. We have

$$X_{\mathcal{H}} = \omega_e^\sharp(d\mathcal{H}), \quad (3-91)$$

with

$$d\mathcal{H} = \frac{\partial \mathcal{H}}{\partial q_e} dq_e + \frac{\partial \mathcal{H}}{\partial q} dq + \frac{\partial \mathcal{H}}{\partial \rho_e} d\rho_e + \frac{\partial \mathcal{H}}{\partial \rho} d\rho. \quad (3-92)$$

It is instructive to first specify the partial derivatives of \mathcal{H} in terms of K_e , so as to compare the generic equations of motion obtained from \mathcal{H} to those obtained from K_e (cf. Equation (3-70)). Using Equation (3-89), the partial derivatives can be expressed in terms of the contact Hamiltonian K_e :

$$\begin{aligned} \frac{\partial \mathcal{H}}{\partial q} &= -\rho_e \frac{\partial K_e}{\partial q}, \\ \frac{\partial \mathcal{H}}{\partial q_e} &= -\rho_e \frac{\partial K_e}{\partial q_e}, \\ \frac{\partial \mathcal{H}}{\partial \rho} &= -\rho_e \frac{\partial K_e}{\partial p} \frac{\partial p}{\partial \rho} = \frac{\partial K_e}{\partial p}, \\ \frac{\partial \mathcal{H}}{\partial \rho_e} &= -K_e - \rho_e \frac{\partial K_e}{\partial p} \frac{\partial p}{\partial \rho_e} = -K_e - \frac{\partial K_e}{\partial p} \frac{\rho}{\rho_e} = \frac{\partial K_e}{\partial p} p - K_e. \end{aligned} \quad (3-93)$$

The homogeneous Hamiltonian vector field is then

$$X_{\mathcal{H}} = \left(\frac{\partial K_e}{\partial p} p - K_e \right) \frac{\partial}{\partial q_e} + \frac{\partial K_e}{\partial p} \frac{\partial}{\partial q} + \rho_e \frac{\partial K_e}{\partial q_e} \frac{\partial}{\partial \rho_e} + \rho_e \frac{\partial K_e}{\partial q} \frac{\partial}{\partial \rho}. \quad (3-94)$$

The equations of motion q_e and q remain identical to those obtained earlier. This is to be expected since otherwise, the dynamics of the symplectified system could not correspond to the dynamics of the contact Hamiltonian system.

For ρ_e , we have

$$\dot{\rho}_0 = \rho_e \frac{\partial K_e}{\partial q_e} = \rho_e \frac{\partial K_e}{\partial q_e} = \gamma \rho_e \quad \Rightarrow \quad \rho_e = C e^{\gamma t}, \quad (3-95)$$

where C is an integration constant which we can choose to be 1, so $\rho_e(t) = e^{\gamma t}$.

In addition, $\dot{\rho} = \rho_e kq = e^{\gamma t} kq$. Since $p = -\rho/\rho_e$, the dynamics of p can be obtained from $\dot{\rho}_e$ and $\dot{\rho}$ using the product rule:

$$\dot{p} = -\frac{\dot{\rho}}{\rho_e} + \frac{\rho}{\rho_e} \frac{\dot{\rho}_0}{\rho_e} = -kq - \gamma p, \quad (3-96)$$

which is equivalent to the expression obtained in Section 3-2-3.

Observe that these equations of motion are invariant under the earlier defined group action $\blacktriangleleft \mathbb{R}_x$, which means that the vector field indeed preserves the Liouville structure. The other condition is that it preserves ω_e , but this is satisfied rather trivially as a result of the mapping ω_e^\sharp .

Liouville submanifolds In Section 3-2-3 we devoted considerable attention to the fact that the contact Hamiltonian should numerically be equal to zero for the equations of motion to represent a physical trajectory. This is equivalent to stating that the trajectories lie in Legendre submanifolds.

As pointed out by van der Schaft [41] and Libermann and Marle [24], because of the equivalence between contact and Liouville structures, the notion of Legendre submanifolds can be lifted to the symplectified space as well. Indeed, from Equation (3-74) we can observe that if α_e pulls back to zero on the trajectories in the contact manifold, so should ϑ_e on the lifted trajectories, for they only differ by multiplication with ρ_e . These are called *Liouville submanifolds*; they are a special subclass of Lagrangian submanifolds¹⁹

Using Equation (3-94), we find that

$$X_{\mathcal{H}} \lrcorner \vartheta_e = -K_e, \quad (3-97)$$

which means that the contact Hamiltonian (i.e. the total energy in the system) must be equal to zero for the lifted trajectories to lie in a Liouville submanifold.

For yet another perspective regarding this point, we can make use of the symplectic nature of the homogeneous Hamiltonian. Indeed, no matter what the value of K_e is, the homogeneous Hamiltonian \mathcal{H} *must* be constant over time because it does not explicitly depend on it. Since the dynamics are symplectic, we can simply use Poisson brackets to support this fact:

$$\dot{\mathcal{H}} = \{\mathcal{H}, \mathcal{H}\} + \frac{\partial \mathcal{H}}{\partial t} = 0. \quad (3-98)$$

Hence, we can set the Hamiltonian equal to a constant, say $\mathcal{H}(t) = \mathcal{H}_0$. But, we also know from $\mathcal{H} = \rho_e K_e = e^{\gamma t} K_e$. It is now very easy to see that K_e either decays exponentially (if $\gamma > 0$), for it then cancels exactly the exponential growth of ρ_e , or it equals to zero. This is equivalent to Equation (3-62). On Liouville submanifolds, both the homogeneous Hamiltonian and the contact Hamiltonian vanish, which is equivalent to the particular choice of $\mathcal{H}_0 = 0$.

If we assume that the dynamics take place on a Liouville submanifold, the Hamiltonian vector field becomes

$$X_{\mathcal{H}}|_{\mathcal{H}_0=0} = -\frac{1}{m} \left(\frac{\rho}{\rho_e} \right) \frac{\partial}{\partial q} + \frac{1}{m} \left(\frac{\rho}{\rho_e} \right)^2 \frac{\partial}{\partial q_e} + \rho_e k q \frac{\partial}{\partial \rho} + \gamma \rho_e \frac{\partial}{\partial \rho_e}. \quad (3-99)$$

If this vector field is be projected to $\mathbb{P}T^*Q_e$ we obtain Equation (3-71) using the pushforward of the projection map σ .

Relation with the Caldirola-Kanai Hamiltonian

In this section, we show that the homogeneous Hamiltonian is equivalent to a well-known existing model for the damped harmonic oscillator, the Caldirola-Kanai Hamiltonian (and Lagrangian).

¹⁹Lagrangian submanifolds satisfy the weaker condition that the symplectic 2-form ω_e vanishes when restricted to them. This is implied by the vanishing of ϑ_e , but the converse is not necessarily true.

The Caldirola-Kanai Hamiltonian, commonly attributed to Caldirola [1] and Kanai [2], is a method to describe the linearly damped harmonic oscillator using a Lagrangian or Hamiltonian function that explicitly depends on time. It was originally motivated for the purposes of quantum mechanics.

We depart from the Lagrangian function for it depends directly on the physical coordinates q and \dot{q} , as opposed to the Hamiltonian. The Caldirola-Kanai Lagrangian is

$$L_{\text{CK}}(q, \dot{q}, t) = e^{\gamma t} \left(\frac{1}{2} m \dot{q}^2 - \frac{1}{2} k q^2 \right). \quad (3-100)$$

The correct equations of motion are readily derived through the Euler-Lagrange equations:

$$\begin{aligned} \frac{d}{dt} \left(\frac{\partial L_{\text{CK}}}{\partial \dot{q}} \right) - \frac{\partial L_{\text{CK}}}{\partial q} &= 0, \\ \frac{d}{dt} (e^{\gamma t} m \dot{q}) + e^{\gamma t} k q &= 0, \\ e^{\gamma t} (m \ddot{q} + m \gamma \dot{q} + k q) &= 0, \\ m \ddot{q} + m \gamma \dot{q} + k q &= 0. \end{aligned} \quad (3-101)$$

The Caldirola-Kanai Hamiltonian is obtained from the Lagrangian by means of a Legendre transform. The Legendre transform is effected with respect to the *canonical momentum*

$$\rho = \frac{\partial L_{\text{CK}}}{\partial \dot{q}} = e^{\gamma t} m \dot{q}, \quad (3-102)$$

which is manifestly different from the kinematic momentum $p = m \dot{q} = \rho e^{-\gamma t}$.

The Hamiltonian is then equal to

$$H_{\text{CK}} = \rho \dot{q} - L_{\text{CK}} = \frac{\rho^2}{2m} e^{-\gamma t} + \frac{1}{2} k q^2 e^{\gamma t}. \quad (3-103)$$

Because the Hamiltonian is explicitly time-dependent, the associated Hamiltonian vector field will be time-dependent as well²⁰.

The construction of the vector field associated with a time-dependent Hamiltonian follows the same construction rules as a normal Hamiltonian using the isomorphism defined by ω^\sharp , but ‘frozen’ at each instant of t . The Hamiltonian vector field on T^*Q is

$$X_{H_{\text{CK}}} = -e^{\gamma t} k q \frac{\partial}{\partial \rho} + e^{-\gamma t} \frac{\rho}{m} \frac{\partial}{\partial q}. \quad (3-105)$$

²⁰A *time-dependent vector field* on a manifold N is a mapping $X : \mathbb{R} \times N \rightarrow TN$ such that for each $t \in \mathbb{R}$, the restriction X_t of X to $N \times \{t\}$ is a vector field on N [24]. An additional construction of importance, called the *suspension* of the vector field, is the mapping

$$\tilde{X} : \mathbb{R} \times N \rightarrow T(\mathbb{R} \times N) \quad (t, n) \mapsto ((t, 1), (n, X(t, n))), \quad (3-104)$$

that is to say, the suspension lifts the vector field to the extended space that also includes t and assigns the time coordinate with a trivial velocity of 1 [19].

The suspension of this vector field on $\mathbb{R} \times T^*Q$ is

$$\tilde{X}_{H_{CK}} = -e^{\gamma t} kq \frac{\partial}{\partial \rho} + e^{-\gamma t} \frac{\rho}{m} \frac{\partial}{\partial q} + \frac{\partial}{\partial t}. \quad (3-106)$$

The suspension is important because it allows us to perform the time-dependent transformation from the canonical momentum ρ to the kinematic momentum p : $\phi : (q, \rho, t) \mapsto (q, e^{\gamma t} p, t)$. The transformed vector field in terms of the physical coordinates p, q, t is

$$\phi_*(\tilde{X}_{H_{CK}}) = (-kq - \gamma p) \frac{\partial}{\partial p} + \frac{p}{m} \frac{\partial}{\partial q} + \frac{\partial}{\partial t}. \quad (3-107)$$

The extra term in p arises as a consequence of the fact that the mapping from ρ to p depends also on t .

The similarity between the derivation of the equations of motion — in particular, the crucial role of the product rule — and the one given by Equation (3-96) is striking. Indeed, if we substitute into the Caldirola-Kanai Hamiltonian $-\rho_e = e^{\gamma t}$, we obtain

$$H_{CK} = -\frac{\rho^2}{2m\rho_e} - \rho_e \frac{1}{2} kq^2 = -\rho_e \left[\frac{1}{2m} \left(\frac{\rho}{\rho_e} \right)^2 + \frac{1}{2} kq^2 \right], \quad (3-108)$$

which is precisely equal to the homogeneous Hamiltonian given in Equation (3-90) excluding the term in q_e . The dependence on q_e is not required, since it is replaced by an explicit dependence on time that would otherwise be used to produce the exponential factor $e^{\gamma t}$.

Many interpretations have already been given for the particular form of H_{CK} ; for example through time-dependent canonical transformations, or by a rescaling of time itself (see i.a. Tokieda and Endo [51], Caldirola [1] and Bravetti et al. [6]). Here we can see that the Caldirola-Kanai can be regarded as directly equivalent to the homogeneous Hamiltonian system, where the dynamics of the additional coordinates ρ_e and q_e are replaced by their explicit solution in time. Additionally, the role of the ‘mysterious’ canonical momentum ρ is explained as being a coordinate of the symplectified space, or as a homogeneous coordinate for the underlying contact space²¹.

3-2-5 The harmonic oscillator with serial damping

In this section, we extend the method outlined in Section 3-2-3 to a harmonic oscillator with two dampers: one in series and one in parallel. This system will play an important role in Chapter 4.

System dynamics

The harmonic oscillator with two dampers is shown in Figure 3-8, together with the corresponding bond graph representation. Comparing this to Figure 3-3, there is another 0-junction present in the system that compares flows (velocities) rather than efforts (forces). The equations of motion can be readily derived:

$$\begin{aligned} m\ddot{q}_1 &= -kq - b_p \dot{q}_1 \\ kq &= b_s(\dot{q}_1 - \dot{q}) \end{aligned} \quad (3-109)$$

²¹This has caused considerable confusion in literature, as stated by Schuch [52].



Figure 3-8: Schematic of the harmonic oscillator with two dampers: one in series and one in parallel. The corresponding bond graph representation is shown on the right.

Due to the presence of the serial damper, the situation is somewhat curious, since there are two positions in the system; one measuring the spring deflection q and the position of the mass q_1 . The subscript ‘1’ refers to the fact that q_1 is the position measured at the 1-junction in the bond graph shown in Figure 3-3. However, the node connecting the serial damper and the spring has no mass, and therefore no second-order dynamics: as such, the overall order of the system is two.

Position is stored in the spring, but momentum is stored in a mass. Hence, we let $p = m\dot{q}_1$ — but $\dot{q} \neq p/m$ in general. That is to say, the spring is naturally associated with a position coordinate, while the mass has momentum, though its position does not partake in the dynamics directly.

Using the damping coefficients $\gamma_s := k/b_s$ and $\gamma_p := b_p/m$, the equations of motion become:

$$\begin{aligned}\dot{q} &= -\gamma_s q + p/m \\ \dot{p} &= -\gamma_p p - kq.\end{aligned}\tag{3-110}$$

Contact Hamiltonian system

In order to establish the contact structure for the harmonic oscillator with two dampers, we must find the expression for the work done by the system on the dampers. We will do so using the structure of the bond graph shown in Figure 3-8.

Bonds carry two signals: an effort and a flow. Both can be assigned with a ‘direction’; they are always opposite. The direction indicates whether either the effort or flow should be regarded as the ‘input’ of the element attached to the bond. For example, *traditionally* (though this is a matter of convention), an I-element takes efforts as an input, and returns a flow. That is to say, one applies a force to a mass, with a change in velocity as a result. Conversely, a spring is stretched along a certain distance to return a force proportional to it; it takes a flow and returns an effort [53]. In a bond graph, this is indicated by a causality stroke, which is placed at the side of the bond that determines the flow.

If a causality convention is chosen, all the I- and C-elements in the bond graph should conform to this convention²². This is *not* the case for R-elements; they are *indifferent to causality*. The

²²Not doing so leads to a differential algebraic system (DAE).

reason for this is that there is no integral/derivative present in the mathematical description of their dynamic behavior: they relate an effort and flow, which are both time derivatives. So, depending on the system architecture, a particular R-element may receive an effort and return a flow, or vice versa [53].

This can be observed from Figure 3-8: the serial damper (on the 0-junction) receives an effort and returns a flow, while the parallel damper receives a flow and returns an effort (1-junction). This distinction is reflected in the work form associated with the damper. For the parallel damper, we have

$$\beta_p = \underbrace{\gamma_p p}_{\text{EFFORT}} \times \underbrace{\mathrm{d}q}_{\text{FLOW}}. \quad (3-111)$$

The variable that is ‘varied’ externally is the flow, hence $\mathrm{d}q$.

For the serial damper, we have the opposite situation. Here, the effort is varied externally, which is equal to $-\mathrm{d}p$. The minus sign is a consequence of the power direction in the bond connecting the 1-junction and 0-junction²³. The flow is equal to $\dot{q}_1 - \dot{q} = kq/b_s = \gamma_s q$ (using Equation (3-109)). Hence, we have

$$\beta_s = \underbrace{\gamma_s q}_{\text{FLOW}} \times \underbrace{-\mathrm{d}p}_{\text{EFFORT}}. \quad (3-112)$$

Combining these work forms, we find the contact form for the system with two dampers:

$$\alpha = \mathrm{d}U - \gamma_p p \mathrm{d}q + \gamma_s q \mathrm{d}p. \quad (3-113)$$

The exterior derivative of the contact form α is then equal to

$$\mathrm{d}\alpha = (\gamma_s + \gamma_p) \mathrm{d}q \wedge \mathrm{d}p, \quad (3-114)$$

and the Reeb vector field is simply

$$R_\alpha = \frac{\partial}{\partial U}. \quad (3-115)$$

Now to find the Hamiltonian and the system dynamics. In the following, we will only consider the horizontal component of the Hamiltonian vector field, for the various reasons pointed out in Sections 3-2-3 and 3-2-4. The horizontal component is given by (cf. Equation (3-32)):

$$\begin{aligned} X_K^{\text{hor}} &= \mathrm{d}\alpha^\sharp(\mathrm{d}K - (R_\alpha \lrcorner \mathrm{d}K)\alpha) \\ &= \mathrm{d}\alpha^\sharp\left(\left(\frac{\partial K}{\partial q} + \gamma_p p \frac{\partial K}{\partial U}\right) \mathrm{d}q + \left(\frac{\partial K}{\partial p} - \gamma_s q \frac{\partial K}{\partial U}\right) \mathrm{d}p\right). \end{aligned} \quad (3-116)$$

The mapping $\mathrm{d}\alpha^\sharp$ acts on the basis 1-forms as follows:

$$\mathrm{d}\alpha^\sharp(\mathrm{d}p) = \frac{1}{\gamma_s + \gamma_p} \left(\frac{\partial}{\partial q} + \gamma_p p \frac{\partial}{\partial U} \right) \quad \mathrm{d}\alpha^\sharp(\mathrm{d}q) = \frac{1}{\gamma_s + \gamma_p} \left(-\frac{\partial}{\partial p} + \gamma_s q \frac{\partial}{\partial U} \right). \quad (3-117)$$

²³Intuitively, it is clear from Figure 3-8 that the force acting *on* the damper is proportional to the *decrease* in momentum. Also, in Equation (3-110) we can observe that the damping force is negatively proportional to \dot{q}_1 , which is itself positively proportional to the momentum of the mass.

The extra terms in $\frac{\partial}{\partial U}$ appear again to ensure that the vector field is horizontal.

Using the same reasoning applied in Section 3-2-3, we can observe that the contact Hamiltonian must be proportional to the sum of the mechanical and internal energy of the system. In addition, we wish to cancel the factor $(\gamma_s + \gamma_p)$ present in the mapping $d\alpha^\sharp$ by multiplying the contact Hamiltonian with the same factor. Hence we, have

$$K = (\gamma_s + \gamma_p) \left(\frac{p^2}{2m} + \frac{1}{2} k q^2 + U \right). \quad (3-118)$$

Assuming again that $K = 0$, the contact Hamiltonian vector field is then:

$$X_K = X_K^{\text{hor}} = \left(\frac{p}{m} - \gamma_s q \right) \frac{\partial}{\partial q} + (-kq - \gamma_p p) \frac{\partial}{\partial p} + \left(\gamma_p \frac{p^2}{m} + \gamma_s k q^2 \right) \frac{\partial}{\partial U}, \quad (3-119)$$

since the cross terms in $\frac{\partial}{\partial U}$ cancel out. Next to the familiar dissipated power for the parallel damper, we also have the dissipated power of the serial damper

$$\gamma_s k q^2 = \underbrace{\gamma_s q}_{\text{FLOW}} \times \underbrace{k q}_{\text{EFFORT}}, \quad (3-120)$$

in the dynamics of U . Hence, this vector field yields the correct dynamics for p and q as given by Equation (3-110), in addition to the internal energy U .

3-3 Jacobi structures for general systems

In this section, we take the ideas outlined in Sections 3-1 and 3-2 one step further to more general mechanical systems. In particular, we will focus on multi-degree of freedom (MDOF) systems. As it turns out, a contact structure is not sufficient to describe such systems. Instead, we use a generalization of contact and symplectic structures, being *Jacobi structures*.

To illustrate the need for a Jacobi structure, we use the mechanical MDOF system shown in Figure 3-9. The corresponding equations of motion are

$$\begin{aligned} \dot{q}^1 &= \frac{p_1}{m_1}, \\ \dot{q}^2 &= \frac{p_2}{m_2}, \\ \dot{p}_1 &= -\frac{b_1}{m_1} p_1 - \frac{b_2}{m_1} p_1 + \frac{b_2}{m_2} p_2 - k_1 q^1 - k_2 q^1 + k_2 q^2, \\ \dot{p}_2 &= -\frac{b_2}{m_2} p_2 + \frac{b_2}{m_1} p_1 - k_3 q^2 - k_2 q^2 + k_2 q^1. \end{aligned} \quad (3-121)$$

To proceed with the method discussed in Section 3-2-3, we have to find the work form that specifies the work done by the system on the dampers. The work done on the first damper (b_1) is

$$\beta_1 = \left(\frac{b_1}{m_1} \right) p_1 dq^1. \quad (3-122)$$



Figure 3-9: Multi-degree of freedom mechanical system with two masses, two dampers, and three springs. The corresponding bond graph representation is shown below.

The second damper (b_2) is placed between the two masses; the flow is relative. The effort is proportional to this flow; i.e.

$$\beta_2 = b_2 \left(\frac{p_2}{m_2} - \frac{p_1}{m_1} \right) d(q^2 - q^1). \quad (3-123)$$

Hence, the contact 1-form that specifies the dissipation is

$$\begin{aligned} \alpha &= dU - \left(\frac{b_1}{m_1} \right) p_1 dq^1 - b_2 \left(\frac{p_2}{m_2} - \frac{p_1}{m_1} \right) d(q^2 - q^1) \\ &= dU - \left[\left(\frac{b_1}{m_1} + \left(\frac{b_2}{m_1} \right) \right) p_1 - \left(\frac{b_2}{m_2} \right) p_2 \right] dq^1 - \left[\left(\frac{b_2}{m_2} \right) p_2 - \left(\frac{b_2}{m_1} \right) p_1 \right] dq^2. \end{aligned} \quad (3-124)$$

From this expression, we can observe a crucial difference with the contact forms of the single degree of freedom systems (cf. Equations (3-45) and (3-113)). In contrast to the single-degree of freedom case given in the previous section, α is here *not* of the form

$$dU - \gamma \vartheta, \quad (3-125)$$

where ϑ is the Liouville form on the cotangent bundle of the configuration manifold T^*Q . This has important ramifications, for the Liouville form (and its exterior derivative) facilitates the ‘pairing’ between the position and momentum coordinates. In the case of a single degree of freedom system, the pairing is trivial because there is only one momentum and one position coordinate. For more complicated systems this is no longer the case, as illustrated Equation (3-124).

The exterior derivative of α is

$$\begin{aligned} d\alpha = & \left[\frac{b_1}{m_1} + \left(\frac{b_2}{m_1} \right) \right] dq^1 \wedge dp_1 - \left(\frac{b_2}{m_2} \right) dq^1 \wedge dp_2 \\ & + \left(\frac{b_2}{m_2} \right) dq^2 \wedge dp_2 - \left(\frac{b_2}{m_1} \right) dq^2 \wedge dp_1, \end{aligned} \quad (3-126)$$

which indicates indeed that there is also a ‘mixing’ of p_1 and q_2 and p_2 and q_1 in the resulting 2-form. As a result, the mapping $d\alpha^\sharp$ will not produce the mapping that we would expect in the purely symplectic case.

From a conceptual standpoint, this is not quite surprising: there is no inherent reason why the form that describes dissipation should somehow also include the ‘pairing’ structure: they are fundamentally different, and both are required for the geometric description of the mechanical system. In the previous section, we were indeed rather ‘lucky’ to find, in *that particular case*, that the dissipation form α also included the pairing structure. This severely limits the applicability of contact Hamiltonian systems to dissipative mechanical systems.

The multi-degree of freedom systems for which α is of the form $dU - \gamma\vartheta$ are those that do exhibit no damping on the relative velocities of the masses, and for which all dampers have the same damping coefficient. This is a very restrictive requirement, and we wish to do better. To do so, we introduce a generalization of contact and symplectic structures called a *Jacobi* structure in the next section, and subsequently apply it to the system shown in Figure 3-9.

3-3-1 Jacobi structures

A *Jacobi structure* on a manifold M is a bilinear mapping of the functions on M [54]

$$\{ , \} : C^\infty(M) \times C^\infty(M) \rightarrow C^\infty(M) : (f, g) \mapsto \{f, g\} \quad (3-127)$$

called the *Jacobi bracket*. This mapping needs to satisfy three properties:

- (i) it must be *skew-symmetric*

$$\{f, g\} = -\{g, f\}, \quad (3-128)$$

- (ii) it satisfies the *Jacobi identity*

$$\{f, \{g, h\}\} + \{h, \{f, g\}\} + \{g, \{h, f\}\} = 0, \quad (3-129)$$

- (iii) it is *local*

$$\text{supp } \{f, g\} \subset \text{supp } f \cap \text{supp } g, \quad (3-130)$$

where supp denotes the support of a function.

Manifolds equipped with a Jacobi structure are called *Jacobi manifolds*.

It can be shown that any Jacobi structure can be uniquely defined in terms of a bivector field²⁴ Λ and a vector field R . The corresponding Jacobi bracket is then given by: [24, 54]

$$\{f, g\} = \Lambda(df, dg) + f(R \lrcorner dg) - g(R \lrcorner df). \quad (3-131)$$

²⁴A *bivector* is the contravariant counterpart of a 2-form: it is a skew-symmetric tensor with valence $(2, 0)$ [55].

Not just any combination of a bivector field and vector field give rise to a Jacobi structure. As shown by Lichnerowicz [56], Λ and R must satisfy two conditions:

$$[\![\Lambda, \Lambda]\!] = 2R \wedge \Lambda \quad [\![R, \Lambda]\!] = 0, \quad (3-132)$$

where $[\![\cdot, \cdot]\!]$ is the *Schouten bracket*²⁵. A Jacobi manifold is therefore a triple (M, Λ, R) [24].

A Jacobi structure induces a mapping from the functions on the manifold to the vector fields on the manifold (sometimes called the *Hamiltonian correspondence*) [7, 58] defined as follows:

$$\Psi : C^\infty(M) \rightarrow \mathfrak{X}(M) : \quad X_f = \Lambda^\sharp(df) + fR, \quad (3-134)$$

where f is the Hamiltonian function, X_f the associated Hamiltonian vector fields. The sharp mapping Λ^\sharp is defined as:

$$\Lambda^\sharp : T^*M \rightarrow TM : \quad \Lambda^\sharp(\eta) = \Lambda \lrcorner \eta, \quad (3-135)$$

or equivalently

$$\Lambda(\eta, \chi) = \Lambda^\sharp(\eta) \lrcorner \chi. \quad (3-136)$$

We will now see that both symplectic and contact manifolds are particular instances of Jacobi manifold, including the Hamiltonian systems defined on them.

Symplectic manifolds are Jacobi

For a symplectic manifold (M, ω) with dimension $2n$, the vector field R is simply zero and the bivector Λ field is defined by:

$$\Lambda(\eta, \chi) = \omega(\omega^\sharp(\eta), \omega^\sharp(\chi)) \quad \eta, \chi \in \Omega^1(M), \quad (3-137)$$

with ω^\sharp defined as in Equation (3-7).

If ω is expressed in Darboux coordinates, i.e.

$$\omega = \sum_{i=1}^n dq^i \wedge dp_i, \quad (3-138)$$

then the associated bivector can be found to be Equation (3-134):

$$\Lambda = \sum_{i=1}^n \frac{\partial}{\partial q^i} \wedge \frac{\partial}{\partial p_i}. \quad (3-139)$$

The associated Jacobi bracket reverts to the familiar Poisson bracket on the symplectic manifold. A Poisson structure is a particular instance of a Jacobi structure where the vector field R is equal to zero. This makes the Poisson/Jacobi bracket into a *derivation* on the algebra of smooth functions (over the real numbers): consequently, Poisson brackets satisfy the Leibniz property in addition to the conditions for Jacobi brackets given above [54].

²⁵The Schouten bracket of an r -vector field A and an s -vector field B on a manifold is a $(r+s-1)$ -vector field $[\![A, B]\!]$, defined by its action on a closed $(r+s-1)$ -form ζ as follows:

$$[\![A, B]\!](\zeta) = (-1)^{rs+s} A \lrcorner d(B \lrcorner \zeta) + (-1)^r B \lrcorner d(A \lrcorner \zeta). \quad (3-133)$$

For $r = s = 1$, the Schouten bracket simply reverts to the ordinary Lie bracket [57].

Contact manifolds are Jacobi

A strictly contact manifold²⁶ (M, α) with dimension $2n + 1$ is also a Jacobi manifold. The vector field $R = R_\alpha$ is the Reeb vector field. and the bivector Λ is equal to

$$\Lambda(\eta, \chi) = d\alpha(d\alpha^\sharp(\eta), d\alpha^\sharp(\chi)), \quad (3-140)$$

where $d\alpha^\sharp$ is defined as in Equation (3-31) and η, χ are semi-basic 1-forms on M .

If α is expressed in Darboux coordinates:

$$\alpha = dq^0 - \sum_{i=1}^n p_i dq^i, \quad (3-141)$$

then

$$R = \frac{\partial}{\partial q^0}. \quad (3-142)$$

The expression for the bivector can be found as follows through the action of Λ^\sharp on a general 1-form $\zeta \in \Gamma(T^*M)$ (by comparison with Equation (3-134)):

$$\begin{aligned} \Lambda^\sharp(\zeta) &= d\alpha^\sharp(\zeta - (R \lrcorner \zeta)\alpha) \\ &= \sum_{i=1}^n \left(\frac{\partial}{\partial q^i} \wedge \frac{\partial}{\partial p_i} \right) \lrcorner (\zeta - (R \lrcorner \zeta)\alpha) \\ &= \sum_{i=1}^n \left(\frac{\partial}{\partial q^i} \wedge \frac{\partial}{\partial p_i} \right) \lrcorner \zeta - \sum_{i=1}^n \left(\frac{\partial}{\partial q^i} \wedge \frac{\partial}{\partial p_i} \right) \lrcorner ((R \lrcorner \zeta)\alpha) \\ &= \sum_{i=1}^n \left(\frac{\partial}{\partial q^i} \wedge \frac{\partial}{\partial p_i} \right) \lrcorner \zeta - \sum_{i=1}^n p_i \frac{\partial}{\partial p_i} (R \lrcorner \zeta) \\ &= \sum_{i=1}^n \left(\frac{\partial}{\partial q^i} \wedge \frac{\partial}{\partial p_i} \right) \lrcorner \zeta - \left(\sum_{i=1}^n p_i \frac{\partial}{\partial p_i} \wedge \frac{\partial}{\partial q^0} \right) \lrcorner \zeta. \end{aligned} \quad (3-143)$$

From this expression, we gather that

$$\Lambda = \sum_{i=1}^n \left(\frac{\partial}{\partial q^i} \wedge \frac{\partial}{\partial p_i} \right) + \left(\sum_{i=1}^n p_i \frac{\partial}{\partial p_i} \wedge \frac{\partial}{\partial q^0} \right). \quad (3-144)$$

We will now apply the Jacobi structure to general mechanical systems.

3-3-2 Jacobi structure of mechanical systems

The geometric structure of a mechanical system has four components:

²⁶For contact structures that are not globally determined by a single contact form, Marle [54] introduced the concept of a *Jacobi bundle*.

- An odd-dimensional manifold $M = T^*Q \times \mathbb{R}$, where Q is the configuration manifold. It is extended by one dimension to incorporate the dissipated (internal) energy U and therefore always odd-dimensional. In the following, we assume the ‘Darboux’ coordinates $(q^1, \dots, q^n, p_1, \dots, p_n, U)$. This manifold has a bundle structure $M \xrightarrow{\pi} T^*Q$, where π is the projection map that ‘forgets’ the U -coordinate.
- A closed 2-form with constant rank $2n$, defined as the negative of the exterior derivative of the Liouville form on T^*Q :

$$\omega = -d\vartheta = \sum_{i=1}^n dq^i \wedge dp_i, \quad (3-145)$$

i.e. ω is the canonical symplectic 2-form on T^*Q .

- A *dissipation form* α that encodes the work done by the system on its environment:

$$\alpha = dU - \beta, \quad (3-146)$$

where $\beta = \pi^*\beta_{T^*Q}$ is a pullback of a form on T^*Q , which means that it cannot depend on U . When there is no dissipation, $\beta = 0$.

- A *Hamiltonian function* $K \in C^\infty(M)$, equal to the sum of the mechanical energy of the system and the internal energy:

$$K = E + U, \quad (3-147)$$

with $E = E(q^1, \dots, q^n, p_1, \dots, p_n)$ the mechanical energy of the system.

In the purely conservative case discussed in Section 3-1, there is no dissipation, so the extra dimension in U does not play a role, and the system may be completely described on T^*Q with its symplectic structure.

For the simple dissipative mechanical systems in Section 3-2, the form α would both encode the pairing structure *and* the dissipation form, since $d\alpha$ would be of the form $dU - \gamma\vartheta$. We now separate both functionalities (i.e. pairing and dissipation) to distinct components, for which the symplectic and contact systems are particular cases.

The Jacobi structure for general mechanical systems is constructed in an analogous manner to the one for contact manifolds, apart from the fact that we now have a separate 2-form ω , instead of using $d\alpha$. We can already expect that this will work given the right conditions, for the derivations in Section 3-2 did not use the fact that $d\alpha$ is indeed the exterior derivative of α .

However, not just any ω and α will make this work. Recall that the maximum nonintegrability of α is equivalent to $\alpha \wedge (d\alpha)^n$ being a volume form on the contact manifold. Along the same line, we require the following condition on ω and α :

$$\alpha \wedge (\omega)^n \neq 0 \quad (3-148)$$

everywhere on M ; that is to say, it is a volume form on M [7]. If M , ω and α are defined as given above, this condition is clearly satisfied:

$$\alpha \wedge (\omega)^n = n! \, dU \wedge \left(\bigwedge_{i=1}^n dq^i \wedge dp_i \right). \quad (3-149)$$

If Equation (3-148) is satisfied we can — similarly to the discussion in Section 3-2-2 — define the splitting of the tangent bundle as follows:

$$T^*M = \ker \alpha \oplus \ker \omega. \quad (3-150)$$

Vector fields in the kernel of α are called *horizontal*, while vector fields in the kernel of ω are *vertical*. Define the *Reeb vector field* R (for this Jacobi structure) as the unique vector field that satisfies the following conditions:

$$R \lrcorner \alpha = 1 \quad R \lrcorner \omega = 0. \quad (3-151)$$

In Darboux coordinates, we have

$$R = \frac{\partial}{\partial U}. \quad (3-152)$$

In addition, define *semi-basic forms* as the forms that annihilate the vertical vector fields; in Darboux coordinates, they are forms that have no component in dU .

The decompositions of vector fields into horizontal and vertical components, and of 1-forms into semi-basic components and multiples of α are analogous to Equations (3-25) and (3-26) respectively.

The construction of Λ is analogous to the case of contact manifolds: the sharp mapping first isolates the semi-basic component of the argument, after it is mapped to a horizontal vector field through ω^\sharp :

$$\Lambda^\sharp(\zeta) = \omega^\sharp(\zeta - (R \lrcorner \zeta)\alpha). \quad (3-153)$$

Using the coordinates defined above, we find:

$$\Lambda = \sum_{i=1}^n \left(\frac{\partial}{\partial q^i} \wedge \frac{\partial}{\partial p_i} \right) - \frac{\partial}{\partial U} \wedge \left[\sum_{i=1}^n \left(\frac{\partial}{\partial q^i} \wedge \frac{\partial}{\partial p_i} \right) \lrcorner \beta \right]. \quad (3-154)$$

The dynamics of the general mechanical system are then equal to

$$X_K = \Lambda^\sharp(dK), \quad (3-155)$$

assuming again that K is numerically equal to zero, so as to make the vertical component of the Hamiltonian vector field disappear.

For computational convenience, this mapping can also be represented by a matrix:

$$\begin{aligned} \begin{pmatrix} \dot{q} \\ \dot{p} \\ \dot{U} \end{pmatrix} &= \left[\begin{pmatrix} 0 & I_n & 0 \\ -I_n & 0 & 0 \\ 0 & 0 & 0 \end{pmatrix} - \begin{pmatrix} 0 \\ 0 \\ 1 \end{pmatrix} \wedge \begin{pmatrix} 0 & I_n & 0 \\ -I_n & 0 & 0 \\ 0 & 0 & 0 \end{pmatrix} \begin{pmatrix} \beta_q \\ \beta_p \\ 0 \end{pmatrix} \right] (\nabla K) \\ &= \left[\begin{pmatrix} 0 & I_n & 0 \\ -I_n & 0 & 0 \\ 0 & 0 & 0 \end{pmatrix} - \begin{pmatrix} 0 & 0 & -\beta_p \\ 0 & 0 & \beta_q \\ \beta_p & -\beta_q & 0 \end{pmatrix} \right] (\nabla K) \\ &= \begin{pmatrix} 0 & I_n & \beta_p \\ -I_n & 0 & -\beta_q \\ -\beta_p & \beta_q & 0 \end{pmatrix} (\nabla K), \end{aligned} \quad (3-156)$$

where β_q and β_p represent the q - and p -components of the form β , and ∇K is the gradient of K . The minus sign in front of the β_p -components is usually canceled because those components often already carry a minus sign as a consequence of the power direction of the bond connecting the 0- and 1-junctions on which they are defined (e.g. in the case of the serial damper in Section 3-2-5).

Application to 2-DOF mechanical system

We now revisit the mechanical system shown in Figure 3-9. The four structure components are

- The manifold $M = \mathbb{R}^5 = T^*Q \times \mathbb{R}$, for which we choose coordinates (q^1, q^2, p_1, p_2, U) .
- The 2-form ω is the canonical symplectic structure on T^*Q :

$$\omega = dq^1 \wedge dp_1 + dq^2 \wedge dp_2. \quad (3-157)$$

- The dissipation form is given by Equation (3-124):

$$\beta = \left[\left(\frac{b_1}{m_1} + \frac{b_2}{m_1} \right) p_1 - \left(\frac{b_2}{m_2} \right) p_2 \right] dq^1 + \left[\left(\frac{b_2}{m_2} \right) p_2 - \left(\frac{b_2}{m_1} \right) p_1 \right] dq^2. \quad (3-158)$$

- The Hamiltonian is equal to the sum of kinetic, potential, and internal energy in the system:

$$K = \frac{p_1^2}{2m_1} + \frac{p_2^2}{2m_2} + \frac{1}{2}k_1(q^1)^2 + \frac{1}{2}k_3(q^2)^2 + \frac{1}{2}k_2(q^2 - q^1)^2 + U. \quad (3-159)$$

The expression for β is given by Equation (3-124) as a part of the dissipation form α . The exterior derivative of K is

$$dK = \left(\frac{p_1}{m_1} \right) dp_1 + \left(\frac{p_2}{m_2} \right) dp_2 + [k_1 q^1 + k_2 (q^1 - q^2)] dq^1 + [k_3 q^2 + k_2 (q^2 - q^1)] dq^2 + dU. \quad (3-160)$$

Using either Equations (3-154) and (3-155) or Equation (3-156), we obtain the correct equations of motion for the system:

$$\begin{aligned} \dot{q}^1 &= \frac{p_1}{m_1}, \\ \dot{q}^2 &= \frac{p_2}{m_2}, \\ \dot{p}_1 &= -\frac{b_1}{m_1} p_1 - \frac{b_2}{m_1} p_1 + \frac{b_2}{m_2} p_2 - k_1 q^1 - k_2 q^1 + k_2 q^2, \\ \dot{p}_2 &= -\frac{b_2}{m_2} p_2 + \frac{b_2}{m_1} p_1 - k_3 q^2 - k_2 q^2 + k_2 q^1, \\ \dot{U} &= b_1 \frac{p_1^2}{m_1^2} + b_2 \frac{p_2^2}{m_1^2} + b_2 \frac{p_2^2}{m_2^2} - 2b_2 \frac{p_1 p_2}{m_1 m_2}. \end{aligned} \quad (3-161)$$

The reason why the equation for U is always correct is that we force the vector field to annihilate the dissipation form α ; as such, any work done by the dampers must constitute the change in U . Because the Hamiltonian is equal to zero, there are no other contributions to \dot{U} .

Observe from Equation (3-161) that the rate of change of U can be written in terms of the *Rayleigh dissipation matrix*:

$$\dot{U} = \begin{pmatrix} \frac{p_1}{m_1} & \frac{p_2}{m_2} \end{pmatrix} \begin{pmatrix} b_1 + b_2 & -b_2 \\ -b_2 & b_2 \end{pmatrix} \begin{pmatrix} \frac{p_1}{m_1} \\ \frac{p_2}{m_2} \end{pmatrix}. \quad (3-162)$$

It is important to point out though that our method does not rely on the fact that the damping force relies on the momenta/velocities in a linear fashion: we made no assumptions on β , apart from the fact that it does not depend on U . Hence, any type of force that performs work in the direction of the generalized coordinates can be incorporated in this fashion. This is in contrast with the Rayleigh method.

Nonautonomous systems

For the purposes of control, the above formalism may also be extended with external inputs; i.e. flow sources, effort sources, or sources that contribute to the internal energy. In the port-Hamiltonian formalism proposed by Van Der Schaft [59], the external sources are simply added to their respective Hamiltonian functions. It is then possible to interconnect several mechanical systems by means of power-preserving connections.

When subject to external inputs, the vector field X governing the dynamics of the mechanical system is the superposition of the time-dependent ‘input vector field’ X_u and the Hamiltonian vector field generated by the Jacobi-structure:

$$X = X_u + X_K. \quad (3-163)$$

In matrix form, the equations of motion given by Equation (3-156) become

$$\begin{pmatrix} \dot{\mathbf{q}} \\ \dot{\mathbf{p}} \\ \dot{U} \end{pmatrix} = \begin{pmatrix} 0 & I_n & \boldsymbol{\beta}_p \\ -I_n & 0 & -\boldsymbol{\beta}_q \\ -\boldsymbol{\beta}_p & \boldsymbol{\beta}_q & 0 \end{pmatrix} (\nabla K) + \begin{pmatrix} \mathbf{u}_q \\ \mathbf{u}_p \\ u_U \end{pmatrix}, \quad (3-164)$$

where \mathbf{u}_q , \mathbf{u}_p and u_U represent the flow sources, effort sources and source of internal energy (i.e. a heat source).

Chapter 4

Split-Quaternion Representations of Dynamical Systems

In this chapter, we propose split-quaternions as an alternative representation of linear two-dimensional dynamical systems instead of the traditional state space representation. This representation is based on the fact that the algebras of split-quaternions and two-dimensional linear matrices are isomorphic. We argue that the split-quaternion representation allows for easier system classification and computation of the system solution. In addition, we also relate the shape of the solution trajectory of an underdamped system to the associated split-quaternion.

First, we introduce the notion of split-quaternions in Section 4-1 and how they correspond to matrices. Second, in Section 4-2, we relate the split-quaternions to general two-dimensional linear dynamical systems. Finally, in Section 4-3, we use the damped harmonic oscillator as a representative system so as to give physical interpretation to the split-quaternion representation and analyze the shape of the solution trajectories.

The discussion in Section 4-1 mainly concerns facts about split-quaternions that have been known in the past. Their application to dynamical systems (i.e. the subject of Section 4-2 and Section 4-3) has not been researched in the previously; as such, the results presented in these sections are all new.

4-1 The algebra of split-quaternions

In this section, we present the split-quaternion number system, its basic properties, and its relation with two-dimensional matrices.

4-1-1 Basic properties of split-quaternions

Like conventional quaternions, the split-quaternions form a number system that consists of linear combinations of four basis elements, which are denoted by 1 , \hat{i} , \hat{j} , and \hat{k} .¹ The algebra of split-quaternions is associative but not commutative — formally speaking, we are dealing with an algebraic structure called a *noncommutative (unital) ring*. The multiplication table for the split-quaternion algebra is shown in Table 4-1. The set of split-quaternions is denoted by $\hat{\mathbb{H}}$, since \mathbb{H} is reserved for conventional quaternions.²

Table 4-1: Multiplication table for the split-quaternion algebra.

	1	\hat{i}	\hat{j}	\hat{k}
1	1	\hat{i}	\hat{j}	\hat{k}
\hat{i}	\hat{i}	-1	\hat{k}	$-\hat{j}$
\hat{j}	\hat{j}	$-\hat{k}$	1	$-\hat{i}$
\hat{k}	\hat{k}	\hat{j}	\hat{i}	1

The distinctive feature that sets split-quaternions apart from conventional quaternions resides in the diagonal elements of Table 4-1. For quaternions, all basis elements but 1 square to -1 , which is not the case for the split-quaternions (only \hat{i} does). This is also the reason why split-quaternions are ‘split’, for this difference in sign makes their norm (to be defined later) into an indefinite quadratic form. That is to say, whereas quaternions have a ‘metric signature’ (in a very imprecise sense of the word metric) of $(+, +, +, +)$, the split-quaternions have $(+, +, -, -)$. The difference ‘metric’ signature makes the split-quaternion number system different from its conventional quaternion counterpart.

Importantly, the split-quaternion algebra can also be seen as an *algebra*; i.e. a four-dimensional vector space over the real numbers combined with the split-quaternion product operation. More specifically, the split-quaternions form a *unital noncommutative associative algebra*.

The dihedral group

On their own, the basis elements of the split-quaternions $\{1, \hat{i}, \hat{j}, \hat{k}\}$ form a *finite group* under multiplication, namely the *dihedral group* D_4 . This group represents all the symmetries of a square: the identity, a 90-degree rotation, and two reflections, as illustrated in Figure 4-1 [61].

The structure of the dihedral group can be visualized by means of its *cycle graph* in Figure 4-2. Many important properties of the split-quaternion algebra and the applications in this chapter can be traced back to the shape of this cycle graph. One example is the ‘split’ nature of the quaternions: the \hat{i} -element generates an order-4 cycle, while \hat{j} and \hat{k} generate order-2 cycles. In contrast, the cycle graph for conventional quaternions is entirely symmetric for all these elements [61].

¹Even though they behave similarly, the imaginary unit i is not to be confused with the split-quaternion basis element \hat{i} , because they each belong to an entirely different number system.

²The set of (split-)quaternions ‘ \mathbb{H} ’ is named in honor of sir William Rowan Hamilton, who also developed the Hamiltonian formalism: the fruits of his work truly form the central theme in this thesis [60].

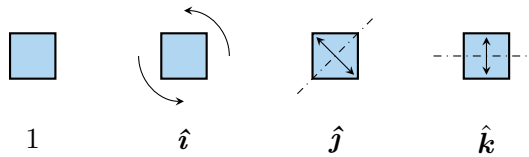


Figure 4-1: The dihedral group D_4 is the symmetry group of a square. This group is isomorphic to the group formed by $1, \hat{i}, \hat{j}$ and \hat{k} under multiplication.

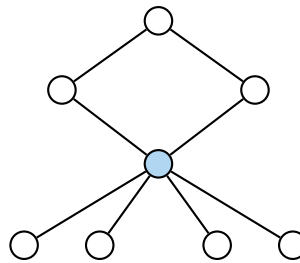


Figure 4-2: The cycle graph of the dihedral group D_4 . There are five cycles: one of order four which represents the rotations (or the element \hat{i}) of the square, and four order-2 cycles, which are all the possible reflections. The colored element represents the identity.

Split-quaternion (total) norm

Similar to conventional quaternions, we make a distinction between the *scalar* or *real part* and the *vector part* of a split-quaternion. For an arbitrary split-quaternion $a \in \hat{\mathbb{H}}$, [62]

$$a = a_0 + a_1 \hat{i} + a_2 \hat{j} + a_3 \hat{k} \quad (4-1)$$

the real part is

$$\text{sca}(a) := a_0, \quad (4-2)$$

and the vector part is

$$\text{vec}(a) := a_1 \hat{i} + a_2 \hat{j} + a_3 \hat{k}. \quad (4-3)$$

Because the vector part and real part are used so often in this chapter, we adopt a more convenient shorthand notation for them, instead of `sca()` and `vec()`. Given any split-quaternion, the real part is denoted by the same symbol with a subscript of 0, without having to explicitly define the split-quaternion components as we did in Equation (4-1). In addition, the vector part is denoted by the symbol of the split-quaternion, but set in **boldface**. For instance, for the split-quaternion b , we denote its real part by $b_0 := \text{sca}(b)$ and its vector part by $\mathbf{b} := \text{vec}(b)$. An alternative expression for b is then

$$b = b_0 + \mathbf{b}. \quad (4-4)$$

In addition, every split-quaternion has a unique *conjugate* split-quaternion, which has the same real part but the opposite vector part:

$$\begin{aligned} a^* &:= \text{sca}(a) - \text{vec}(a) \\ &= a_0 - \mathbf{a} \\ &= a_0 - a_1 \hat{i} - a_2 \hat{j} - a_3 \hat{k}. \end{aligned} \quad (4-5)$$

Using the conjugate, we can define the *squared split-quaternion norm*:

$$\mathcal{N}: \hat{\mathbb{H}} \rightarrow \mathbb{R} : \mathcal{N}(a) := aa^* = a_0^2 + a_1^2 - a_2^2 - a_3^2. \quad (4-6)$$

The split-quaternion norm is (in stark contrast to the norm defined for quaternions) *indefinite*: it can be positive, negative or zero. Split-quaternions can therefore be categorized into three regimes based on the sign of their squared norm. In the tradition of special relativity, these regimes are named

- a is *timelike* if $\mathcal{N}(a) > 0$,
- a is *lightlike* if $\mathcal{N}(a) = 0$,
- a is *spacelike* if $\mathcal{N}(a) < 0$.

Like the space of split-quaternions, Minkowski spacetime is also four-dimensional. However, the signature of the Minkowski metric is different from the split-quaternion signature: it is either $(-, +, +, +)$ or equivalently $(+, -, -, -)$ depending on the sign convention one chooses to adhere to. The terminology (i.e. spacelike, timelike, lightlike) applies nonetheless [63, 64].

Based on the squared split-quaternion norm, the *split-quaternion norm* is then defined as

$$\|\cdot\|: \hat{\mathbb{H}} \rightarrow \mathbb{C} : \|a\| := \sqrt{\mathcal{N}(a)} = \sqrt{a_0^2 + a_1^2 - a_2^2 - a_3^2}. \quad (4-7)$$

Because of the indefiniteness of \mathcal{N} , $\|a\|$ is an imaginary number if a is spacelike, for its squared norm is negative in that case.

Vector norm

Apart from the split-quaternion norm, we may also define a (squared) norm that only considers the *vector part* of the split-quaternion. The *squared vector norm* is defined in accordance with the total squared split-quaternion norm given by Equation (4-6):

$$\mathcal{N}(\mathbf{a}) = a_1^2 - a_2^2 - a_3^2. \quad (4-8)$$

This is not an abuse of notation, for \mathbf{a} can be seen as a split-quaternion in its own right with the same vector part as a but with a zero scalar part. It is therefore a valid argument for the split-quaternion norm, and we can use the same function with no ambiguity. The *vector norm* is then defined in accordance

$$\|\mathbf{a}\| = \sqrt{\mathcal{N}(\mathbf{a})} = \sqrt{a_1^2 - a_2^2 - a_3^2}. \quad (4-9)$$

In the remainder of this chapter, the distinction between the squared norm of the entire split-quaternion and its squared vector norm plays a crucial role. Therefore, we will refer to $\mathcal{N}(a)$ as the squared *total* norm, and to $\mathcal{N}(\mathbf{a})$ as the squared *vector* norm. Likewise, we refer to $\|a\|$ as the *total* norm, and to $\|\mathbf{a}\|$ as the *vector* norm of that split-quaternion.

The quadratic form given in Equation (4-8) is also not positive-definite. As a result, we can establish a classification based on the vector norm instead of the total norm as well:

- \mathbf{a} is *timelike* / a has a timelike vector if $\mathcal{N}(\mathbf{a}) > 0$,
- \mathbf{a} is *lightlike* / a has a lightlike vector if $\mathcal{N}(\mathbf{a}) = 0$,
- \mathbf{a} is *spacelike* / a has a spacelike vector if $\mathcal{N}(\mathbf{a}) < 0$.

Because one can classify based on both the (squared) squared norm and the (squared) total norm, one may identify nine hypothetical cases, since each falls into one of three regimes. However, the squared vector norm is not completely independent from the squared total norm: observe that

$$\mathcal{N}(a) < 0 \Rightarrow \mathcal{N}(\mathbf{a}) < 0, \quad (4-10)$$

which is to say that *a spacelike split-quaternion always has a spacelike vector part*. The converse is not necessarily true. Furthermore, *a lightlike split-quaternion must have a lightlike or spacelike vector part*, i.e.

$$\mathcal{N}(a) = 0 \Rightarrow \mathcal{N}(\mathbf{a}) \leq 0 \quad (4-11)$$

These two statements rule out three hypothetical combinations for the regimes of the total norm and the vector norm (spacelike - timelike, spacelike - lightlike and lightlike - timelike). Hence, six possible combinations remain; they are listed in Table 4-2.

Table 4-2: All the possible combinations of the regime of the split-quaternion and the regime of its vector part. Spacelike split-quaternions can only have a spacelike vector, while lightlike split-quaternions can only have lightlike or spacelike vector parts. The numbering of these cases coincides with the classification of dynamical systems in Section 4-2-2.

		$\mathcal{N}(\mathbf{a})$		
		spacelike	lightlike	timelike
$\mathcal{N}(a)$	spacelike	①	—	—
	lightlike	②	③	—
	timelike	④	⑤	⑥

The classification given by Table 4-2 is very important because it corresponds directly to the qualitative classification of dynamical systems discussed in Section 4-2-2.

In the remainder of this chapter, the split-quaternion properties that are defined above are used profusely. For the convenience of the reader, an overview of these properties and their definitions is provided in Table 4-3.

Lorentzian 3-space

In contrast to the overall split-quaternion, the vector part of the split-quaternion does live in a space with a Lorentz structure, having three dimensions instead of four. In general, the *Lorentzian n-space* is defined as the real vector \mathbb{R}^n space equipped with the *Lorentzian inner product*.

$$\langle \mathbf{a}, \mathbf{b} \rangle_L := a_1 b_1 - a_2 b_2 - \dots - a_n b_n, \quad \mathbf{a}, \mathbf{b} \in \mathbb{R}^n. \quad (4-12)$$

Since the Lorentzian inner product has signature $(+, -, \dots, -)$, the Lorentzian n -space is denoted by $\mathbb{R}^{1,n-1}$. For $n = 4$, the Lorentzian space is equal to *Minkowski spacetime*, which forms the mathematical setting of the theory of special relativity.

Table 4-3: Overview of the split-quaternion properties that are often used in this chapter.

Terminology	Notation	Definition	Expression
Split-quaternion	a		$a_0 + a_1\hat{\mathbf{i}} + a_2\hat{\mathbf{j}} + a_3\hat{\mathbf{k}}$
Conjugate split-quaternion	a^*	$a - \text{vec}(a)$	$a_0 - a_1\hat{\mathbf{i}} - a_2\hat{\mathbf{j}} - a_3\hat{\mathbf{k}}$
Scalar part	$\text{sca}(a) = a_0$		a_0
Vector part	$\text{vec}(a) = \mathbf{a}$		$a_1\hat{\mathbf{i}} + a_2\hat{\mathbf{j}} + a_3\hat{\mathbf{k}}$
Squared (total) norm	$\mathcal{N}(a)$	aa^*	$a_0^2 + a_1^2 - a_2^2 - a_3^2$
(Total) norm	$\ \mathbf{a}\ $	$\sqrt{\mathcal{N}(a)}$	$\sqrt{a_0^2 + a_1^2 - a_2^2 - a_3^2}$
Squared vector norm	$\mathcal{N}(\mathbf{a})$	$\mathbf{a}\mathbf{a}^*$	$a_1^2 - a_2^2 - a_3^2$
Vector norm	$\ \mathbf{a}\ $	$\sqrt{\mathcal{N}(\mathbf{a})}$	$\sqrt{a_1^2 - a_2^2 - a_3^2}$

Based on the Lorentzian inner product³, the *Lorentz norm* can be defined as follows:

$$\|\mathbf{a}\| = \sqrt{\langle \mathbf{a}, \mathbf{a} \rangle_L}, \quad (4-13)$$

For the Lorentzian 3-space $\mathbb{R}^{1,2}$, the Lorentzian norm coincides with the vector norm for split-quaternions defined in Equation (4-8). Hence, if the vector part of a split-quaternion is regarded as a three-dimensional object in its own right (rather than a split-quaternion with zero real part), it is an element of $\mathbb{R}^{1,2}$. For this space, we view the split-quaternion basis elements $\hat{\mathbf{i}}, \hat{\mathbf{j}}, \hat{\mathbf{k}}$ as *unit basis vectors* to distinguish the vector components.

Next to the Lorentzian inner product, we can also define a *Lorentzian cross product*, which exists only for $\mathbb{R}^{1,2}$. Given two vectors \mathbf{a}, \mathbf{b} , in $\mathbb{R}^{1,2}$ their Lorentzian cross-product is defined as: [62]

$$\mathbf{a} \times_L \mathbf{b} := \det \begin{pmatrix} -\hat{\mathbf{i}} & \hat{\mathbf{j}} & \hat{\mathbf{k}} \\ a_1 & a_2 & a_3 \\ b_1 & b_2 & b_3 \end{pmatrix} \quad \mathbf{a}, \mathbf{b} \quad (4-14)$$

$$= (a_3b_2 - a_2b_3)\hat{\mathbf{i}} + (a_3b_1 - a_1b_3)\hat{\mathbf{j}} + (a_1b_2 - a_2b_1)\hat{\mathbf{k}}, \quad (4-15)$$

where we have assumed $\hat{\mathbf{i}}, \hat{\mathbf{j}}, \hat{\mathbf{k}}$ as basis vectors.

The split-quaternion product can be conveniently expressed in terms of the Lorentzian inner product and cross product. For two split-quaternions a and b with their respective vector parts \mathbf{a} and \mathbf{b} , we have the following relation:

$$ab = a_0b_0 - \langle \mathbf{a}, \mathbf{b} \rangle_L + a_0\mathbf{b} + b_0\mathbf{a} + \mathbf{a} \times_L \mathbf{b}. \quad (4-16)$$

4-1-2 Relation with two-dimensional matrix algebra

In this section, we demonstrate how the split-quaternion algebra relates to the algebra of real 2×2 -matrices.

³Because the Lorentzian inner product fails to be positive definite, it is not strictly an inner product, but rather a *pseudo-inner product*. Likewise, the Lorentzian norm is called a *pseudonorm*.

Algebra isomorphisms

Formally, an algebra is a vector space combined V over a field \mathbb{F} , combined with an \mathbb{F} -bilinear product operation [48]:

- The split-quaternion algebra is an algebra over the field real numbers ($\mathbb{F} = \mathbb{R}$), where the multiplication is the split-quaternion multiplication (see Table 4-1);
- The 2×2 -matrices also form an \mathbb{R} -vector space; the product operation is matrix multiplication.

An *algebra isomorphism* is an isomorphism between vector spaces that also commutes with the respective product operations in both vector spaces. If (V, \bullet) and (W, \diamond) are vector spaces equipped with their respective product operations \bullet and \diamond , then $\phi : V \rightarrow W$ is an algebra isomorphism if [65]

- ϕ is a vector space isomorphism between V and W , and
- the isomorphism commutes with the product operation, i.e.

$$\phi(\mathbf{v}_1 \bullet \mathbf{v}_2) = \phi(\mathbf{v}_1) \diamond \phi(\mathbf{v}_2) \quad \mathbf{v}_1, \mathbf{v}_2 \in V. \quad (4-17)$$

In the case of the split-quaternions and two-dimensional matrices, it is sufficient to map the basis elements of the split-quaternions to four linearly independent ‘basis’ matrices, and show that the resulting matrices observe the same multiplication rules as defined in Table 4-1. Indeed, define the mapping ϕ by

$$\begin{aligned} \phi : \hat{\mathbb{H}} \rightarrow \mathbb{R}^{2 \times 2} : \quad 1 &\mapsto \begin{pmatrix} 1 & 0 \\ 0 & 1 \end{pmatrix} & \hat{\mathbf{i}} &\mapsto \begin{pmatrix} 0 & 1 \\ -1 & 0 \end{pmatrix} \\ \hat{\mathbf{j}} &\mapsto \begin{pmatrix} 0 & 1 \\ 1 & 0 \end{pmatrix} & \hat{\mathbf{k}} &\mapsto \begin{pmatrix} 1 & 0 \\ 0 & -1 \end{pmatrix} \end{aligned} \quad (4-18)$$

It is easily verified that (i) these matrices span $\mathbb{R}^{2 \times 2}$ and (ii) that the multiplication rules for split-quaternions are in accordance when mapped to the respective matrices under matrix multiplication. Due to the bilinearity of the product, any linear combination of the basis elements will therefore satisfy the rules as well. Hence, we have established an algebra isomorphism between the split-quaternions and the 2×2 -matrices.

Based on the mapping ϕ for the basis vectors, a general quaternion a maps to:

$$\phi(a_0 + a_1 \hat{\mathbf{i}} + a_2 \hat{\mathbf{j}} + a_3 \hat{\mathbf{k}}) = \begin{pmatrix} a_0 + a_3 & a_1 + a_2 \\ a_2 - a_1 & a_0 - a_3 \end{pmatrix}. \quad (4-19)$$

Likewise, the inverse mapping of an arbitrary matrix yields

$$\phi^{-1} \begin{pmatrix} b_0 & b_1 \\ b_2 & b_3 \end{pmatrix} = \frac{b_0 + b_3}{2} + \left(\frac{b_1 - b_2}{2} \right) \hat{\mathbf{i}} + \left(\frac{b_1 + b_2}{2} \right) \hat{\mathbf{j}} + \left(\frac{b_0 - b_3}{2} \right) \hat{\mathbf{k}}. \quad (4-20)$$

Relation between matrix and split-quaternion properties

A striking feature of the isomorphism ϕ is that it maps the natural properties of the split-quaternion to the natural properties of the associated matrix. Given that $A = \phi(a)$ with $a \in \hat{\mathbb{H}}$ and $A \in \mathbb{R}^{2 \times 2}$, we have the following correspondence:

- The *sum of matrices* is equivalent to the *sum of the split-quaternions*. If $A = \phi(a)$ and $B = \phi(b)$, then

$$A + B = \phi(a + b). \quad (4-21)$$

- *Matrix multiplication* is equivalent to *split-quaternion multiplication*. If $A = \phi(a)$ and $B = \phi(b)$, then

$$AB = \phi(ab). \quad (4-22)$$

- The *adjugate* of the matrix maps to the *conjugate* of the split-quaternion:⁴

$$\text{adj}(A) = \phi(a^*). \quad (4-23)$$

- The *trace* of the matrix coincides with twice the *real or scalar part* of the split-quaternion:

$$\frac{\text{tr}(A)}{2} = \text{sca}(a) = a_0. \quad (4-24)$$

- The *determinant* of the matrix is equal to the *squared total norm* of the split-quaternion:

$$\det(A) = \mathcal{N}(a). \quad (4-25)$$

- The equivalence of the determinant and the split-quaternion norm suggests that the *multiplicative inverse* of a split-quaternion does not always exist: it must be nonzero. In that case, it is clear that

$$\phi(a^{-1}) = A^{-1} \quad \mathcal{N}(a) \neq 0. \quad (4-26)$$

The determinant property also shows us what the regime of the product of two split-quaternions is; this is shown in Table 4-4.

Table 4-4: Regime transition under the action of split-quaternion multiplication. The timelike split-quaternions form a group under multiplication, the lightlike and spacelike split-quaternions do not: lightlike split-quaternions do not have an inverse and the spacelike split-quaternions are not closed.

\times	<i>space</i>	<i>light</i>	<i>time</i>
<i>space</i>	time	light	space
<i>light</i>	light	light	light
<i>time</i>	space	light	time

⁴The adjugate of a matrix is the transpose of its cofactor matrix [50].

- Importantly, the *eigenvalues* of a 2×2 -matrix A can be expressed in terms of its trace and its determinant:

$$\lambda_A = \frac{\text{tr}(A) \pm \sqrt{\text{tr}^2(A) - 4 \det(A)}}{2}. \quad (4-27)$$

The argument of the square root in the above expression is equal to the *negative of the squared vector norm* of a . We therefore have:

$$\lambda_A = \frac{2a_0 \pm \sqrt{4a_0^2 - 4\mathcal{N}(a)}}{2} = a_0 \pm i\|a\|, \quad (4-28)$$

where $\|a\|$ is imaginary if a is spacelike. Hence, the *real part and the vector norm the split-quaternion coincide with the real and imaginary parts of the eigenvalues of the matrix*, where the latter is multiplied by the imaginary unit i . When the vector either is spacelike or timelike, the i cancels, and the overall eigenvalue is real. This striking correspondence is the main reason for the benefits of the split-quaternion representation of dynamical systems, which is discussed in Section 4-2-2.

An overview of the correspondence between matrix and split-quaternion properties is given in Table 4-5.

Table 4-5: Overview of the correspondence between the algebra of split-quaternions and the algebra of 2×2 matrices, given that $A = \phi(a)$ and $B = \phi(b)$. In the top section, we compare matrices to split-quaternions, which means that they are related by the isomorphism ϕ . The bottom section compares scalar properties: these are numerically equal.

Matrix		Split-quaternion
Sum	$A + B$	$a + b$
Matrix product	AB	ab
Inverse	A^{-1}	a^{-1}
Adjugate	$\text{adj}(A)$	a^*
Determinant	$\det(A)$	$\mathcal{N}(a)$
Trace	$\frac{\text{tr}(A)}{2}$	a_0
Eigenvalues	λ_A	$a_0 + ai$
		Scalar part & vector norm

4-2 Dynamical systems as split-quaternions

In this section, we show how split-quaternions can be used to represent two-dimensional linear dynamical systems in their full generality. We commence in Section 4-2-1 by establishing the split-quaternion representation of a dynamical system. Subsequently, in Section 4-2-2 we show how the split-quaternion representation leads to a more convenient procedure for system classification. Finally, we exploit the split-quaternion properties to compute the solution of the corresponding dynamical system in Section 4-2-3.

4-2-1 The Lie algebra of vector fields

A linear dynamical system is specified by a linear vector field on a vector space. In our context, the vector space is \mathbb{R}^2 . Combined with the Lie bracket, these vector fields form a so-called *Lie algebra*. We demonstrate in this section how the Lie algebra of vector fields can be specified in terms of split-quaternions.

Lie algebras

The split-quaternions form an associative, noncommutative unital algebra over the real numbers, which is isomorphic (as an algebra) to the algebra of 2×2 -matrices. Every associative algebra can be turned into a *Lie algebra* by defining the *Lie bracket* as the *commutator* of the multiplication operator of the algebra⁵. For the split-quaternion algebra, the Lie bracket is defined as

$$[,] : \hat{\mathbb{H}} \times \hat{\mathbb{H}} \rightarrow \hat{\mathbb{H}} : [a, b] := ab - ba. \quad (4-29)$$

In analogous fashion, we have the equivalent definition for the matrix algebra:

$$[,] : \mathbb{R}^{2 \times 2} \times \mathbb{R}^{2 \times 2} \rightarrow \mathbb{R}^{2 \times 2} : [A, B] := AB - BA. \quad (4-30)$$

Clearly, these Lie algebras are isomorphic.

The Lie algebras defined above are abstract, which is to say that they are not defined in terms of a specific Lie group. The Lie algebra of 2×2 -matrices combined with the bracket defined above isomorphic to the Lie algebra $\mathfrak{gl}(2, \mathbb{R})$ (it is often even defined this way). These are the linear vector fields on a vector space: the vector field is a section of the tangent bundle, and the mapping that defines the section must preserve the linear structure of the vector space.

The algebra $\mathfrak{gl}(2, \mathbb{R})$ is the Lie algebra of the general linear group $GL(2, \mathbb{R})$, which is the group of all automorphisms of \mathbb{R}^2 (as a vector space). Hence, the elements of $GL(2, \mathbb{R})$ are the infinitesimal automorphisms of that vector space. From the vector field perspective, the Lie bracket of vector fields X and Y is equal the *Lie derivative* of X with respect to Y :

$$[X, Y] = \mathcal{L}_X Y. \quad (4-31)$$

If the bracket of X and Y vanishes, X and Y are said to *commute*. If two vector fields commute, then the associated transformations (i.e. elements of $GL(n, \mathbb{R})$) do so as well: it does not matter in which order the transformations are applied.

Basis vector fields

Because of the isomorphism between the Lie algebra of split-quaternions and $\mathfrak{gl}(2, \mathbb{R})$, the linear vector fields (i.e. linear dynamical systems) on \mathbb{R}^2 can be represented by a split-quaternion. Since the linear vector fields are directly represented by a matrix, it suffices to map that matrix to a split-quaternion using Equation (4-20). In particular, because we are dealing with a vector space (of vector fields) we can relate the split-quaternion basis elements each to a specific basis vector field. Any other linear vector field can then be constructed by taking linear combinations of these basis vector fields.

⁵By definition, the multiplication operation is bilinear, and the commutator is alternating. The associative property is needed for the Jacobi identity to be satisfied, which is the third criterion for a Lie algebra [66].

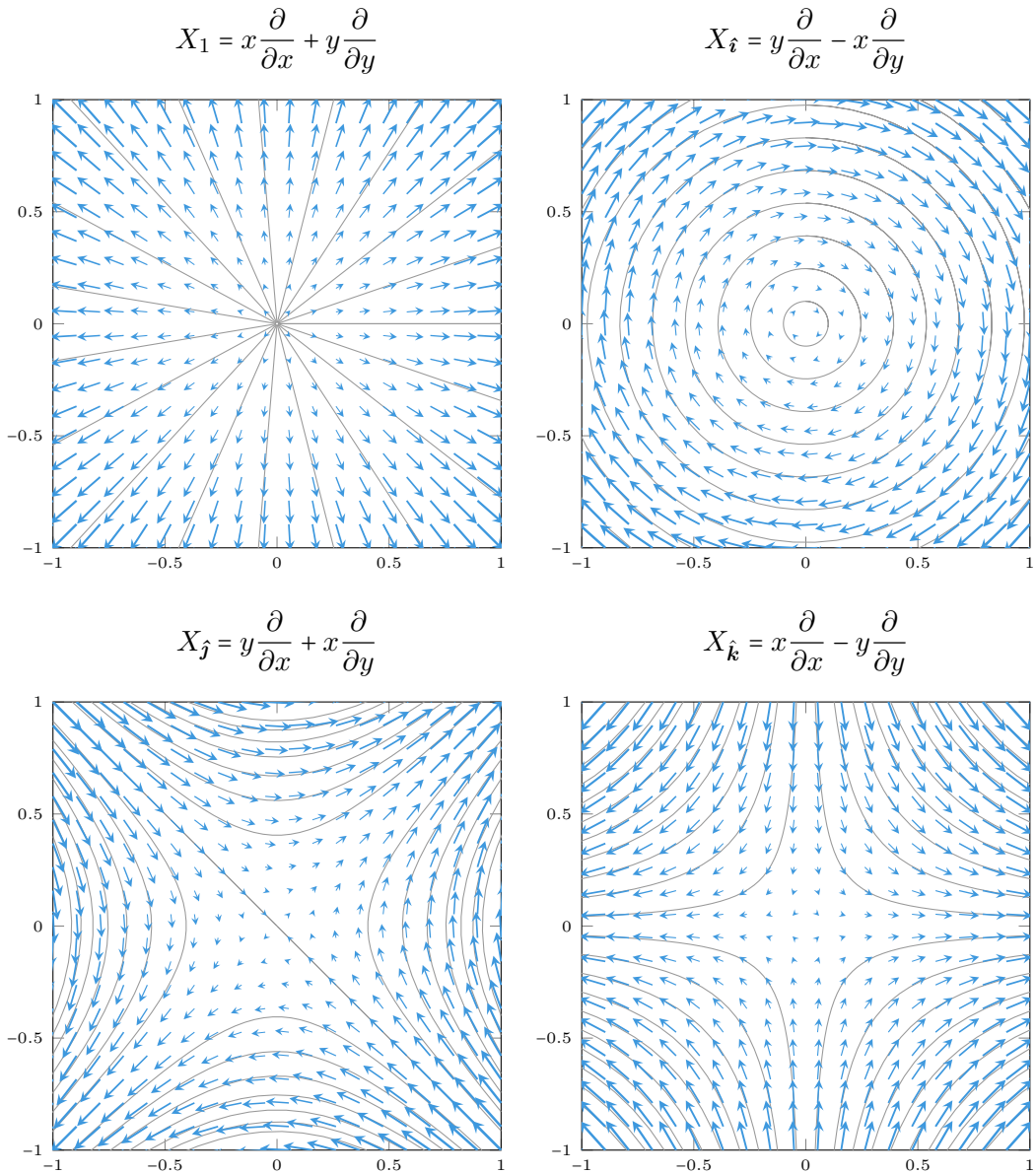


Figure 4-3: Basis vector fields corresponding to the basis elements of the split-quaternions.

The four basis vector fields and their integral curves are visualized in Figure 4-3.

- The identity element 1 corresponds to the identity matrix; the associated vector field X_1 is given by $X_1 = x \frac{\partial}{\partial x} + y \frac{\partial}{\partial y}$, where x and y are coordinates for \mathbb{R}^2 . These are *infinitesimal dilations* of the plane. The integral curves are star-shaped.
- The element \hat{i} corresponds to the vector field $X_{\hat{i}} = y \frac{\partial}{\partial x} - x \frac{\partial}{\partial y}$, which represents an *infinitesimal circular rotation* (clockwise). The integral curves are concentric circles centered at the origin.
- The element \hat{j} corresponds to the vector field $X_{\hat{j}} = y \frac{\partial}{\partial x} + x \frac{\partial}{\partial y}$, which represents an *infinitesimal squeeze mapping* or *infinitesimal hyperbolic rotations*. The integral curves

are rectangular hyperbolae, whose asymptotes are the lines specified by the equations $x = y$ and $x = -y$.

- Finally, $\hat{\mathbf{k}}$ corresponds to the vector field $X_{\hat{\mathbf{k}}} = x \frac{\partial}{\partial x} - y \frac{\partial}{\partial y}$. This vector field also represents an *infinitesimal squeeze mapping* or *hyperbolic rotation*, but the asymptotes of the hyperbolae are the x - and y -axis instead.

Volume-preserving vector fields Importantly, X_i , X_j and X_k are *volume-preserving transformations*: the vector fields are divergence-free. Any linear combination of these vector fields also preserves volume. Because the divergence of a linear vector field is equal to the trace of its matrix representation, these are all the matrices with *zero trace*. As a result, the vector part of a split-quaternion (or a split-quaternion with zero real part) represents the volume-preserving component of the vector field.

The volume-preserving linear transformations form a subgroup of $GL(2, \mathbb{R})$: this is the special linear group $SL(2, \mathbb{R})$. If represented as a matrix subgroup of $GL(2, \mathbb{R})$, $SL(2, \mathbb{R})$ consists of all the matrices with a determinant of 1. The associated algebra $\mathfrak{sl}(2, \mathbb{R})$ is isomorphic to the algebra of traceless matrices, or equivalently, the split-quaternions with no real part.

Because we are dealing with \mathbb{R}^2 , the conservation of volume is the same as conservation of *area* — this is manifestly *not* the case for higher dimensions. Indeed, the special linear group $SL(n, \mathbb{R})$ is isomorphic to the *symplectic group* $Sp(n)$ only if $n = 2$. The associated Lie algebra $\mathfrak{sp}(2)$ comprises the volume-preserving vector fields, which are also called *symplectic* or *Hamiltonian*⁶. The Hamiltonian function that generates each of these vector fields through the symplectic form $\omega = dx \wedge dy$ is simply equal to the implicit equation of the integral curves. An overview of the split-quaternion - vector field correspondence and the Hamiltonian functions (if applicable) is given in Table 4-6.

Table 4-6: Vector field representation of the split-quaternion basis elements. The Hamiltonian is the function that generates the associated vector field through Hamilton's equations: $\dot{x} = \frac{\partial H}{\partial y}$ and $\dot{y} = -\frac{\partial H}{\partial x}$.

$\hat{\mathbb{H}}$	$\mathbb{R}^{2 \times 2}$	Vector field	Hamiltonian	Transformation
1	$\begin{pmatrix} 1 & 0 \\ 0 & 1 \end{pmatrix}$	$x \frac{\partial}{\partial x} + y \frac{\partial}{\partial y}$	—	Dilation
\hat{i}	$\begin{pmatrix} 0 & 1 \\ -1 & 0 \end{pmatrix}$	$y \frac{\partial}{\partial x} - x \frac{\partial}{\partial y}$	$\frac{1}{2}(x^2 + y^2)$	Clockwise rotation
\hat{j}	$\begin{pmatrix} 0 & 1 \\ 1 & 0 \end{pmatrix}$	$y \frac{\partial}{\partial x} + x \frac{\partial}{\partial y}$	$\frac{1}{2}(y^2 - x^2)$	Squeeze mapping
\hat{k}	$\begin{pmatrix} 1 & 0 \\ 0 & -1 \end{pmatrix}$	$x \frac{\partial}{\partial x} - y \frac{\partial}{\partial y}$	xy	Squeeze mapping

⁶In general, every symplectic vector field is Hamiltonian, but not the other way around. As a consequence of the Poincaré Lemma (a special case of the de Rham cohomology) these notions are identical for contractible spaces. Clearly, \mathbb{R}^2 falls under this category.

Commuting vector fields The *center* of a Lie algebra consists of all those elements for which the Lie bracket operation produces zero, *regardless* of which other algebra element is the second argument. For $\mathfrak{gl}(2, \mathbb{R})$, these are all the scalar multiples of the identity, which are the split-quaternions that have *no vector part*. For this reason, the real part and vector part of the split-quaternion coincide with a natural decomposition of the associated vector field into a volume/area preserving component of the vector field, and the infinitesimal increase (or decrease) in volume. These components can be considered *independently* precisely because the associated transformations commute.

4-2-2 System classification with split-quaternions

In this section, we demonstrate how the properties of the split-quaternion representation can be exploited to classify the associated dynamical system in a convenient and exhaustive manner. In system theory, the classification of a linear dynamical system gives one an idea about the overall qualitative behavior of the system solution. Moreover, this practice is vital for the study of nonlinear systems too: the linearization of a nonlinear system around one of its fixed points replicates in many cases the correct behavior (cf. the Hartman-Grobmann theorem) [67]. This means that qualitative findings derived from the linearized system remain to be true — at least locally — for the nonlinear system as well.

Consider the linear dynamical system given by the differential equation

$$\dot{\mathbf{x}} = A\mathbf{x} \quad A \in \mathbb{R}^{2 \times 2}, \quad (4-32)$$

where A is the *state matrix*; we henceforth denote the associated split-quaternion by $a := \phi^{-1}(A)$. Usually, (the fixed point of) a linear dynamical system is classified based on the eigenvalues of A into one of several categories:

- saddle point,
- source or sink,
- spiral,
- center,
- ...

Other types of fixed points may arise when A has one or more zero eigenvalues. As will become clear, it are especially those degenerate cases which are handled remarkably well by the split-quaternion representation, i.e. without being considered exceptions to the rule.

The classification procedure using the split-quaternion representation makes use of three properties (cf. Section 4-1-2):

- (i) The regime of the squared total norm $\mathcal{N}(a)$, equal to the determinant of A ;
- (ii) The regime of the squared vector norm $\mathcal{N}(\mathbf{a})$, equal to the square of the imaginary part of the eigenvalues of A ;
- (iii) The regime of the real part a_0 , equal to half the trace of A .

The classic *Poincare diagram* can be restated in terms of split-quaternion properties, as shown in Figure 4-4. For the split-quaternion representation, this diagram classifies based on the

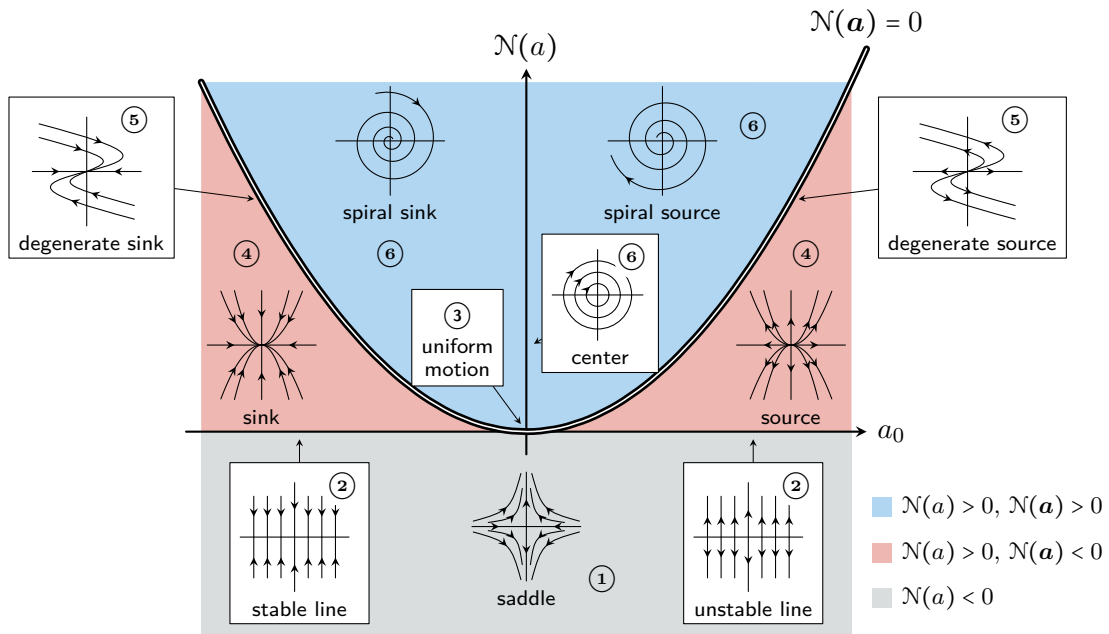


Figure 4-4: The split-quaternion Poincaré diagram is based on the regime combinations defined in Table 4-2. The determinant axis coincides with the squared norm of the split quaternion being 0. The parabolic double stroke line corresponds to the split-quaternions with zero vector norm. A further distinction is made with the scalar part of the split-quaternion, which, for each of the regimes, determines (asymptotic) (in)stability.

regime (i.e. sign) of both the total and vector norm, and the real part which determines stability in some cases.

However, this classification in Figure 4-4 not completely exhaustive, for it does not distinguish between the degenerate cases when $N(\mathbf{a}) = 0$. We will therefore discuss all the regime combinations listed in Table 4-2 and the corresponding class of dynamical systems in more detail; adhering to the same numbering scheme.

Spacelike total norm

- ① For spacelike split-quaternions, there is only one possibility: a negative split-quaternion norm corresponds to a negative determinant, which means that the fixed point is a *saddle point*. We can distinguish one particular case: if the scalar part of the split-quaternion is zero ($a_0 = 0$), the saddle is balanced and generates a proper *squeeze mapping*, which is a symplectomorphism of the phase space. The split-quaternion is therefore Hamiltonian. An example of the latter is the linearization of the unstable fixed point of a rotational pendulum.

Lightlike total norm

- ② *Spacelike vector norm*: in this case, there is not just a single fixed point but an entire fixed line in the phase space. This fixed line is stable or unstable depending on the sign of a_0 .

- ③ *Lightlike vector norm*: this case is degenerate to the second degree; it coincides with the origin in the Poincaré diagram. The associated vector field is purely translational. An example is an object in uniform motion.

Timelike total norm

- ④ *Spacelike vector norm*: this case gives rise to eigenvalues that are purely real; the fixed point is called a *node*. Depending on the sign of the scalar part, the fixed point can be an unstable node or *source* ($a_0 > 0$) or a stable node or *sink* ($a_0 < 0$). An example of such a system is the overdamped harmonic oscillator.
- ⑤ *Lightlike vector norm*: in this case, the two eigenvalues are equal to each other. This can be easily seen from Equation (4-28):

$$\lambda_A = a_0 \pm \|\mathbf{a}\|i = a_0 \quad a_0 \neq 0, \quad (4-33)$$

i.e. both eigenvalues are equal to the real part of a . From the perspective of the matrix, we have

$$\mathcal{N}(\mathbf{a}) = \det \left(A - \frac{\text{tr } A}{2} I \right). \quad (4-34)$$

If the squared vector norm vanishes, the null space of the matrix $A - a_0 I$ is

There are then two subcategories to be distinguished, corresponding to whether the associated matrix is diagonalizable or not:

- (a) If the matrix is diagonalizable, it *must* be a scalar multiple of the identity [68]. This is because the rank of the matrix $A - \lambda I$ must be equal to 0 for the eigenspace to be two-dimensional; $A - \lambda I$ i.e. the zero matrix. The corresponding split-quaternion is then *purely real*; i.e. $a = \lambda$. Because it has no vector part, the vector is then lightlike in the most trivial fashion. The associated fixed point is a *star*, which can either be stable or unstable depending on the sign of the real part (this particular case is not shown in Figure 4-4).
- (b) Conversely, if *the vector norm is zero but the vector part is not*, the matrix is not diagonalizable: the null space of $A - \lambda I$ is one-dimensional, and can therefore not be spanned by two independent eigenvectors. The fixed point is an *improper node*, which is again stable or unstable depending on the sign of the real part. An example of this type of system is the critically damped harmonic oscillator.
- ⑥ *Timelike vector norm*: this is the case where the eigenvalues of A are complex. If $a_0 = 0$, the eigenvalues are imaginary and the fixed point is a *center*. Again, for $a_0 > 0$ it is an *unstable spiral node* and for $a_0 < 0$ a *stable spiral node*. An example is an underdamped (or even undamped) harmonic oscillator.

It is clear from the present discussion that the split-quaternions offer a very natural representation of linear dynamical systems, in particular because of the relation between the split-quaternion norms and real part, and the eigenvalues of the state matrix. All six cases are again summarized in Table 4-7.

Table 4-7: Overview of the classification of fixed points based on the regime of the associated split-quaternion and its vector part.

#	$\mathcal{N}(a)$	$\mathcal{N}(\mathbf{a})$	Fixed point
①	spacelike	spacelike	Saddle
②	lightlike	spacelike	Line
③	lightlike	lightlike	Uniform motion
④	timelike	spacelike	Source / sink
⑤	timelike	lightlike	Degenerate node
⑥	timelike	timelike	Spiral node / center

4-2-3 The exponential function of split-quaternions

In order to obtain the system solution, one usually computes the matrix exponential of the state matrix A . In this section, we demonstrate that the same can be done for the split-quaternion representation, which has some computational advantages. The exponential function for split-quaternions is defined in an analogous fashion to its matrix equivalent, i.e. in terms of a Taylor-like series:

$$\exp : \hat{\mathbb{H}} \rightarrow \hat{\mathbb{H}} : \exp(a) := \sum_{k=0}^{\infty} \frac{a^k}{k!}. \quad (4-35)$$

Because this definition is completely analogous to the one for matrices, the exponentials in the split-quaternion domain or the matrix domain are equivalent, given the isomorphism ϕ defined by Equation (4-19):

$$\exp(a) = \phi^{-1}(\exp(\phi(a))). \quad (4-36)$$

In this expression, the first ‘exp’ refers to the split-quaternion exponential, while the second ‘exp’ is the matrix exponential.

To evaluate the exponential function of a split-quaternion, let us first use the following property of the (split-quaternion) exponential⁷ [69]

$$[a, b] = 0 \Rightarrow \exp(a + b), \quad (4-37)$$

i.e. we can only decompose the exponential of a sum if the two elements *commute*. We can regard an arbitrary split-quaternion

$$a = a_0 + a_1\hat{\mathbf{i}} + a_2\hat{\mathbf{j}} + a_3\hat{\mathbf{k}} \quad (4-38)$$

as the sum of the real part a_0 and the vector part $a_1\hat{\mathbf{i}} + a_2\hat{\mathbf{j}} + a_3\hat{\mathbf{k}}$. As discussed in Section 4-2-1, the real part is distinguished from the other three parts in the sense that it commutes with every other element. As a result, we have:

$$\exp(a) = e^{a_0} \exp(a_1\hat{\mathbf{i}} + a_2\hat{\mathbf{j}} + a_3\hat{\mathbf{k}}). \quad (4-39)$$

It is important to emphasize that this is *not* possible for the other individual vector components, since $\hat{\mathbf{i}}, \hat{\mathbf{j}}$ and $\hat{\mathbf{k}}$ do *not* commute with each other. We therefore only have to be

⁷This is a consequence of the Baker-Campbell-Haussdorff formula, which applies to Lie algebras in general.

considered with the evaluation of $\exp(\mathbf{a})$. To do so, recall that we can consider the vector part of a split-quaternion to be a split-quaternion in its own right, but with zero real part. We have by definition, that $\mathbf{a}^* = -\mathbf{a}$, which means that the squared vector norm is simply the negative of the square of the vector part, i.e.:

$$\mathcal{N}(\mathbf{a}) = \mathbf{a}\mathbf{a}^* = -\mathbf{a}^2. \quad (4-40)$$

Let us now introduce the concept of *unit split-quaternion vectors*, which are vector split-quaternions with a vector norm of ± 1 . The unit vector may be obtained by normalization of the vector part:

$$\hat{\mathbf{a}} = \frac{\mathbf{a}}{\sqrt{|\mathcal{N}(\mathbf{a})|}}, \quad \mathcal{N}(\mathbf{a}) \neq 0, \quad (4-41)$$

which squares to

$$\hat{\mathbf{a}}^2 = -\mathcal{N}(\hat{\mathbf{a}}) = -\frac{\mathcal{N}(\mathbf{a})}{|\mathcal{N}(\mathbf{a})|} = -\text{sgn}(\mathcal{N}(\mathbf{a})), \quad \mathcal{N}(\mathbf{a}) \neq 0. \quad (4-42)$$

Normalizing lightlike vectors is not possible, because they have all the same length of zero: there is no point in making the distinction between vector and unit vector.

Based on the regime of the vector part, three possibilities arise: [70, 71]

- If \mathbf{a} is timelike, then $\hat{\mathbf{a}}^2 = -1$. We can therefore say that the unit vector ‘behaves’ like the imaginary unit i ($i^2 = -1$). In general, we can identify the split-quaternion (with timelike vector part) $a_0 + \|\mathbf{a}\|\hat{\mathbf{a}}$ with the *complex number* $a_0 + \|\mathbf{a}\|i$.
- If \mathbf{a} is lightlike, then $\hat{\mathbf{a}}^2 = 0$, and the notion of the unit vector is not well-defined. Because the vector is nilpotent with degree 2, it is analogous to the nilpotent unit ε (for which we have that $\varepsilon^2 = 0$). Split-quaternions with timelike vector part can be identified with the *dual number* $a_0 + \varepsilon$.
- Finally, if \mathbf{a} is spacelike, then $\hat{\mathbf{a}}^2 = 1$. The unit vector behaves like the idempotent unit j , with defining property $j^2 = 1$ ($j \notin \mathbb{R}$).⁸ Likewise, a split-quaternion with spacelike vector part is analogous to the *split-complex number* (or hyperbolic number) $a_0 + \|\mathbf{a}\|j$.

The connection between split-quaternions and the generalized complex numbers⁹ (i.e. complex, dual and split-complex) sheds some additional light on the behavior of the eigenvalues of the associated matrix A by means of the root locus plot (see Equation (4-28)). A typical branch of the root locus consists of a complex pole pair approaching the real axis when the gain is increased. When they finally collide on the real axis, they each go their opposite ways on the real axis, essentially breaking the symmetry with respect to the real axis.

In contrast, the split-quaternions and their relation with hypercomplex numbers paint a slightly more elegant picture, which is shown in Figure 4-5:

⁸Again, we must take care not to confuse the hyperbolic unit with the split-quaternion basis element j . They behave the same and are related in the sense that they give rise to ‘split’ behavior, but are part of a very different number systems.

⁹For a more detailed account of generalized complex numbers, the reader is referred to Harkin and Harkin [71].

- As shown above, when the pole pair is complex, the associated split-quaternion vector is timelike. The eigenvalues are naturally conjugate with respect to the real axis, i.e.

$$\lambda_A = a_0 \pm \|\mathbf{a}\| \mathbf{i}. \quad (4-43)$$

- When the pole pair collides on the real axis (often called the *branch point*), the imaginary part of the eigenvalue is zero, and the vector is lightlike. Observe that we can make the case that, because the branches continue separately afterward, they cannot be *exactly* the same. Indeed, the eigenvalues are

$$\lambda_A = a_0 \pm \varepsilon. \quad (4-44)$$

The nilpotent unit ε is often interpreted as a differential, or an infinitesimally small quantity.¹⁰ We argue that, in this case, the pole pair is still conjugate, but the poles differ only by an infinitesimal amount.

- When the gain is increased even further, the poles are real and the symmetry with respect to the real axis is broken. However, we can infer from the preceding discussion that the imaginary part is now hyperbolic instead, i.e.

$$\lambda_A = a_0 \pm \|\mathbf{a}\| \mathbf{j}. \quad (4-45)$$

Of course, it is possible to project these points on the real axis, but this obscures the natural symmetry of the root locus branch. In Figure 4-5, we therefore place the hyperbolic part on a third axis.

Let us now return to the exponential function. We can manipulate the definition of $\exp(a)$ as follows:

$$\begin{aligned} \exp(a) &= e^{a_0} \left(\sum_{k=0}^{\infty} \frac{\mathbf{a}^k}{k!} \right) \\ &= e^{a_0} \left[\sum_{k=0}^{\infty} \frac{(\mathbf{a}^2)^k}{(2k)!} + \sum_{k=0}^{\infty} \frac{\mathbf{a}(\mathbf{a}^2)^k}{(2k+1)!} \right]. \end{aligned}$$

Furthermore, if \mathbf{a} is not lightlike, we have:

$$\exp(a) = e^{a_0} \left[\sum_{k=0}^{\infty} \frac{\|\mathbf{a}\|^{2k} (\hat{\mathbf{a}}^2)^k}{(2k)!} + \hat{\mathbf{a}} \sum_{k=0}^{\infty} \frac{\|\mathbf{a}\|^{2k+1} (\hat{\mathbf{a}}^2)^k}{(2k+1)!} \right].$$

Once again, there are three possibilities, depending on the regime of \mathbf{a} :

¹⁰A common application of dual numbers is automatic differentiation: because higher powers vanish, they can be used to generate first-order polynomial approximations. The unit ‘circle’ for dual numbers consists of two vertical lines crossing the horizontal axis at ± 1 . These lines can again be interpreted as linear approximations of the actual unit circle (or unit hyperbola) associated with (split-)complex numbers. The plane is spanned by the \mathbf{j} -axis and the real axis is the split-complex plane. The ‘projection’ to the real axis is in this plane a reflection with respect to the light cone (first diagonal).

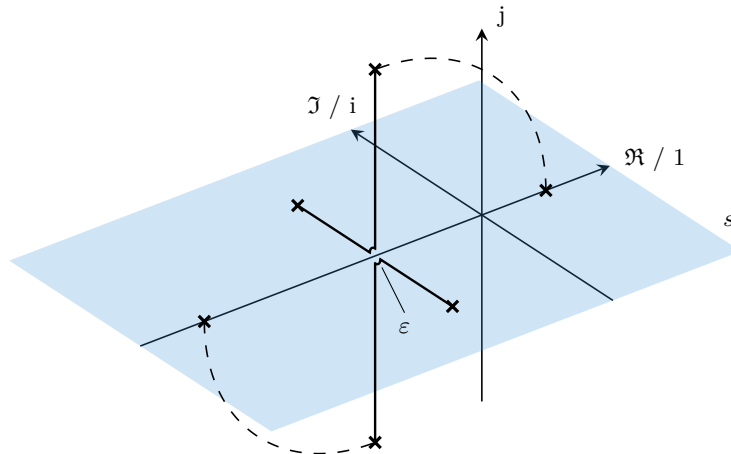


Figure 4-5: A generalized version of a root locus plot in terms of hypercomplex numbers. The traditional root locus is set in the complex s -plane (shown in blue), but we added a third axis for the hyperbolic part of the eigenvalue. When the gain is increased, the initially complex pole pair ventures towards the real axis. If the pole pair is critically damped, both poles are separated from the real axis by an infinitesimal distance of ε . Increasing the gain even more pushes the pole pair into the hyperbolic regime (the associated split-quaternion vector is now spacelike). Observe that in this picture, the symmetry with respect to the real axis is preserved. In the traditional root locus, these points are projected onto the real axis, indicated by the dashed lines.

- If \mathbf{a} is *timelike*, then the above expression reverts to

$$\begin{aligned} \exp(\mathbf{a}) &= e^{a_0} \left[\sum_{k=0}^{\infty} \frac{\|\mathbf{a}\|^{2k} (-1)^k}{(2k)!} + \hat{\mathbf{a}} \sum_{k=0}^{\infty} \frac{\|\mathbf{a}\|^{2k+1} (-1)^k}{(2k+1)!} \right], \\ &= e^{a_0} [\cos(\|\mathbf{a}\|) + \hat{\mathbf{a}} \sin(\|\mathbf{a}\|)]. \end{aligned} \quad (4-46)$$

This is roughly equivalent to the Euler identity for complex numbers.

- Secondly, if \mathbf{a} is *lightlike*, we can simply use the definition of the exponential in its original form:

$$\begin{aligned} \exp(\mathbf{a}) &= e^{a_0} \sum_{k=0}^{\infty} \frac{\mathbf{a}^k}{k!}, \\ &= e^{a_0} \left[1 + \mathbf{a} + \sum_{k=2}^{\infty} \frac{\mathbf{a}^{k-2} \mathbf{a}^2}{k!} \right], \\ &= e^{a_0} (1 + \mathbf{a}). \end{aligned} \quad (4-47)$$

- Finally, if \mathbf{a} is *spacelike*, we have

$$\begin{aligned} \exp(\mathbf{a}) &= e^{a_0} \left[\sum_{k=0}^{\infty} \frac{\|\mathbf{a}\|^{2k}}{(2k)!} + \hat{\mathbf{a}} \sum_{k=0}^{\infty} \frac{\|\mathbf{a}\|^{2k+1}}{(2k+1)!} \right], \\ &= e^{a_0} [\cosh(\|\mathbf{a}\|) + \hat{\mathbf{a}} \sinh(\|\mathbf{a}\|)]. \end{aligned} \quad (4-48)$$

The dynamical system given in Equation (4-32) has the following solution [72]

$$\mathbf{x}(t) = \exp(At)\mathbf{x}_0 = \phi(\exp(at))\mathbf{x}_0 \quad t \in \mathbb{R}^+, \quad (4-49)$$

where the exponential of at takes the following value:

$$\exp(at) = \begin{cases} e^{a_0 t} [\cos(\|\mathbf{a}\|t) + \hat{\mathbf{a}} \sin(\|\mathbf{a}\|t)] & \mathbf{a} \text{ timelike}, \\ e^{a_0 t} (1 + \|\mathbf{a}\|t) & \mathbf{a} \text{ lightlike}, \\ e^{a_0 t} [\cosh(\|\mathbf{a}\|t) + \hat{\mathbf{a}} \sinh(\|\mathbf{a}\|t)] & \mathbf{a} \text{ spacelike}. \end{cases} \quad (4-50)$$

Computing the split-quaternion exponential instead of the traditional matrix exponential avoids the need for either generalized eigenvectors (in the degenerate case) and/or complex eigenvectors, which arguably offers a computational advantage.

In the next section, we replace the general dynamical system by a mechanical system so as to give the split-quaternion representation a physical interpretation.

4-3 Application to mechanical systems

We will now proceed by using a mechanical prototype example instead of the generic dynamical system of the preceding section. This mechanical system is the harmonic oscillator with two dampers: one in series and one in parallel, as discussed in Section 3-2-5. The reason for this particular mechanical system is twofold: first, it helps to establish the connection between this chapter and Chapter 3, and second, it allows us to gain a physical intuition behind the split-quaternion representation.

Furthermore, the oscillator with two dampers is chosen because the corresponding state transition matrix the extra damper fills the one entry in the state matrix that would otherwise remain zero in the case of the conventional damped harmonic oscillator. Therefore, this system can represent (in theory) all the possible two-dimensional systems discussed in the previous section.

4-3-1 Equations of motion

The harmonic oscillator with two dampers is shown in Figure 3-8, and its equations of motion are given by Equation (3-109). In matrix form, the equations of motion are:

$$\begin{pmatrix} \dot{q} \\ \dot{p} \end{pmatrix} = \begin{pmatrix} -\frac{k}{b_s} & \frac{1}{m} \\ -k & -\frac{b_p}{m} \end{pmatrix} \begin{pmatrix} q \\ p \end{pmatrix}.$$

Alternatively, using the $\gamma_p := b_p/m$, $\gamma_s := k/b_s$, and $\Omega_n := \sqrt{k/m}$, we have the following:

$$\begin{pmatrix} \dot{q} \\ \dot{p} \end{pmatrix} = \underbrace{\begin{pmatrix} -\gamma_s & \frac{1}{m} \\ -m\Omega_n^2 & -\gamma_p \end{pmatrix}}_A \begin{pmatrix} q \\ p \end{pmatrix}. \quad (4-51)$$

Although the above matrix can represent all possible linear two-dimensional systems *in theory*, we will make some assumptions regarding the parameters in order to enforce that the system is indeed an actual oscillator:

- (i) The damping coefficients are larger than or equal to zero: $\lambda_s \geq 0, \lambda_p \geq 0$;
- (ii) The mass is strictly positive: $m > 0$;
- (iii) The spring constant is strictly positive: $k > 0$.

These assumptions imply that the determinant of the matrix given in Equation (4-51) is strictly larger than zero, which precludes the fixed point from being a saddle ①, an (un)stable line ② or uniform motion ③. Furthermore, because the damping is positive of zero, the system is stable in the sense of Lyapunov (i.e. the solutions are at least bounded).

The split-quaternion associated with the state matrix of the doubly damped system can easily be found using the mapping defined by Equation (4-20). We must, however, be careful when dealing with physical systems, because the entries of the A -matrix are not dimensionless.

In a vector space, units are associated with the basis vectors, not with the vector components. For example, consider a two-dimensional vector space spanned by an axis for apples and an axis for pears. If we wish to represent that someone possesses three apples and four pears, the *components* of that vector are $(3, 4)$, and the *unit vectors* are $(1 \text{ apple}, 1 \text{ pear})$.

Along the same line, we must define the units in the state matrix in the split-quaternion basis elements $1, \hat{\mathbf{i}}, \hat{\mathbf{j}}, \hat{\mathbf{k}}$. To do so, define the reference quantities and m_0, t_0 . The basis elements are then mapped in terms of these reference quantities:

$$\phi(1) = \begin{pmatrix} \frac{1}{t_0} & 0 \\ 0 & \frac{1}{t_0} \end{pmatrix}, \quad \phi(\hat{\mathbf{i}}) = \begin{pmatrix} 0 & \frac{1}{m_0} \\ -\frac{m_0}{t_0^2} & 0 \end{pmatrix}, \quad (4-52)$$

$$\phi(\hat{\mathbf{j}}) = \begin{pmatrix} 0 & \frac{1}{m_0} \\ \frac{m_0}{t_0^2} & 0 \end{pmatrix}, \quad \phi(\hat{\mathbf{k}}) = \begin{pmatrix} \frac{1}{t_0} & 0 \\ 0 & -\frac{1}{t_0} \end{pmatrix}. \quad (4-53)$$

If we would use SI units, $m_0 = 1 \text{ kg}$ and $t_0 = 1 \text{ s}$.

Using these reference quantities, the split-quaternion associated with the state matrix given in Equation (4-51) becomes

$$a = -\frac{1}{2}(t_0\gamma_s + t_0\gamma_p)1 + \frac{1}{2}\left(\frac{m_0}{m} + \frac{m\Omega_n^2 t_0^2}{m_0}\right)\hat{\mathbf{i}} + \frac{1}{2}\left(\frac{m_0}{m} + \frac{m\Omega_n^2 t_0^2}{m_0}\right)\hat{\mathbf{j}} + \frac{1}{2}(t_0\gamma_p - t_0\gamma_s)\hat{\mathbf{k}}. \quad (4-54)$$

Clearly, all the components of the split-quaternion are dimensionless. This really is not too wild of an idea: after all, the split-quaternion represents the matrix itself, and *not* the two-dimensional vector space that it acts on. The units are inherited from the vector space, so we should add them only when returning from the split-quaternions back to the realm of the matrices.

The preceding argument only explains why we can work around this issue without performing illegal operations, but it does not give a satisfactory answer as to why we would be interested to add numbers that are seemingly incompatible. Indeed, observe that γ_s and γ_p have the

same units, whereas $\frac{1}{m}$ and Ω_n^2 do not. So, in which sense can the $\hat{\mathbf{i}}$ and $\hat{\mathbf{j}}$ -components be of any significance? To answer this question, note that the rescaling of units is a linear transformation on the vector space given by a diagonal matrix (with nonzero diagonal entries):

$$N = \begin{pmatrix} \nu_1 & 0 \\ 0 & \nu_2 \end{pmatrix} \quad \nu_1, \nu_2 \in \mathbb{R}^*, \quad (4-55)$$

which form the group isomorphic to $(\mathbb{R}^*)^2$. This transformation of the vector space manifests itself on the A -matrix as

$$A' = N^{-1}AN. \quad (4-56)$$

It is easy to see that the basis matrices (or vector fields) for 1 and $\hat{\mathbf{k}}$ are invariant under this transformation, while the $\hat{\mathbf{i}}$ and $\hat{\mathbf{j}}$ -matrices are not (that is, without making use of the reference quantities).

A geometric explanation is that the eigenvectors of the identity matrix and the $\hat{\mathbf{k}}$ -matrix point along the axes; and are therefore invariant under rescaling of these axes. As a result of this fact, the $\hat{\mathbf{i}}$ and $\hat{\mathbf{j}}$ components will not transform properly under a unit transformation. For example, it is common practice in physics to rescale the state space of the undamped harmonic oscillator as follows [4, 73]

$$p \mapsto \frac{p}{m} \quad q \mapsto m\Omega q, \quad (4-57)$$

such that the Hamiltonian reverts to the standard quadratic form $\frac{1}{2}(q^2 + p^2)$. This is precisely the transformation that removes the $\hat{\mathbf{j}}$ -component of the split-quaternion. This would essentially resolve this unit problem, because it only arises when we attempt to make the *distinction* between the $\hat{\mathbf{i}}$ and $\hat{\mathbf{j}}$ -component. However, we are interested in the full range of geometrical properties that the trajectories in the phase plane can exhibit, including those that are not invariant under the action of the structure group $(\mathbb{R}^*)^2$.

As a final argument, we can say that the rescaling of the axes, while common in physics and mathematically allowed, is of little use for engineers, since they tend to stick to SI units in the first place. The scale of the axes is therefore a physical reality. This is why we choose not to discard the $\hat{\mathbf{j}}$ -component by rescaling.

To conclude, it is not so much the case that unit transformations are not allowed in the split-quaternion space, but the question as to what the units of the $\hat{\mathbf{j}}$ -components are is moot. Unfortunately, the notation in Equation (4-54) is rather obfuscating. Hence, we take the freedom to choose $m_0 = 1(\text{kg})$ and $t_0 = 1(\text{s})$, and write the split-quaternion as follows:

$$a = -\frac{1}{2}(\gamma_s + \gamma_p) + \frac{1}{2}\left(\frac{1}{m} + m\Omega_n^2\right)\hat{\mathbf{i}} + \frac{1}{2}\left(\frac{1}{m} - m\Omega_n^2\right)\hat{\mathbf{j}} + \frac{1}{2}(\gamma_p - \gamma_s)\hat{\mathbf{k}}. \quad (4-58)$$

Leaving out the reference quantities requires the silent understanding that all the components are dimensionless, and that we are not just adding apples and pears.

In the next section, we investigate the influence that each of the split-quaternion components has on the physical behavior of the mechanical system.

4-3-2 Physical interpretation of the split-quaternion representation

In this section, we look at various aspects of the split-quaternion representation and relate them to the physical properties of the oscillator described in the previous section.

Squared total norm

The squared total norm of the split-quaternion given in Equation (4-58) is equal to

$$\mathcal{N}(a) = m\Omega_n^2 + \gamma_p\gamma_s. \quad (4-59)$$

The assumptions made earlier regarding the sign of m, k, λ_s and λ_p ensure that this is a positive number; which is to say that the split-quaternion a as a whole is timelike.

The interpretation of the squared total norm is the parameter of the *effective potential energy* in the system. Indeed, when there is no damping, $\mathcal{N}(a)$ is equal to $m\Omega_n^2$, i.e. the spring constant of the oscillator. The second term appears only if both γ_p and γ_s are nonzero. This is because the presence of both dampers introduces a phase shift in the damping. Whereas the parallel damper dissipates in proportion the momentum p , the serial damper damps in proportion to the position q . Hence, their combined presence shifts the phase of the damping action in the cycle of the oscillator. The term $\gamma_p\gamma_s$ can be seen as a correction term to take into account this phase shift, if one were to express the equation entirely in terms of the position of the mass (cf. Equation (3-109)).

Real part

The real part of the split-quaternion representation of the harmonic oscillator with two dampers is (cf. Equation (4-58)),

$$a_0 = -\frac{1}{2}(\gamma_s + \gamma_p). \quad (4-60)$$

This real part therefore effect represents the *combined effect of both dampers*.

As can be observed from Equation (4-50) and Figure 4-3, the real part a_0 appears in the system solution as part of the argument of the exponential that envelopes the inner part of the solution, but it does not influence it in any other fashion. This is a consequence of the fact that the vector fields proportional to X_1 commute with all the other vector fields, as discussed in Section 4-2-1.

In the context of the mechanical system, this commuting of vector fields means that the overall transformation of the state-space that is generated by the vector field can be seen as the composition of two separate transformations.

The first is a purely exponential contraction of the phase space (assuming $\gamma_s, \gamma_p > 0$), which is the overall effect of the dampers. We call this transformation *nonconservative*, for it removes mechanical energy from the system.

Second, we have the remaining transformation that is generated by the combined effect of the vector part \mathbf{a} . The latter cannot be decomposed into separate $\hat{\mathbf{i}}$, $\hat{\mathbf{j}}$ and $\hat{\mathbf{k}}$ transformations, because the vector fields that generate them do not commute. The transformations generated by the vector part of a are *conservative* (in contrast to the exponential contraction): this decomposition of the transformations therefore amounts to separating the dissipative and conservative effects in present in the mechanical system. That is to say, we decompose the system solution into two parts:

$$\exp(at) = \underbrace{\exp(a_0t)}_{\text{dissipative}} \underbrace{\exp(\mathbf{a}t)}_{\text{conservative}}. \quad (4-61)$$

From the above expression, it can be seen that the dissipative component of the solution is rather simple: it is simply a contraction by $e^{a_0 t} = e^{-(\gamma_s + \gamma_p)t}$. This is why we will now focus exclusively on the nature of the second transformation, being the conservative part. From the split-quaternion point of view, this means that we assume that the real part vanishes, and only take the vector part into account.

Vector part

The vector part of a has three components. Based on the associated basis vector fields shown in Figure 4-3 and Equation (4-58), the following observations can be made

- The \hat{i} -component of the split-quaternion gives rise to a rotational vector field that is rotationally symmetric, since the solution trajectories are concentric circles. A positive component gives rise to a clockwise rotation. For the mechanical system, this component is equal to $\frac{1}{2}(\frac{1}{m} + m\Omega_n^2)$; it induces the *oscillatory* or *periodic motion* of the harmonic oscillator.
- The \hat{j} -component of the split-quaternion is a hyperbolic (saddle) vector field, its solution trajectories are hyperbolae whose asymptotes are the diagonals of the phase plane. For the mechanical system, this component is equal to $\frac{1}{2}(\frac{1}{m} - m\Omega_n^2)$: it measures the *imbalance between the two terms that constitute the rotation*. As a result, the combination of the \hat{i} and \hat{j} -components is an ellipse that is stretched or squeezed along its primary axes, but *not* rotated. The undamped harmonic oscillator is of this type.
- Finally, the \hat{k} -component is also a hyperbolic (saddle) vector field whose asymptotes are the horizontal and vertical axis. For the mechanical system, the \hat{k} -component is equal to the *imbalance between the two dampers*, i.e. $\frac{1}{2}(\gamma_p - \gamma_s)$. It also gives rise to a stretch and squeeze of the trajectory, but now along the diagonals of the phase plane. Therefore, it results in a *phase shift* or ‘wobble’ in the trajectory.

The influence of the vector components on the shape of the solution trajectories is visualized in Figure 4-6.

Squared vector norm The vector norm of a split-quaternion is equal to the imaginary part of the eigenvalues of the associated matrix. For the harmonic oscillator with two dampers represented by the split-quaternion in Equation (4-58), the squared vector norm is equal to

$$\mathcal{N}(a) = \Omega_n^2 - \frac{1}{4}(\gamma_s^2 + \gamma_p^2) + \frac{1}{2}\gamma_s\gamma_p = \Omega_n^2 - \left(\frac{1}{2}\gamma_s - \frac{1}{2}\gamma_p\right)^2. \quad (4-62)$$

Provided that the full system exhibits dissipation, i.e. $(\gamma_s + \gamma_p > 0)$, the sign of the squared vector norm determines the regime of the mechanical system:

- if $\mathcal{N}(a) > 0$ (timelike vector), the system is *underdamped* (or undamped);
- if $\mathcal{N}(a) = 0$ (lightlike vector), the system is *critically damped*;
- if $\mathcal{N}(a) < 0$ (spacelike vector), the system is *overdamped*.

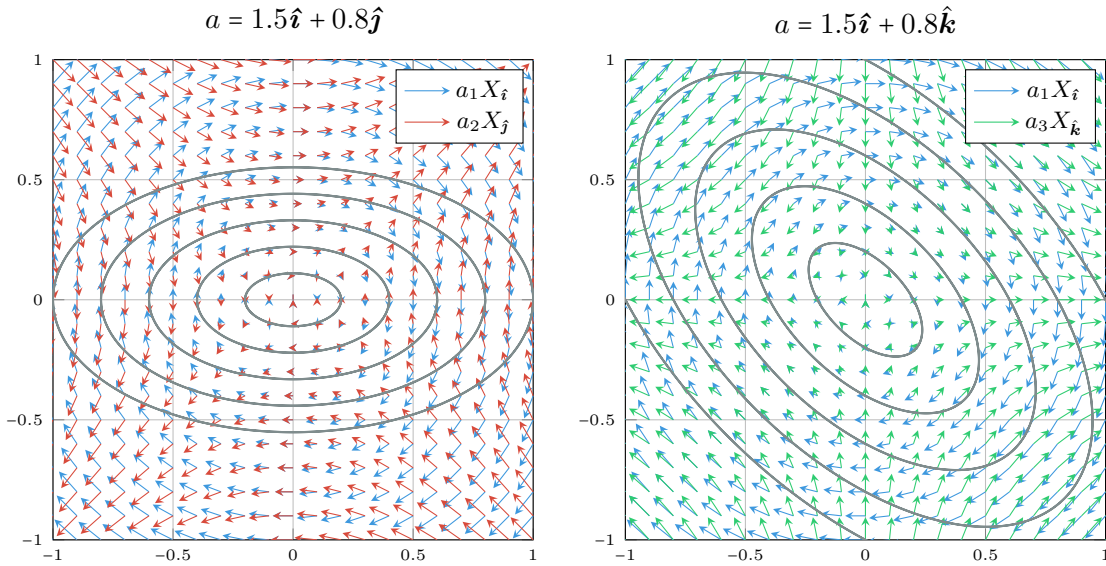


Figure 4-6: Comparison between the influence of the \hat{j} -component (left) and \hat{k} -component on the integral curves of $X_{\hat{i}}$. The \hat{j} component stretches the elliptic trajectory along the horizontal axis and squeezes it by the same amount in the vertical direction, while the \hat{k} component does the same but along axes that are rotated by 45 degrees. As shown by the figures, this is a consequence of the constructive or destructive interference of those vector fields in these particular directions.

This can also be explained in terms of the *damping ratio* ζ of the system. Recall that the eigenvalues of the matrix associated to the split quaternion are given by

$$\lambda_A = a_0 \pm \|\mathbf{a}\| \mathbf{i}. \quad (4-63)$$

The *damping ratio* is defined as

$$\zeta := \frac{\Re(\lambda_A)}{|\lambda_A|} = \frac{a_0}{\sqrt{a_0^2 + \mathcal{N}(\mathbf{a})}}. \quad (4-64)$$

Hence, if $\mathcal{N}(\mathbf{a})$ vanishes (provided that the system is indeed damped, so $a_0 \neq 0$), then $\zeta = 1$ and the system is critically damped. Likewise, if $\mathcal{N}(\mathbf{a}) > 0$, $\zeta < 1$, then the system is underdamped and vice versa.

More generally, one can see that the vector norm measures whether either the ‘circular’ \hat{i} -component is dominant, or otherwise the combination of \hat{j} and \hat{k} . In the former case, the solution trajectory is elliptic, while in the latter case it is hyperbolic.

Normalized vector part By looking only at the vector part of the split-quaternion in Equation (4-58), we have removed the real part from the eigenvalues of the associated matrix. The remaining vector part with the conservative component of the vector field. To show that the real part of the split-quaternion does not influence the eigenvectors of the matrix, observe that

$$(A - \lambda I)\mathbf{v} = [(A + sI) - (s + \lambda)I]\mathbf{v}. \quad (4-65)$$

This implies that adding any scalar multiple of the identity to the matrix adds this scalar to the value of all the eigenvalues, and leaves the eigenvectors unaltered. Since removing the

real part of the split-quaternion corresponds to subtracting a multiple of the identity from the associated matrix, we can see that this does not affect the eigenvectors.

Furthermore, if we normalize the vector part, the vector norm is taken out of the equation as well: since it is equal to the imaginary part of the eigenvalue, what remains are the *eigenvectors* (in alternative form) of the associated matrix.

As discussed in Section 4-1-1, the vector part of a split-quaternion lives in a three-dimensional Lorentzian space $\mathbb{R}^{1,2}$ with basis $(\hat{\mathbf{i}}, \hat{\mathbf{j}}, \hat{\mathbf{k}})$. Because the squared vector (Lorentzian) norm is indefinite, we can distinguish three possible normalizations (cf. Section 4-2-3):

- *timelike* vectors have a positive squared norm, and their normalized length is 1;
- *lightlike* vectors have a squared norm of zero, they cannot be normalized;
- *spacelike* vectors have a negative squared norm, their normalized length is -1.

These normalized (if not lightlike) vectors live on three disconnected subspaces of $\mathbb{R}^{1,2}$:

- If \mathbf{a} is *timelike*, its normalized vector $\hat{\mathbf{a}}$ lives on the *two-sheet unit hyperboloid*, which is the subspace defined as:

$$\{\mathbf{a} \in \mathbb{R}^3 \mid a_1^2 - a_2^2 - a_3^2 = 1\}. \quad (4-66)$$

This space consists of two separate sheets, referred to as the positive and negative sheet, depending on the sign of the $\hat{\mathbf{i}}$ -component.

- If \mathbf{a} is *lightlike*, it cannot be normalized: it lives on the *light cone*, which is defined as:

$$\{\mathbf{a} \in \mathbb{R}^3 \mid a_1^2 - a_2^2 - a_3^2 = 0\}. \quad (4-67)$$

- If \mathbf{a} is *spacelike*, its normalized vector $\hat{\mathbf{a}}$ lives on the *one-sheet unit hyperboloid*, which is defined as:

$$\{\mathbf{a} \in \mathbb{R}^3 \mid a_1^2 - a_2^2 - a_3^2 = -1\}. \quad (4-68)$$

These three subspaces are visualized in Figure 4-7.

Because the vector norm determines the regime of the damped mechanical system, we can state that the two-sheet hyperboloid contains all the normalized underdamped systems, the light cone contains all the critically damped systems and the one-sheet hyperboloid contains all the normalized overdamped systems.

In the next section, we analyze the significance of the normalized vector part in greater detail for the case of an underdamped system.

4-3-3 Geometric analysis of underdamped systems

In this section, the normalized vector part $\hat{\mathbf{a}}$ is related to the specific shape of the integral curves of the dynamical system. The discussion is limited to underdamped systems, i.e. systems for which the split-quaternion vector part is timelike. For these systems, the trajectories are spiral-shaped. Removing the real part from the split-quaternion eliminates the exponential contraction in the spiral. As a result, the conservative version of this trajectory is an

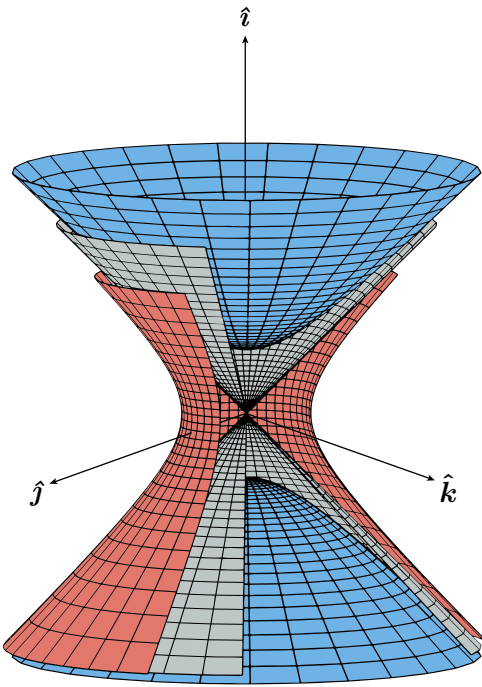


Figure 4-7: The disconnected ‘unit sphere’ in the Lorentzian 3-space. The red surface is the one-sheet hyperboloid, containing all the spacelike unit vectors, or overdamped systems. The gray sheet is the light cone, that contains all the lightlike ‘null’ vectors with zero norm, or critically damped systems. Finally, the two blue surfaces constitute the two-sheet hyperboloid, or underdamped systems.

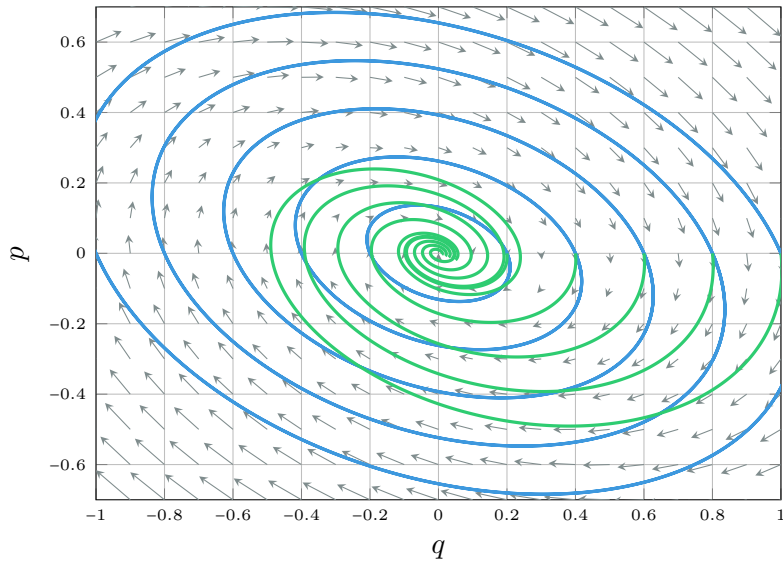


Figure 4-8: Solution trajectories and vector field of an exemplary underdamped system. The green trajectories are the actual solution of the system, while the blue trajectories are the convergent version, i.e. with the real part of the split-quaternion removed.

elliptic trajectory. This ellipse is subject to the same stretch and tilt of the original spiral, as illustrated by Figure 4-8.

For underdamped systems, the eigenvectors are complex. This obscures the direct geometric implications of the eigenvectors on the integral curves, in contrast to other types of fixed points for which the eigenvectors are real (e.g. saddle points or nodes). Within the set of complex eigenvectors (all a complex multiple of each other), there is one specific set for which the real and imaginary part of the eigenvectors are orthogonal. In that particular case, the real and imaginary part of the eigenvectors coincide with the principal axes of the elliptic integral curves. Hence, one must first find the right set of eigenvectors in order to gain insights regarding shape of the integral curves [68].

We argue that the split-quaternion representation, specifically its normalized vector part, offers a more efficient way to extract the geometric information about the integral curves — in particular when the eigenvectors are complex.

For an underdamped system, the normalized vector is given by

$$\hat{\mathbf{a}} = \underbrace{\left(\frac{\frac{1}{m} + m\Omega_n^2}{2\Omega_d} \right) \hat{\mathbf{i}}}_{\hat{a}_1} + \underbrace{\left(\frac{\frac{1}{m} - m\Omega_n^2}{2\Omega_d} \right) \hat{\mathbf{j}}}_{\hat{a}_2} + \underbrace{\left(\frac{\gamma_p - \gamma_s}{2\Omega_d} \right) \hat{\mathbf{k}}}_{\hat{a}_3}. \quad (4-69)$$

Here, Ω_d is the *damped frequency* of the oscillator, which is equal to the vector norm:

$$\Omega_d = \|\mathbf{a}\| = \sqrt{\Omega_n^2 - \left(\frac{1}{2}\gamma_s - \frac{1}{2}\gamma_p \right)^2}. \quad (4-70)$$

Instead of the Cartesian coordinates for the normalized vector part used in Equation (4-69), we will adopt a more parsimonious description in the form of the so-called *pseudospherical coordinates*. These consist of a *hyperbolic angle* τ and a Euclidean angle σ , which specify a point on either one of the sheets of the two-sheet hyperboloid shown in Figure 4-7. The pseudospherical coordinates are related to the Cartesian coordinates through the following relations:

$$\hat{a}_1 = \pm \cosh(\tau) \quad \hat{a}_2 = \sinh(\tau) \cos(\sigma) \quad \hat{a}_3 = \sinh(\tau) \sin(\sigma). \quad (4-71)$$

In addition, we have:

$$\begin{aligned} \cosh(\tau) &= \hat{a}_1, & \sinh(\tau) &= \sqrt{\hat{a}_2^2 + \hat{a}_3^2}, \\ \cos(\sigma) &= \frac{\hat{a}_2}{\sqrt{\hat{a}_2^2 + \hat{a}_3^2}}, & \sin(\sigma) &= \frac{\hat{a}_3}{\sqrt{\hat{a}_2^2 + \hat{a}_3^2}}. \end{aligned} \quad (4-72)$$

The geometry of an elliptic trajectory is determined by its *aspect ratio* and its *tilt angle*, as shown in Figure 4-9. For the aspect ratio many measures exist, of which the *eccentricity* e is the best known. The other measures are listed in Table 4-8; especially the third flattening and third eccentricity play an important role in the remainder of the discussion.

To relate the normalized vector part (in pseudospherical coordinates) to the geometric features of the elliptic integral curves, the solution trajectories of the basis vector fields given by Table 4-6 can be weighed by the vector components to obtain the overall implicit form of the elliptic trajectories.

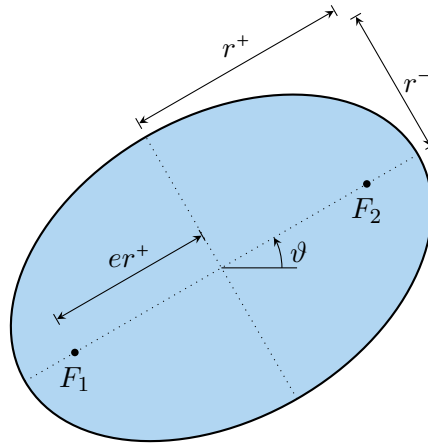


Figure 4-9: Geometric parameters of the ellipse. Its shape is characterized by two lengths: the semi-major axis r_+ and the semi-minor axis r_- . The various measures of the aspect ratio of the ellipse given in Table 4-8 express the relative size of r_+ with respect to r_- in various ways. The (first) eccentricity e parameter locates the focal points F_1, F_2 as a proportion of the semi-major axis. The angle ϑ by which the semi-major axis is rotated with respect to the horizontal is called the *tilt*.

For X_i , the solution curves have the implicit form

$$\frac{1}{2}(q^2 + p^2) = \text{cst}, \quad (4-73)$$

i.e. they are concentric circles of some radius. Second, for X_j , we have the implicit form

$$\frac{1}{2}(p^2 - q^2) = \text{cst}. \quad (4-74)$$

Thirdly, for X_k , the solution trajectories are of the form

$$pq = \text{cst}. \quad (4-75)$$

From the above expression we can find the shape of the actual solution trajectory by weighing each of these curves with the respective components of the normalized vector part:

$$\underbrace{(\hat{a}_1 - \hat{a}_2)}_{:=R} q^2 + \underbrace{2\hat{a}_3}_{:=S} pq + \underbrace{(\hat{a}_1 + \hat{a}_2)}_{:=T} p^2 = \text{cst}. \quad (4-76)$$

The actual radius of the trajectory is immaterial for the discussion, for it depends on the initial condition chosen for the system and does not influence the shape of the ellipse. The above expression is the implicit equation for an ellipse if [74]

$$S^2 - 4RT < 0. \quad (4-77)$$

Substitution shows that this condition is equivalent to a being timelike.

Table 4-8: Commonly used parameters to measure the eccentricity (or alternatively, the flattening) of an ellipse in terms of its semi-major axis r_+ and semi-minor axis r_- [74].

Parameter	Notation	Formula
Semi-major axis	r^+	—
Semi-minor axis	r^-	—
(First) eccentricity	e	$\frac{r_+^2 - r_-^2}{r_+^2}$
Second eccentricity	e'	$\frac{r_+^2 - r_-^2}{r_-^2}$
Third eccentricity	e''	$\frac{r_+^2 - r_-^2}{r_+^2 + r_-^2}$
(First) flattening	f	$\frac{r_+ - r_-}{r_+}$
Second flattening	f'	$\frac{r_+ - r_-}{r_-}$
Third flattening	f''	$\frac{r_+ - r_-}{r_+ + r_-}$

Eccentricity

The eccentricity of the ellipse specified by Equation (4-76) in terms of the parameters R , S and T is equal to [74]

$$e = \sqrt{\frac{2\sqrt{(R-T)^2 + S^2}}{(R+T) + \sqrt{(R-T)^2 + S^2}}} \quad (4-78)$$

Since we have that $R-T = -2\hat{a}_2$, $R+T = 2\hat{a}_1$ and $S = 2\hat{a}_3$, the eccentricity may be expressed as a function of the components of the split-quaternion too:

$$e = \sqrt{\frac{2\sqrt{\hat{a}_2^2 + \hat{a}_3^2}}{q_1 + \sqrt{\hat{a}_2^2 + \hat{a}_3^2}}} \quad (4-79)$$

Finally, using the relations stated in Equation (4-72), this expression can be succinctly written in terms of the pseudospherical coordinates τ and σ :

$$e = \sqrt{\frac{2\sinh(\tau)}{\cosh(\tau) + \sinh(\tau)}} \quad (4-80)$$

Tilt angle

The tilt angle ϑ of the ellipse is defined as the angle between the positive horizontal q -axis and the major axis of the ellipse. Just like the eccentricity, we start from the general expression

in terms of the parameters R, T and S :

$$\tan(\vartheta) = \frac{T - R - \sqrt{(R - T)^2 + S^2}}{S}. \quad (4-81)$$

Again, substituting the split-quaternion components, we have

$$\tan(\vartheta) = \frac{\hat{a}_2 - \sqrt{\hat{a}_2^2 + \hat{a}_3^2}}{\hat{a}_3}. \quad (4-82)$$

Rather unsurprisingly, the \hat{i} -component does not play a role in the tilt angle of the trajectory: from Figure 4-3, we can see that the associated vector field $X_{\hat{i}}$ is indeed rotationally symmetric, in contrast to $X_{\hat{j}}$ or $X_{\hat{k}}$.

Equation (4-82) may be expressed in terms of the pseudospherical coordinates (cf. Equation (4-72)) as well:

$$\tan(\vartheta) = \frac{\cos(\sigma) - 1}{\sin(\sigma)} = -\tan\left(\frac{\sigma}{2}\right). \quad (4-83)$$

Hence, we obtain that the *tilt angle is equal to half the pseudospherical angle, oppositely oriented*:

$$\vartheta = -\frac{\sigma}{2}. \quad (4-84)$$

Orientation

The two-sheet hyperboloid consists of two disconnected surfaces; this begs the question what the significance is of either of those surfaces. The hyperboloids are directed along the \hat{i} -axis; therefore, the sign of the \hat{i} -component of a determines on which hyperboloid the vector is located. Physically, the sign of the \hat{i} -component determines whether the rotational part of the vector field has a clockwise or counterclockwise rotation. By default, $X_{\hat{i}}$ is an infinitesimal clockwise rotation (cf. Figure 4-3): as a result, if a_0 is positive the rotation is clockwise and vice versa.

The obtained relations show that the pseudospherical coordinates σ and τ are directly related to respectively the tilt angle and the eccentricity of the elliptic trajectories. We will now investigate the role of these coordinates in two common projections of the two-sheet hyperboloid, being the *Poincaré model* and the *Cayley-Klein model*. As it turns out, the coordinates in these projections correspond with the eccentricity parameters defined Table 4-8.

Relation with models of the hyperbolic plane

The *hyperbolic plane* is a plane that has everywhere a constant negative Gaussian curvature. The geometry of the hyperbolic plane is known as *hyperbolic geometry*, as opposed to *Euclidean geometry* and *spherical geometry*, which are associated with surfaces of no curvature and constant positive curvature respectively.

In contrast to the Euclidean plane and the sphere (which exhibits spherical geometry), the hyperbolic plane cannot be isometrically embedded in three-dimensional space; this is formalized in Hilbert's theorem on differential geometry [75]. This is why mathematicians must

resort to so-called *models* of the hyperbolic plane. Many are in existence, for example the hyperboloid model, the Poincaré disk, the Cayley-Klein disk, and the Poincaré half-plane. The former three will be of our interest in this context. For more information concerning hyperbolic geometry, the reader is referred to Needham [76, 77] and Thurston [75].

Hyperboloid model The *hyperboloid model* consists simply of the positive sheet of the two-sheet hyperboloid, embedded in the Lorentzian 3-space. In this space, this sheet of the hyperboloid has a constant negative Gaussian curvature equal to -1 [78]. Because of this constant negative curvature, the positive sheet of the two-sheet hyperboloid can serve as a model for the hyperbolic plane.

Both the Poincaré disk and the Cayley-Klein disk arise by projecting the hyperboloid surface to a disk with unit radius in a particular fashion. In the \hat{i} - \hat{j} -plane, these projections are illustrated in Figure 4-10.

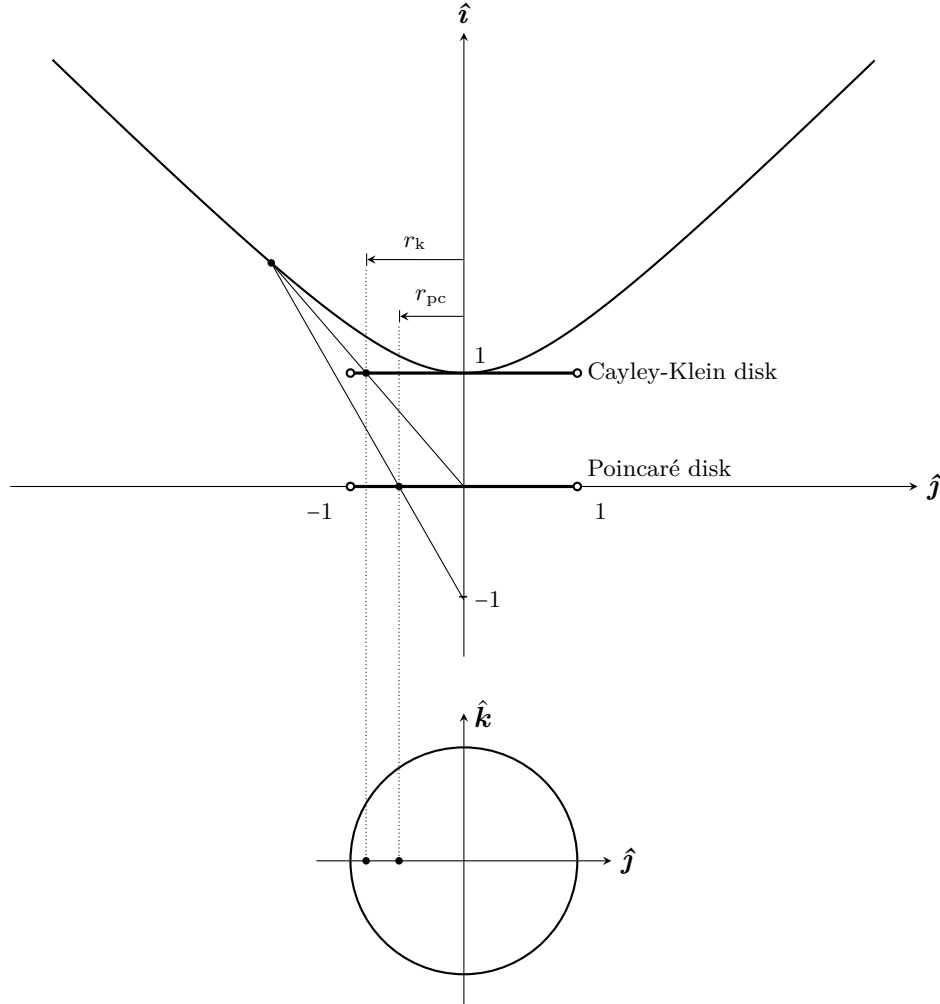


Figure 4-10: Illustration of the projection on the Poincaré disk and the Cayley-Klein disk. The Lorentzian 3-space is intersected along the \hat{i} - \hat{j} -plane; both disks therefore appear as a line segment with radius 1.

The Cayley-Klein disk The Cayley-Klein is the result of *gnomonic projection* of the positive hyperboloid sheet. The advantage of gnomonic projection is that geodesics on the hyperboloid map to straight lines in the disk. On the downside, this projection method is not conformal (it does not preserve angles). As shown in Figure 4-10 and Figure 4-11, the projection of a point on the hyperboloid is the intersection of the line segment of that point with the origin and the disk with unit radius, centered at the point \hat{i} (i.e. the point in Lorentzian 3-space with coordinates $(1, 0, 0)$).

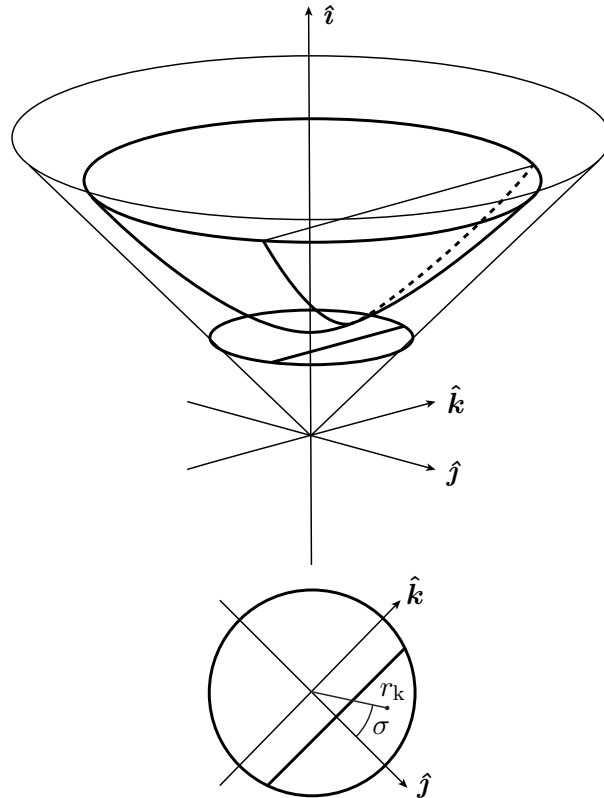


Figure 4-11: The Cayley-Klein disk and the hyperboloid model are related through gnomonic projection. A geodesic of on the hyperboloid model is shown as well, its projected image in the Cayley-Klein disk (also a geodesic) is a straight line. Illustration adapted from Balazs and Voros [78].

If polar coordinates are used to specify a point in the Cayley-Klein disk, the rotation angle σ remains identical to the corresponding pseudospherical coordinate, and from Figure 4-10 it can readily be deduced that the radial coordinate $r_k \in [0, 1]$ is simply equal to

$$r_k = \tanh(\tau). \quad (4-85)$$

We can now use Equation (4-80) to relate the radial coordinate to the eccentricity of the elliptic trajectory (the angular coordinate remains again identical):

$$e = \sqrt{\frac{2 \sinh(\tau)}{\cosh(\tau) + \sinh(\tau)}} = \sqrt{\frac{2r_k}{1 + r_k}}. \quad (4-86)$$

This expression shows that the *radius in the Cayley-Klein disk is equal to the square of the third eccentricity of the elliptic trajectory e''* , also denoted by ‘ m ’ in literature (we will not do so here, for it is already reserved for mass). In terms of the major and minor axes (r_+ and r_- respectively), this we have: [74]

$$r_p = \frac{r_+^2 - r_-^2}{r_+^2 + r_-^2} = (e'')^2. \quad (4-87)$$

The Poincaré disk The *Poincaré disk* is the image of the positive hyperboloid sheet under *stereographic projection* with respect to the point $-\hat{\mathbf{i}}$, i.e. the point in Lorentzian 3-space with coordinates $(-1, 0, 0)$. That is to say, the projection of a point on the hyperboloid on the Poincaré disk is equal to the intersection of the line segment connecting that point with $-\hat{\mathbf{i}}$ and the unit disk centered at the origin. This is illustrated in Figures 4-10 and 4-12.

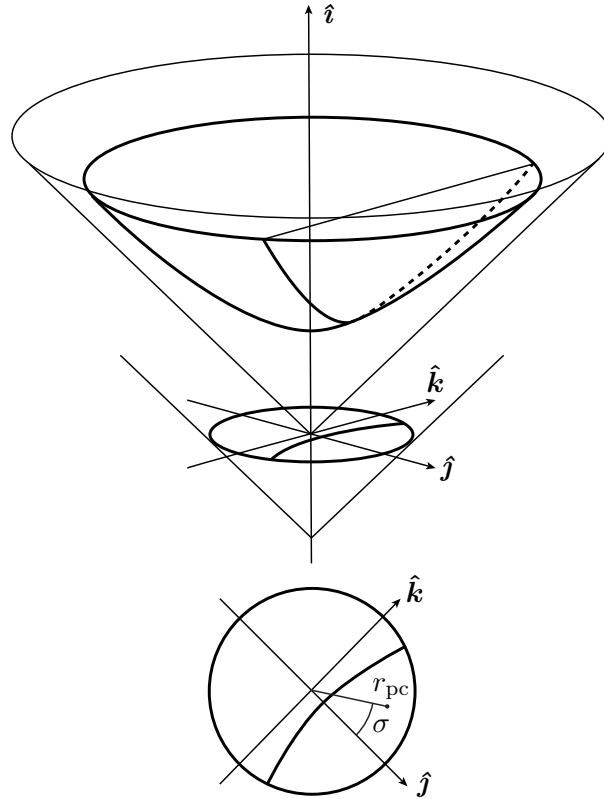


Figure 4-12: The Poincaré disk and the hyperboloid model are related through stereographic projection. A geodesic on the hyperboloid model is shown as well, its projected image in the Poincaré disk (also a geodesic) is part of a circle that intersects the boundary of the disk at right angles. Illustration adapted from Balazs and Voros [78].

If polar coordinates are used in the Poincaré disk, then the Euclidean rotation remains identical, and the radial coordinate is equal to

$$r_{pc} = \tanh\left(\frac{\tau}{2}\right) = \frac{\sinh(\tau)}{1 + \cosh(\tau)}. \quad (4-88)$$

Because stereographic projection projects each point on the positive hyperboloid uniquely onto the Poincaré disk, every point on the disk corresponds to two possible elliptic trajectories: one with clockwise and one with counterclockwise rotation.

As stated by Equation (4-87), the Cayley-Klein radius is equal to the square of the third eccentricity. Along the same line, the radius in the Poincaré disk may be related to a specific measure of elliptic eccentricity as well. Using the double angle formula for \tanh , we have that

$$r_k = \frac{2r_{pc}}{1 + r_{pc}^2}. \quad (4-89)$$

Hence, we gather that the *Poincaré radius is equal to the third flattening of the elliptic trajectory*, commonly denoted by n or f'' . In terms of the major and minor axes of the elliptic trajectory, the Poincaré radius is equal to

$$r_{pc} = \frac{r_+ - r_-}{r_+ + r_-} = f''. \quad (4-90)$$

Relation with eigenvectors

As mentioned, the normalized vector part a encodes the same information as the eigenvectors of the associated matrix A . For an underdamped system, both the eigenvectors and the eigenvalues of the matrix are complex. These complex eigenvectors are not directly interpretable; they can be multiplied by any complex number to obtain another eigenvector of the system. In one particular instance (i.e. a specific length in \mathbb{C}^2), the real and imaginary part of the eigenvectors align with the major and minor axes (r^+, r^-) of the elliptic trajectory, but this requires additional computation to find the correct multiplication factor for the eigenvectors [68].

Conversely, as demonstrated in the above discussion, the normalized split-quaternions are naturally parameterized in way that corresponds directly to the shape parameters of the solution trajectories. As vectors in the phase plane, the semi-major and semi-minor axes can be expressed in terms of σ and τ as follows (where the semi-major axis has length 1):

$$\begin{aligned} \mathbf{r}^+ &= \begin{pmatrix} \cos\left(\frac{\sigma}{2}\right) & \sin\left(\frac{\sigma}{2}\right) \\ -\sin\left(\frac{\sigma}{2}\right) & \cos\left(\frac{\sigma}{2}\right) \end{pmatrix} \begin{pmatrix} 1 \\ 0 \end{pmatrix} \\ \mathbf{r}^- &= \begin{pmatrix} \cos\left(\frac{\sigma}{2}\right) & \sin\left(\frac{\sigma}{2}\right) \\ -\sin\left(\frac{\sigma}{2}\right) & \cos\left(\frac{\sigma}{2}\right) \end{pmatrix} \begin{pmatrix} 0 \\ \frac{1-\tanh\left(\frac{\tau}{2}\right)}{1+\tanh\left(\frac{\tau}{2}\right)} \end{pmatrix}, \end{aligned} \quad (4-91)$$

$$\text{since } \frac{r^-}{r^+} = \frac{1-f''}{1+f''}.$$

The Lorentzian cross-product

Finally, we relate the action of the conservative part of the state matrix on the phase plane to the action of vector part \mathbf{a} of the associated split-quaternion through the Lorentzian cross-product, defined in Equation (4-15).

First, we define the notion of *Lorentz orthogonality* based on the Lorentzian inner product (cf. Equation (4-12)): two vectors are Lorentz-orthogonal if their Lorentzian inner product is equal to zero. In an analogous fashion to the conventional cross product, the Lorentz cross product of two vectors is Lorentz orthogonal to both of those vectors.

Given that \mathbf{a} is the vector part of the split-quaternion representation of the state-transition matrix A , we wish to relate the vector field generated by A to the vector field generated by \mathbf{a} as ‘operator’: $\mathbf{a}_{\times_L}(\mathbf{b}) := \mathbf{a} \times_L \mathbf{b}$. The operator \mathbf{a}_{\times_L} has an invariant linear subspace: the plane that is Lorentz-orthogonal to the vector \mathbf{a} . This is visualized in Figure 4-13. Expressing \mathbf{a}_{\times_L} as a matrix, we get:

$$[\mathbf{a}_{\times_L}](\mathbf{b}) = \begin{pmatrix} 0 & a_3 & -a_2 \\ a_3 & 0 & -a_1 \\ -a_2 & a_1 & 0 \end{pmatrix} \begin{pmatrix} b_1 \\ b_2 \\ b_3 \end{pmatrix}. \quad (4-92)$$

The eigenvalues of $[\mathbf{a}_{\times_L}]$ are $\{0, \pm i\sqrt{a_1^2 - a_2^2 - a_3^2}\}$, i.e. the imaginary part of the eigenvalues is the same as the imaginary part of the eigenvalues of A (or the eigenvalues of A with trace removed), with the addition of zero. The zero direction is colinear with the vector \mathbf{a} . This means that in the Lorentz orthogonal plane, the action of $[\mathbf{a}_{\times_L}]$ is the same as the action of $A - \frac{\text{tr}(A)}{2}I$ (the associated matrix with trace removed) on the phase plane, *given the right basis*.

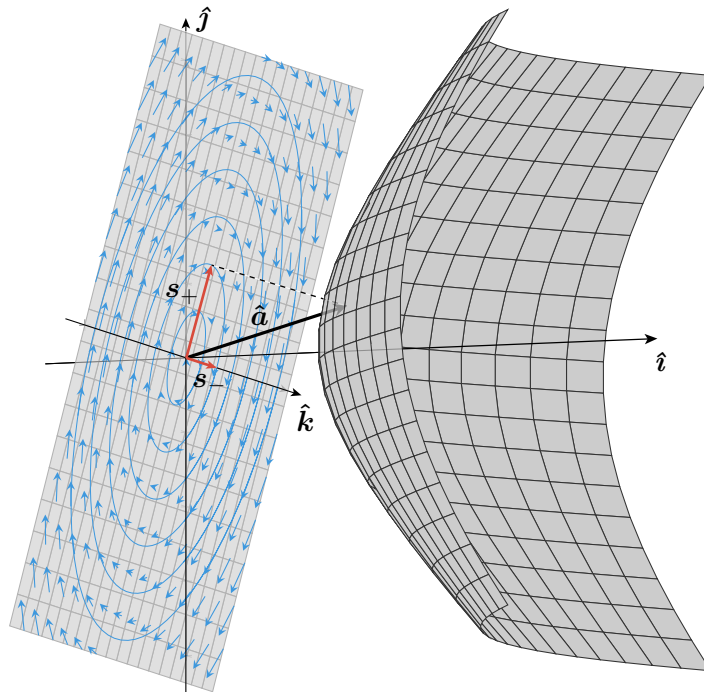


Figure 4-13: Vector field generated by the Lorentzian cross product by \mathbf{a} on the vectors in the plane that is Lorentz-orthogonal to \mathbf{a} . The vectors s_+ and s_- are the principal axes of (one of the) elliptic trajectories. The positive sheet of the hyperboloid is shown as well.

We can find the correct basis by relating the major axes of the elliptic trajectory generated by $[\mathbf{a}_{\times_L}]$, denoted by (s_+, s_-) (also shown in Figure 4-13) to the major axes of the elliptic trajectory (r_+, r_-) given by Equation (4-91).

The semi-major axis \mathbf{s}_+ of the elliptic trajectory generated by the Lorentzian cross-product can be obtained by projecting the matrix \mathbf{a} on the plane that is Lorentz orthogonal to it. The semi-minor axis is simply found by applying the Lorentzian cross-product to the semi-major axis. That is,

$$\mathbf{s}_+ = \mathbf{a} - \frac{\langle \mathbf{a}, \hat{\mathbf{n}} \rangle}{\langle \hat{\mathbf{n}}, \hat{\mathbf{n}} \rangle} \hat{\mathbf{n}}, \quad (4-93)$$

$$\mathbf{s}_- = \hat{\mathbf{a}} \times_L \mathbf{s}_+,$$

where $\hat{\mathbf{n}} = a_1 \hat{\mathbf{i}} - a_2 \hat{\mathbf{j}} - a_3 \hat{\mathbf{k}}$ is the normal vector to the plane that is Lorentz-orthogonal to \mathbf{a} . Please note that we are using two types of orthogonality: both Lorentz and Euclidean. The inner product \langle , \rangle refers to the Euclidean inner product, as opposed to the Lorentzian inner product. We will now prove that \mathbf{s}_+ and \mathbf{s}_- as given above indeed are the principal axes of the elliptic trajectory generated by the Lorentzian cross product.

Proof. For convenience, we will use the normalized vector $\hat{\mathbf{a}}$ in place of \mathbf{a} without loss of generality. A unit normal vector to the Lorentz-orthogonal subspace is

$$\hat{\mathbf{n}} = \hat{a}_1 \hat{\mathbf{i}} - \hat{a}_2 \hat{\mathbf{j}} - \hat{a}_3 \hat{\mathbf{k}}$$

. Following Equation (4-93), the basis vectors are

$$\mathbf{s}_+ = \hat{\mathbf{a}} - \frac{\langle \hat{\mathbf{a}}, \hat{\mathbf{n}} \rangle}{\langle \hat{\mathbf{n}}, \hat{\mathbf{n}} \rangle} \hat{\mathbf{n}} \quad (4-94)$$

$$\mathbf{s}_- = \hat{\mathbf{a}} \times_L \mathbf{s}_+ = -\frac{\langle \hat{\mathbf{a}}, \hat{\mathbf{n}} \rangle}{\langle \hat{\mathbf{n}}, \hat{\mathbf{n}} \rangle} (\hat{\mathbf{a}} \times_L \hat{\mathbf{n}}),$$

because the Lorentz-cross product distributes over addition and $\hat{\mathbf{a}} \times_L \hat{\mathbf{a}} = \mathbf{0}$.

If $(\mathbf{s}_+, \mathbf{s}_-)$ are the major axes of the elliptic trajectory generated by the cross product, then they must be the real and imaginary part of an eigenvector of $[\hat{\mathbf{a}} \times_L]$. Hence, it must be the case that

$$[\hat{\mathbf{a}} \times_L](\mathbf{s}_+ + i\mathbf{s}_-) = \lambda(\mathbf{s}_+ + i\mathbf{s}_-), \quad (4-95)$$

where λ is then an eigenvalue of the matrix [68]. This can be verified by replacing the action of $[\hat{\mathbf{a}} \times_L]$ with the cross product.

Plugging in the definition and exploiting the linearity of the Lorentz cross-product, we obtain:

$$\begin{aligned} \hat{\mathbf{a}} \times_L (\mathbf{s}_+ + i\mathbf{s}_-) &= \hat{\mathbf{a}} \times_L \mathbf{s}_+ + i(\hat{\mathbf{a}} \times_L \mathbf{s}_-) \\ &= \mathbf{s}_- + (\hat{\mathbf{a}} \times_L \mathbf{s}_-)i \\ &= \mathbf{s}_- + (\hat{\mathbf{a}} \times_L (\hat{\mathbf{a}} \times_L \mathbf{s}_+))i \\ &= \mathbf{s}_- - \frac{\langle \hat{\mathbf{a}}, \hat{\mathbf{n}} \rangle}{\langle \hat{\mathbf{n}}, \hat{\mathbf{n}} \rangle} (\hat{\mathbf{a}} \times_L (\hat{\mathbf{a}} \times_L \hat{\mathbf{n}}))i. \end{aligned}$$

The triple cross-product expansion, or *Lagrange formula*, relates the regular cross product to the corresponding dot product:

$$\mathbf{x} \times (\mathbf{y} \times \mathbf{z}) = \mathbf{y} \langle \mathbf{z}, \mathbf{x} \rangle - \mathbf{z} \langle \mathbf{x}, \mathbf{y} \rangle. \quad (4-96)$$

This well-known identity generalizes (easily verified) to the Lorentzian counterpart of the cross- and inner product:

$$\mathbf{x} \times_L (\mathbf{y} \times_L \mathbf{z}) = \mathbf{y} \langle \mathbf{z}, \mathbf{x} \rangle_L - \mathbf{z} \langle \mathbf{x}, \mathbf{y} \rangle_L. \quad (4-97)$$

Using the Lagrange formula, the above expression becomes

$$\begin{aligned} \hat{\mathbf{a}} \times_L (\mathbf{s}_+ + i\mathbf{s}_-) &= \mathbf{s}_- - \frac{\langle \hat{\mathbf{a}}, \hat{\mathbf{n}} \rangle}{\langle \hat{\mathbf{n}}, \hat{\mathbf{n}} \rangle} (\hat{\mathbf{a}} \langle \hat{\mathbf{a}}, \hat{\mathbf{n}} \rangle_L - \hat{\mathbf{n}} \langle \hat{\mathbf{a}}, \hat{\mathbf{a}} \rangle_L)i \\ &= \mathbf{s}_- - \left(\hat{\mathbf{a}} \frac{\langle \hat{\mathbf{a}}, \hat{\mathbf{n}} \rangle_L \langle \hat{\mathbf{a}}, \hat{\mathbf{n}} \rangle}{\langle \hat{\mathbf{n}}, \hat{\mathbf{n}} \rangle} - \hat{\mathbf{n}} \frac{\langle \hat{\mathbf{a}}, \hat{\mathbf{n}} \rangle}{\langle \hat{\mathbf{n}}, \hat{\mathbf{n}} \rangle} \right)i \\ &= \mathbf{s}_- - \left(\hat{\mathbf{a}} - \hat{\mathbf{n}} \frac{\langle \hat{\mathbf{a}}, \hat{\mathbf{n}} \rangle}{\langle \hat{\mathbf{n}}, \hat{\mathbf{n}} \rangle} \right)i \\ &= \mathbf{s}_- - \mathbf{s}_+i. \\ &= -i(\mathbf{s}_+ + i\mathbf{s}_-). \end{aligned}$$

The latter is the scalar multiple of the vector $\mathbf{s}_+ + \mathbf{s}_-$ by $-i$ - hence, this is indeed an eigenvector of the corresponding matrix. This means that indeed, $\mathbf{s}_+ + \mathbf{s}_-$ are the principal axes of the elliptic trajectory generated by the Lorentzian cross-product. ■

Knowing the eigenvectors of both matrices, the state transition matrix A and matrix generated by the Lorentzian cross-product $[\mathbf{a}_{\times_L}]$ can be related through the following similarity transformation:

$$A = T^{-1} [\mathbf{a}_{\times_L}] T, \quad (4-98)$$

where the transformation matrix is constructed from the principal axes in both the phase plane and the Lorentz orthogonal plane:

$$T = (\mathbf{r}_+ \quad \mathbf{r}_-) (\mathbf{s}_+ \quad \mathbf{s}_-)^{-1}. \quad (4-99)$$

Chapter 5

Conclusions and Recommendations

Conclusions

The purpose of this thesis is twofold: first, to establish a fitting geometric framework for mechanical systems with dissipation that also has a clear physical interpretation, and second, to present the properties and advantages of the newly proposed split-quaternion representation of dynamical systems.

Contact manifolds provide a suitable setting for simple mechanical systems, particularly those with only a single degree of freedom. The contact Hamiltonian system reflects the thermodynamic/mechanical information about the system, consisting of a contact 1-form, which represents the first law of thermodynamics, and the Hamiltonian, being the sum of the mechanical and internal energy in the system. The contact form can also be interpreted as a manifestation of the work-heat equivalence as it was initially shown by James P. Joule [79]. Similar to the contact form in thermodynamics being the *Gibbs form*, the contact form in mechanical systems may be called the *Joule form* instead.

The newly proposed framework allows for unifying thermodynamic and mechanical systems that would otherwise be treated separately. Indeed, the Hamiltonian contains both mechanical and thermodynamic energy, and the Joule form specifies the transformation of one into the other. As a result, we expect that this approach can readily be used to handle systems containing thermodynamic and mechanical elements with a single Hamiltonian description.

The physical interpretation of the contact structure makes it straightforward to apply it to any mechanical system simply from inspection. We have shown this by extending the contact Hamiltonian system for the harmonic oscillator with parallel damping to the harmonic oscillator with both a parallel and a serial damper. Apart from the compelling mathematical symmetry of the contact form, being able to handle both types of dampers has essential applications in economic engineering. Whereas the parallel damper acts on the price based on the flow of goods (e.g., a transaction cost), the serial damper acts on the flow of goods based on a price (e.g., depreciation or consumption).

In addition, we have used the symplectified Hamiltonian system to explain the form of the Caldriola-Kanai Hamiltonian, which has been widely regarded as the standard method to incorporate dissipation into the Hamiltonian (in the case of the damped harmonic oscillator). However, the interpretation of the form of the Caldriola-Kanai Hamiltonian has been the subject of debate in the past. We have shown that the form of the Caldriola-Kanai Hamiltonian is a direct consequence of the fact that it is the homogeneous Hamiltonian of the symplectified system with part of the solution substituted in it. Because contact Hamiltonian systems can always be symplectified, a Caldriola-Kanai type expression can be obtained for any such system.

For more general systems, the contact structure does not suffice. This is because the contact structure derives the ‘Hamiltonian isomorphism’ from the contact form, which is conceptually wrong. Indeed, the nature of the dissipation in the system is by no means necessarily related to the symplectic pairing of positions and momenta. This is not a problem for simple mechanical systems because there is only one pairing possible between the position and momentum. The generalized structure that takes care of this is not a contact structure anymore, but the physical interpretations of the associated 1-form and the Hamiltonian remain. As such, the Jacobi structure also allows the unification of thermodynamic and mechanical systems.

The split-quaternion representation of two-dimensional dynamical systems provides immediate insights into the geometric nature of the system. Roughly speaking, the split-quaternion are ‘super-eigenvalues’: they have the same structure (real part plus imaginary part), where the imaginary part also contains the eigenvector information if its magnitude is disregarded.

Deriving the qualitative nature of the system follows almost immediately from inspection of the split-quaternion interpretation. Even the degenerate cases (e.g., if the eigenvalues are not simple) do not have to be handled as exceptions in this procedure. Furthermore, the system solution can be obtained without the need for eigenvectors. This offers, in our opinion, a computational advantage, especially when the eigenvectors are complex.

We also argue that the normalized vector part of the split-quaternion presents the ‘shape information’ of the system more conveniently. This is because the normalized vector is a two-dimensional object, whereas the eigenvectors are specified as two projective two-dimensional objects. As a result, we can represent the shape of a trajectory unambiguously with a point on either the light cone, two-sheet hyperboloid, or one-sheet hyperboloid, depending on the regime of the system (i.e., underdamped, overdamped, and critically damped).

Overall, we fully acknowledge the incontrovertible mathematical fact that because split-quaternions are isomorphic to 2×2 -matrices, they cannot possibly do more than the matrices can. Our point is instead that the chart mapping (in the literal sense) from the split-quaternions translates to the actual behavior of the dynamical system in a more straightforward manner than the matrix representation does.

Recommendations

Economic engineering

In this thesis, we have assigned the geometric infrastructure that underlies Lagrangian mechanics with a compelling economic interpretation: the Lagrange 2-form is analogous to the Slutsky matrix in microeconomics. However, we have not elaborated on this result and recommend that further research in the field of economic engineering puts this hypothesis to the test and investigates its potential consequences.

Geometric structures for dissipative mechanics

We have shown that any contact symplectic manifold can be lifted canonically to a symplectic manifold through a procedure called *symplectification*. We have applied this to the contact Hamiltonian system of the damped harmonic oscillator and demonstrated its correspondence with the Caldriola-Kanai method. However, we have not symplectified the contact Hamiltonian system for the oscillator with serial and parallel damper; this can be an interesting subject for future research. According to our views, it should also be possible to derive a Caldriola-Kanai-type Hamiltonian via this method for the damper with two oscillators. Moreover, *every* contact can be symplectified, so a Caldriola-Kanai type system can be derived for any mechanical system that can be written as a contact Hamiltonian system.

Along the same line, it has been shown that any Jacobi structure can be lifted to a manifold with a homogeneous Poisson structure; this is called *Poissonization* (symplectification is a particular case of this) [54]. Hence, it might be possible to extend the practice of symplectification to the Jacobi structure for general mechanical systems.

On a more general note regarding the proposed Jacobi structure, we have not formally proven that the proposed structure always meets the required conditions to be a Jacobi manifold. Also, since there have been extensions for e.g., the Noether theorem and symplectic reduction to contact manifolds, there may also be equivalent theorems for Jacobi manifolds. As such, more research is required to investigate the mathematical properties of this specific type of Jacobi structure in greater detail.

From the perspective of control theory, the ‘Jacobi systems’ as described in this thesis can be used in the framework of port-Hamiltonian systems (see Van Der Schaft [59]) and the associated control formalism to facilitate energy-based control for general mechanical systems.

Finally, we would be interested to see whether a Hamilton-Jacobi-type equation can be developed for Jacobi manifolds as well (at least for this particular class of Jacobi structures).

Split-quaternion representation of dynamical systems

We have limited ourselves to using the split-quaternions to analyze the dynamical system more conveniently. However, we have not ventured into the field of control using the split-quaternion representation. Although, from a purely mathematical perspective, the split-quaternions cannot do more than their matrix counterparts, their properties might make some practices in control easier. For example, algorithms for pole placement are typically

fairly numerically unreliable, which might be improved by using split-quaternions instead. For precisely the same reason, the split-quaternion representation may also prove advantageous for system identification.

Arguably the most prominent limitation of the split-quaternions is that they are not immediately applicable to dynamical systems of dimensions greater than two. However, it may be possible to consider larger (even-dimensional) systems as interconnections of several atomic split-quaternion systems (representing a single pole pair). In any case, control applications often focus on the *dominant* pole pair, which can, of course easily represented by a single split-quaternion.

We have shown that the models of the hyperbolic plane can serve as a maps for the normalized vector part of the split-quaternions, and have related the shape parameters of the solution trajectories of an underdamped system. It is relatively straightforward to extend these ideas to critically damped and underdamped systems, but it is not covered in this thesis. Finally, we have not touched upon an important feature of the hyperbolic plane and its models: geodesics. These represent the paths of the shortest distance connecting two points on the hyperboloid (or in the Poincaré or Cayley-Klein disks). The measure of distance in the Lorentz space as a whole is specified by the Lorentzian norm, which is equivalent to the magnitude of the imaginary part of the eigenvalue. It is not altogether clear what the meaning of these paths is in terms of the associated dynamical system: they represent a specific path from the shape of one trajectory to another, thereby remaining in the same regime. We find this question a very compelling subject for future research.

Appendix A

Geometry of Lagrangian Mechanics

Just like the cotangent bundle, the tangent bundle admits a canonical structure, which is called the *vertical endomorphism*. Its construction is slightly more convoluted than the canonical symplectic structure of the cotangent bundle, but nevertheless essential for a proper geometric interpretation of Lagrangian mechanics.

A-1 The double tangent bundle

The *double tangent bundle* is the tangent bundle to TQ , denoted by TTQ . This space has not one, but two canonical vector bundle structures, defined by different projection maps from TTQ to TQ . First, there is the trivial projection π_{TQ} that forgets about the tangent elements to TQ . Secondly, there is $(\pi_Q)_*$ the pushforward (tangent map) of the projection map $\pi_Q : TQ \rightarrow Q$ [19].

$$\begin{array}{ccc} & T(TQ) & \\ (\pi_Q)_* \swarrow & & \searrow \pi_{TQ} \\ TQ & & TQ \\ \pi_Q \searrow & & \swarrow \pi_Q \\ Q & & \end{array}$$

Vectors on the tangent bundle TQ (they live in $T(TQ)$) are called vertical if they are part of the kernel of $(\pi_Q)_*$. These vectors point entirely in the direction of the fiber: in the Lagrangian formalism, they reflect a pure change in velocity, and no change in the generalized position.

The *vertical lift* Ψ maps a vector on Q to a vertical vector on TQ [17].

$\Psi_v : T_q Q \rightarrow T_v T_q Q$:

$$\Psi_v(\mathbf{w}) f = \frac{d}{dt} f(\mathbf{v} + t\mathbf{w}) \Big|_{t=0} \quad q \in Q, \quad \mathbf{v}, \mathbf{w} \in T_q Q, \quad f \in C^\infty(TQ). \tag{A-1}$$

In components, the effect of the vertical lift is as follows:

$$\Psi_v : \quad \mathbf{w} = w^i \frac{\partial}{\partial q^i} \Big|_q \quad \mapsto \quad \Psi_v(\mathbf{w}) = w^i \frac{\partial}{\partial v^i} \Big|_{(q,v)}. \quad (\text{A-2})$$

The vertical lift can also lift entire sections of TQ by simply applying the vertical lift pointwise.

Using the concept of the vertical lift, we can define the *vertical isomorphism* S from the double tangent bundle to itself, first by projecting with $(\pi_Q)_*$ and then lifting again:

$$S : TTQ \rightarrow TTQ : \quad S(q, v) u = (\Psi_v \circ (\pi_Q)_*) u \quad u \in T_{(q,v)} TQ. \quad (\text{A-3})$$

The action of S can also be stated in the form of the following diagram:

$$\begin{array}{ccc} TTQ & \xrightarrow{S} & TTQ \\ (\pi_Q)_* \downarrow & & \uparrow \Psi \\ TQ & \xrightarrow{\text{id}_{TQ}} & TQ \end{array} .$$

The action of the vertical endomorphism on the chart-induced basis is:

$$S : \quad \frac{\partial}{\partial q^i} \Big|_{(q,v)} \mapsto \frac{\partial}{\partial v^i} \Big|_{(q,v)} \quad \frac{\partial}{\partial v^i} \Big|_{(q,v)} \mapsto 0. \quad (\text{A-4})$$

The vertical isomorphism is therefore a tensor of valence $(1, 1)$ — it takes a vector and produces another. Locally, S can be expressed as:

$$S = \frac{\partial}{\partial v^i} \otimes dq^i. \quad (\text{A-5})$$

with \otimes being the tensor product [17].

The Lagrangian formalism only applies to second-order vector fields. A second-order vector field is a vector field X such that $(\pi_Q \circ X) = \text{id}_{TQ}$; i.e. the following diagram commutes: [19]

$$\begin{array}{ccccc} & & TTQ & & \\ & (\pi_Q)_* \swarrow & & \nwarrow X & \\ TQ & \xleftarrow{\text{id}_{TQ}} & & & TQ \end{array} .$$

The identity on TQ is $\text{id}_{TQ} : (q, v) \mapsto (q, v)$. Therefore, for a vector field X to be second order, we should have that the component in $\frac{\partial}{\partial q^i}$ that is picked out by $(\pi_Q)_*$ should be equal to v^i ; for example

$$X = \sum_{i=1}^n \left[v^i \frac{\partial}{\partial q^i} + F^i \frac{\partial}{\partial v^i} \right]. \quad (\text{A-6})$$

The corresponding differential equations are

$$\frac{dq^i}{dt} = v^i \quad \frac{dv^i}{dt} = F^i, \quad (\text{A-7})$$

which means that the second-order vector field coincides with the notion of a second-order differential equation in q^i .

A-2 The Euler-Lagrange equations

With the infrastructure established in the preceding section, we can now define the precise geometric setting of Lagrangian mechanics. Given a Lagrangian function $L \in C^\infty(TQ)$, define the *Lagrange 1-form*¹

$$\vartheta_L := dL \circ S = \sum_{j=1}^n \frac{\partial L}{\partial v^j} dq^j. \quad (\text{A-8})$$

Observe that the Lagrange 1-form is also equal to the pullback of the Liouville form under the Legendre transformation: $\vartheta_L = (\mathbb{F}L)^*\vartheta$ [19]. Secondly, we define the *Lagrange 2-form* as: [17, 19]

$$\omega_L := -d\vartheta_L = \frac{\partial^2 L}{\partial v^i \partial v^j} dq^j \wedge dv^i + \frac{\partial^2 L}{\partial q^i \partial v^j} dq^j \wedge dq^i. \quad (\text{A-9})$$

Because the exterior derivative and the pullback commute, the Lagrange 2-form is equal to the pullback of the symplectic 2-form under the Legendre transform. If the rank of the Hessian $\frac{\partial^2 L}{\partial v^i \partial v^j}$ is full (and constant), then ω_L is nondegenerate and therefore defines a symplectic structure on TQ . However, observe that ω_L being symplectic or not depends on the nature of the Lagrangian, while the symplectic structure in the Hamiltonian setting is canonically derived from the cotangent bundle itself — there is no need for the Hamiltonian to be regular.

The final ingredient for the Euler-Lagrange equations is the *energy function*

$$E := Z(L) - L, \quad (\text{A-10})$$

where $Z = \sum v^i \frac{\partial}{\partial v^i}$ is the Liouville vector field on TQ .

The *Lagrangian vector field* X_L is then the unique vector field that satisfies the equation: [27]

$$X_L \lrcorner \omega_L = dE, \quad (\text{A-11})$$

In components, the right hand side of this equation is:

$$\begin{aligned} dE &= \sum_{i,j} \left(\frac{\partial^2 L}{\partial v^j \partial q^i} v^j dq^i + \frac{\partial^2 L}{\partial v^j \partial v^i} v^j dv^i + \frac{\partial L}{\partial v^j} dv^j \right) - dL, \\ dE &= \sum_{i,j} \left(\frac{\partial^2 L}{\partial v^j \partial q^i} v^j dq^i + \frac{\partial^2 L}{\partial v^j \partial v^i} v^j dv^i - \frac{\partial L}{\partial q^j} dq^j \right). \end{aligned} \quad (\text{A-12})$$

Let $X_L = \sum_i \left(A^i \frac{\partial}{\partial q^i} + B^i \frac{\partial}{\partial v^i} \right)$; the left hand side can then be written as follows:

$$X_L \lrcorner \omega_L = - \sum_{i,j} A^i \frac{\partial^2 L}{\partial q^i \partial v^j} dq^j + \sum_{i,j} A^j \frac{\partial^2 L}{\partial q^i \partial v^j} dq^i - \sum_{i,j} B^i \frac{\partial^2 L}{\partial v^i \partial v^j} dq^j + \sum_{i,j} A^j \frac{\partial^2 L}{\partial v^i \partial v^j} dv^i. \quad (\text{A-13})$$

Comparing this expression with Equation (A-12), it is immediately clear that

$$A^j \frac{\partial^2 L}{\partial v^i \partial v^j} = v^j \frac{\partial^2 L}{\partial v^i \partial v^j}. \quad (\text{A-14})$$

¹Cariñena [17] calls ϑ the Euler-Poincaré 1-form.

We therefore have that $A^j = v^j$, but *only* if the Hessian of L with respect to the velocities is nonsingular. If this is indeed the case (i.e. L is regular), and the condition implies that the vector field X_L is second-order. We can use this knowledge to obtain a second condition (since the terms in dq^i cancel):

$$\sum_i B^i \frac{\partial^2 L}{\partial v^i \partial v^j} = \frac{\partial L}{\partial q^j} - \sum_i v^i \frac{\partial^2 L}{\partial q^i \partial v^j}. \quad (\text{A-15})$$

The Hessian of L in the velocities $M_{ij} = \frac{\partial^2 L}{\partial v^i \partial v^j}$ is also called the mass matrix of the system. We have already assumed that this matrix is invertible. As such, we have that

$$\sum_i \frac{\partial^2 L}{\partial v^i \partial v^j} \frac{d^2 q^j}{dt^2} + \sum_i \frac{\partial^2 L}{\partial q^i \partial v^j} \frac{dq^i}{dt} = \frac{\partial L}{\partial q^j}, \quad (\text{A-16})$$

or equivalently

$$\frac{d}{dt} \left(\frac{\partial L}{\partial v^j} \right) - \frac{\partial L}{\partial q^j} = 0. \quad (\text{A-17})$$

This is the traditional form of the Euler-Lagrange equations.

Provided that X_L is a second-order vector field, the equation Equation (A-11) is equivalent to the following statement:

$$\mathcal{L}_{X_L} \vartheta_L = dL. \quad (\text{A-18})$$

The equivalence is easily shown using the Cartan formula:

$$\mathcal{L}_{X_L} \vartheta_L = dL$$

$$d(X_L \lrcorner \vartheta_L) + X_L \lrcorner d\vartheta_L = dL$$

$$d(X_L \lrcorner \vartheta_L) - X_L \lrcorner \omega_L = dL$$

The fact that X_L is second-order implies that $X_L \lrcorner \vartheta_L = Z(L)$. Therefore

$$d(Z(L)) - X_L \lrcorner \omega_L = dL$$

$$X_L \lrcorner \omega_L = dZ(L) - L$$

$$X_L \lrcorner \omega_L = dE.$$

Lagrangians are not unique: from Equation (A-11) we can deduce that the addition of a closed 1-form (as a map from $TQ \rightarrow \mathbb{R}$) to the Lagrangian will not alter the Euler-Lagrange equations. The closed 1-forms on Q therefore constitute the *gauge group* of Lagrangian mechanics. An equivalent statement is that the Euler-Lagrange equations remain invariant if a total derivative is added to the Lagrangian function [19].

Appendix B

Contact Geometry

This appendix provides a short introduction to the basic concepts of contact geometry that are relevant in this thesis.

B-1 Contact structures

A *contact element* on a manifold M is a point $m \in M$ combined with a tangent hyperplane $\xi_m \subset T_m M$ (a subspace of the tangent space with codimension 1). The word ‘contact’ refers to the intuitive notion that if two submanifolds touch, they share a contact element: they are *in contact*. Being in contact is a slightly weaker notion than tangency, for the magnitude of the ‘velocity’ does not matter in the former case [23].

Contact elements to a two-dimensional manifold are simply lines through the origin in the tangent space. Contact elements to a three-dimensional manifold are planes through the origin, etc.

A *contact manifold* is a manifold M (of dimension $2n + 1$) with a *contact structure*, which is a smooth field (or distribution) of contact elements on M . Locally, any contact element determines a 1-form α (up to multiplication by a nonzero scalar) whose kernel constitutes the tangent hyperplane distribution, i.e.

$$\xi_m = \ker \alpha_m \tag{B-1}$$

This α is called the (local) *contact form*, and it acts like a ‘normal (co-)vector’ to the hyperplane. For the field hyperplanes to be a constant structure, it must satisfy a nondegeneracy condition: it should be *nonintegrable*. This can be expressed as the the Frobenius condition for nonintegrability: [14, 19, 23]

$$\alpha \wedge (d\alpha)^n \neq 0. \tag{B-2}$$

Integrable distributions would have this expression vanish everywhere. Roughly equivalent statements are that (i) one cannot find foliations of M such that ξ is everywhere tangent to it, or (ii) that $d\alpha|_{\xi}$ is a *symplectic form*.

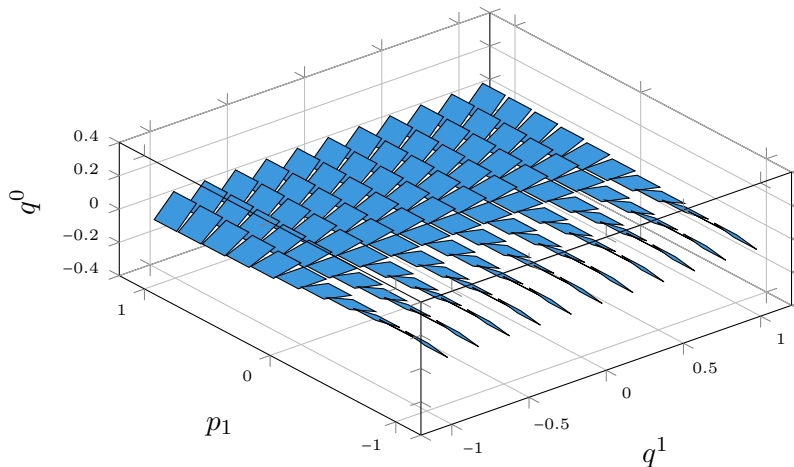


Figure B-1: The standard contact structure on \mathbb{R}^3 , given by the contact form $\mathrm{d}q^0 - p_1 \mathrm{d}q^1$; the hyperplanes tilt more in the increasing y -direction.

The contact form for a contact structure may not be globally defined (e.g. in the case of the bundle of contact elements, cf. Section 3-2-4). A contact form can only be defined globally if the quotient TM/ξ is a trivial line bundle, i.e. the orientation of the contact structure is preserved across the entire manifold [25].

The *Darboux theorem* for contact manifolds asserts that it is always possible to find local coordinates $(q^0, q^1, \dots, q^n, p_1, \dots, p_n)$, expressed in which the contact 1-form is of the form

$$\mathrm{d}q^0 - \sum_{i=1}^n p_i \mathrm{d}q^i. \quad (\text{B-3})$$

This is also called the *standard* or *natural contact structure*. The standard contact structure on \mathbb{R}^3 is illustrated in Figure B-1.

Finally, it is clear that the contact form singles out a special direction in the tangent space at every point of the manifold. This direction is given by the unique *Reeb vector field*,

$$R_\alpha \in \mathfrak{X}(M) : \quad R_\alpha \lrcorner \mathrm{d}\alpha = 0 \quad \text{and} \quad R_\alpha \lrcorner \alpha = 1. \quad (\text{B-4})$$

The special direction identified by the Reeb vector field is referred to as the *vertical* direction. Likewise, vector field components in the direction of the Reeb vector field are vertical.

In contrast, *horizontal vector fields* are those that vanish when contracted with the contact 1-form itself.

It is worth pointing out that the Reeb vector field depends on the choice of contact 1-form, and is therefore not uniquely defined up to a multiplicative constant for a given contact structure.

B-2 The manifold of contact elements

A contact manifold is a manifold with a contact structure. One can, however, associate a *canonical* $(2n - 1)$ -dimensional contact manifold to *any* n -dimensional manifold Q , just like

one can always find a canonical symplectic structure on T^*Q . Roughly speaking, this attaches a fiber containing all possible contact elements to every point of the manifold Q . As it turns out, this *manifold of contact elements* has a natural contact structure.

The manifold of contact elements CQ of an n -dimensional manifold Q is defined as [23]

$$CQ := \{(q, \xi_q) \mid q \in Q \text{ and } \xi_q \text{ a hyperplane on } T_q Q\}. \quad (\text{B-5})$$

This manifold CQ has dimension $2n - 1$.

It is clear that CQ has a natural bundle structure, being $C \xrightarrow{\pi} Q$ where the bundle projection π forgets the contact element:

$$\pi : CQ \rightarrow Q : (q, \xi_q) \mapsto q. \quad (\text{B-6})$$

Importantly, it can be shown that the manifold of contact elements to Q is isomorphic to the *projectivization of the cotangent bundle* to Q , which we denoted by $\mathbb{P}T^*Q$. This projectivization can be defined in terms of an equivalence relation between two nonzero elements in the cotangent bundle at every point in the manifold:

$$\eta, \chi \in T_q^*Q \setminus \{\mathbf{0}\} : (q, \eta) \sim (q, \chi) \Leftrightarrow \eta = \lambda \chi, \quad \lambda \in \mathbb{R}_0, \text{ for all } q \in Q. \quad (\text{B-7})$$

The equivalence relation identifies all the covectors in the cotangent space that are a nonzero multiple of each other. It is precisely this identification that takes care of the ambiguity in Equation (B-1), in that any nonzero multiple of a 1-form has the same kernel, and therefore gives rise to the same contact structure. $\mathbb{P}T^*Q$ is then the quotient set of T^*Q (without zero section) with respect to the equivalence relation \sim .

Visually, the projectivization of an n -dimensional vector space is the space of all *lines* through the origin in that vector space, which has dimension $n - 1$. It can be shown that this space is bundle-isomorphic to the manifold CQ [23].

As shown in Figure B-2, coordinates of the equivalence class of 1-forms are ‘projective coordinates’, $[p_0 : p_1 : \dots : p_{n-1}]$, where p_i are coordinates for T_q^*Q . The projective coordinates acknowledge the invariance under multiplication by a nonzero number. The tuple $(1, p_1, \dots, p_n)$ provides coordinates that cover most of $\mathbb{P}T^*Q$, i.e. all points where p_0 is nonzero.

Now, it remains to be shown that the manifold of contact elements is itself a contact manifold. Indeed, there is a canonical field of hyperplanes *on* CQ , which lifts the hyperplane tangent to Q to a hyperplane tangent to CQ (this is akin to the tautological trick played in the symplectic structure of the cotangent bundle). The contact structure distinguishes the curves in CQ that are lifted versions from curves in Q . This is illustrated in Figure B-3 [30]. Said otherwise, a tangent vector on CQ lies in the hyperplane defined by the contact structure if its projection down on Q lies in the hyperplane on Q defined by the given point on the CQ . This contact structure is associated with the 1-form:

$$\alpha = dq^0 + \sum_{i=1}^{n-1} p_i dq^i, \quad (\text{B-8})$$

given where we chose the particular chart assuming that $p_0 \neq 0$.

The canonical contact structure on the manifold of contact elements is visualized in Figure B-3 for a falling object. The base manifold Q is two-dimensional, containing time t and position

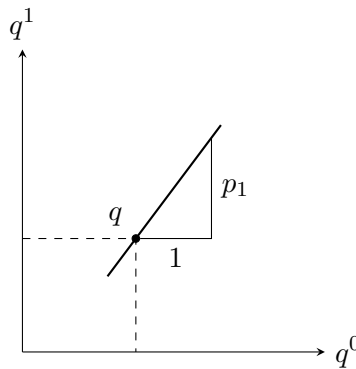


Figure B-2: A point in the manifold of contact elements on $Q = \mathbb{R}^2$. A coordinate system for CQ consists of $q = (q^0, q^1)$ to indicate a point on Q , and projective coordinates $[p_0 : p_1]$, which denote the contact element at that point. Without loss of generalization, one can choose $p_0 = 1$, and the remaining coordinate p_1 covers all but one points in the projective space. A potential confusion rests in this two-dimensional example, since both the ‘hyperplane’ and the equivalence class of 1-forms are both lines in the tangent and cotangent space respectively. This is not the case for higher-dimensions, for which $n - 1 \neq 1$.

q . A curve γ in Q can be seen as a path parameterized in time, i.e. $\gamma : t \mapsto (t, q(t))$. The contact elements are lines in the tangent spaces to Q : they locally represent the *slope* that an arbitrary curve $q(t)$ can have. Hence, the contact variable v is in this case literally interpreted as the velocity of the object. The contact structure is then

$$\alpha = dq - v dt. \quad (\text{B-9})$$

When the curve on Q is lifted to CQ (i.e. the space including the velocity), the contact structure forces the velocity coordinate v to be equal to the actual velocity of the curve in Q ; i.e. it selects those curves in CQ that are lifted from the base manifold.

B-3 Contact Hamiltonian systems

Just like in the symplectic case, the contact Hamiltonian formalism defines an automorphism between a function on the contact manifold $K \in C^\infty(M)$, and an associated ‘Hamiltonian’ vector field $X_K \in \mathfrak{X}(M)$. While the isomorphism is rather straightforward for symplectic manifolds, the contact counterpart is more involved: this is the prime reason behind the computational advantage of symplectification, as opposed to performing the calculations directly on the contact manifold.

Coordinate-free derivation

Given a contact manifold (M, ξ) with contact form α (i.e. $\xi \in \ker \alpha$), the tangent bundle M can be decomposed into two subbundles: [23, 24]

$$TM = \ker \alpha \oplus \ker d\alpha, \quad (\text{B-10})$$

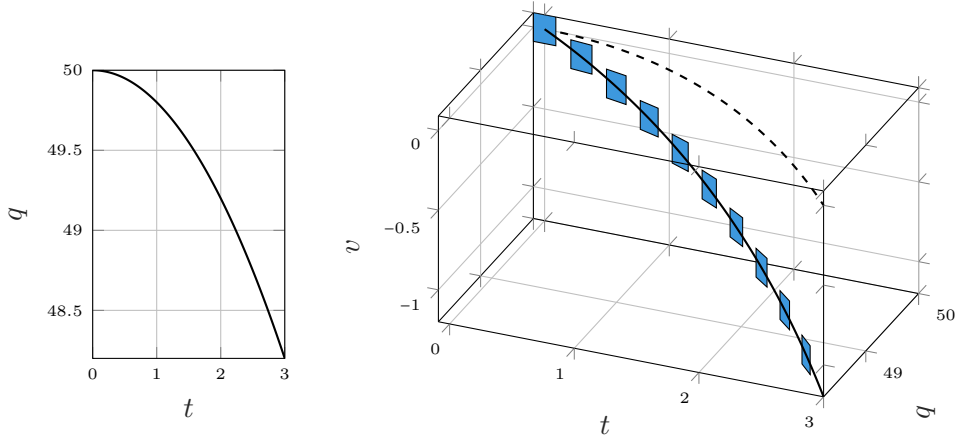


Figure B-3: Intuitive picture of the canonical contact on the manifold of contact elements. In this case, let $(t, q) \in Q$, and let v be a coordinate for the contact (line) element. The standard contact form is then $dq - v dt$. On the left, the curve corresponding to a falling object is shown in Q . When this curve is ‘lifted’ to CQ , the contact structure imposes that it be locally tangent to the contact structure, or that $v = \frac{dq}{dt}$. If the vertical direction is projected down onto the $(q - t)$ -plane ($C(Q) \rightarrow Q$), the hyperplanes defined by the contact structure are line elements tangent to the trajectory, making v the actual velocity of the curve.

where \oplus denotes the Whitney sum. The first subbundle is referred to as the *horizontal* bundle, the second as the *vertical* bundle. The vertical subbundle is of rank 1 and its fiber is spanned by the Reeb vector field (cf. Equation (B-4)). As mentioned to in Appendix B-1, *any* vector field $X \in \mathfrak{X}(M)$ may be decomposed accordingly. This decomposition is unique and given by

$$X = \underbrace{(X \lrcorner \alpha)R_\alpha}_{X^{\text{ver}}} + \underbrace{[X - (X \lrcorner \alpha)R_\alpha]}_{X^{\text{hor}}}. \quad (\text{B-11})$$

Observe that indeed $X^{\text{ver}} \in \ker d\alpha$ and $X^{\text{hor}} \in \ker \alpha$ [23, 24, 80].

We now wish to find the relation between the contact Hamiltonian $K \in C^\infty(M)$ and the associated Hamiltonian vector field $X_K \in \mathfrak{X}(M)$. This one-to-one relation is uniquely determined by two conditions. Firstly, we impose that¹

$$K := -X_K \lrcorner \alpha. \quad (\text{B-12})$$

This condition already provides us with the vertical component of the Hamiltonian vector field, namely

$$X_K^{\text{ver}} = -KR_\alpha. \quad (\text{B-13})$$

Secondly, the automorphism generated by the Hamiltonian vector field must be a *contact automorphism*: it must preserve the contact structure. This condition is encoded in terms of the Lie derivative:²

$$X_K \text{ is an infinitesimal contact automorphism} \Leftrightarrow \mathcal{L}_{X_K} \alpha = s\alpha, \quad (\text{B-14})$$

¹This is the sign convention observed by Bravetti et al. [6] en van der Schaft [41], as opposed to Libermann and Marle [24].

²Terminology differs somewhat in literature on this point: some authors, such as de León and Lainz [80] only refer to contactomorphisms as the special case where $g = 0$; while the more general case is called *conformal* contactomorphisms.

where $s \in C^\infty(M)$. The function s is there because $s\alpha$ and α give rise to the same hyperplane distribution. Using Cartan's 'magic' formula, the Lie derivative can be expanded as follows:

$$\mathcal{L}_{X_K} \alpha = s\alpha$$

$$d(X_K \lrcorner \alpha) + X_K \lrcorner d\alpha = s\alpha$$

$$-dK + X_K \lrcorner d\alpha = s\alpha$$

Contracting both sides with the Reeb vector field yields:

$$\begin{aligned} R_\alpha \lrcorner (-dK + X_K \lrcorner d\alpha) &= R_\alpha \lrcorner (s\alpha) \\ -R_\alpha \lrcorner dK + R_\alpha \lrcorner X_K \lrcorner d\alpha &= s R_\alpha \lrcorner \alpha \\ -R_\alpha \lrcorner dK - X_K \lrcorner R_\alpha \lrcorner d\alpha &= s. \end{aligned}$$

Hence, we have $s = -R_\alpha \lrcorner dK$. Because the vertical component of X_K is spanned by the Reeb vector field, its contraction with $d\alpha$ vanishes. As a result, we can rewrite the previous expression in terms of the *horizontal* component of X_K :

$$X_K \lrcorner d\alpha = X_K^{\text{hor}} \lrcorner d\alpha = [dK - (R_\alpha \lrcorner dK)\alpha], \quad (\text{B-15})$$

We must therefore recover X_K^{hor} from the above expression. Define the mapping

$$\alpha^\flat : TM \rightarrow T^*M : X \mapsto X \lrcorner d\alpha, \quad (\text{B-16})$$

when restricted to the space of horizontal vector fields, this mapping is an isomorphism onto the 'semi-basic' forms³. Define the inverse mapping of α^\flat by α^\sharp , such that

$$X_K^{\text{hor}} = \alpha^\sharp(dK - (R_\alpha \lrcorner dK)\alpha). \quad (\text{B-17})$$

As such, the Hamiltonian vector field associated to the contact Hamiltonian K is

$$X_K = KR_\alpha + \alpha^\sharp(dK - (R_\alpha \lrcorner dK)\alpha). \quad (\text{B-18})$$

Coordinate expression

Given the contact manifold (M, ξ) with contact form

$$dq^0 - \sum_{i=1}^n p_i dq^i, \quad (\text{B-19})$$

and define the contact Hamiltonian $K = K(q^0, q^1, \dots, q^n, p_1, \dots, p_n)$. The vertical component of the Hamiltonian vector field is straightforward (cf. Equation (B-4)):

$$X_K^{\text{ver}} = -K \frac{\partial}{\partial q^0}. \quad (\text{B-20})$$

³Semi-basic forms are forms that vanish when contracted with a vertical vector field [24].

For the horizontal component, first evaluate the right hand side of Equation (B-15) in coordinates:

$$X_K^{\text{hor}} \lrcorner d\alpha = \sum_{i=1}^n \left(\frac{\partial K}{\partial q^i} + p_i \frac{\partial K}{\partial q^0} \right) dq^i + \frac{\partial K}{\partial p_i} dp^i. \quad (\text{B-21})$$

In terms of the basis vectors, the mapping α^\flat is

$$\frac{\partial}{\partial q^i} \mapsto dp_i \quad \frac{\partial}{\partial p_i} \mapsto -dq^i \quad \frac{\partial}{\partial q^0} \mapsto 0 \quad i = 1, \dots, n. \quad (\text{B-22})$$

The inverse transformation is slightly ambiguous at first sight, since any $\frac{\partial}{\partial q^0}$ cannot be recovered directly from the ‘forward’ mapping. However, we know that α^\sharp must produce a horizontal vector field. Therefore, first perform the inverse mapping in the q^i, p_i -components to obtain

$$-\sum_{i=1}^n \left(\frac{\partial K}{\partial q^i} + p_i \frac{\partial K}{\partial q^0} \right) \frac{\partial}{\partial p_i} + \sum_{i=1}^n \frac{\partial K}{\partial p_i} \frac{\partial}{\partial q^i}. \quad (\text{B-23})$$

Contracting this expression with α produces $-\sum_{i=1}^n p_i \frac{\partial K}{\partial p_i}$. Hence, we can use this knowledge to find the actual horizontal component:

$$X_K^{\text{hor}} = \sum_{i=1}^n p_i \frac{\partial K}{\partial p_i} \frac{\partial}{\partial q^0} - \sum_{i=1}^n \left(\frac{\partial K}{\partial q^i} + p_i \frac{\partial K}{\partial q^0} \right) \frac{\partial}{\partial p_i} + \sum_{i=1}^n \frac{\partial K}{\partial p_i} \frac{\partial}{\partial q^i}. \quad (\text{B-24})$$

As such, the coordinate expression of Equation (B-18) is

$$X_K = \left(\sum_{i=1}^n p_i \frac{\partial K}{\partial p_i} - K \right) \frac{\partial}{\partial q^0} - \sum_{i=1}^n \left(\frac{\partial K}{\partial q^i} + p_i \frac{\partial K}{\partial q^0} \right) \frac{\partial}{\partial p_i} + \sum_{i=1}^n \frac{\partial K}{\partial p_i} \frac{\partial}{\partial q^i}. \quad (\text{B-25})$$

Furthermore, we have

$$\mathcal{L}_{X_K} \alpha = -\frac{\partial K}{\partial q^0} \alpha, \quad (\text{B-26})$$

and

$$\mathcal{L}_{X_K} K = -K \frac{\partial K}{\partial q^0}. \quad (\text{B-27})$$

Bibliography

- [1] P. Caldirola, “Forze Non Conservative Nella Meccanica Quantistica,” *Il Nuovo Cimento*, vol. 18, no. 9, pp. 393–400, 1941.
- [2] E. Kanai, “On the Quantization of the Dissipative Systems,” *Progress of Theoretical Physics*, vol. 3, no. 4, pp. 440–442, 1948.
- [3] C. Hutters and M. Mendel, “Overcoming the dissipation obstacle with Bicomplex Port-Hamiltonian Mechanics,” *IFAC-PapersOnLine*, 2020.
- [4] G. Dedene, “Oscillators and Complex Hamiltonian Calculus,” *Physica*, vol. 371, no. 103A, pp. 371–378, 1980.
- [5] S. G. Rajeev, “A Canonical Formulation of Dissipative Mechanics using Complex-Valued Hamiltonians,” *Annals of Physics*, vol. 322, no. 7 SPEC. ISS., pp. 1541–1555, 2007.
- [6] A. Bravetti, H. Cruz, and D. Tapias, “Contact Hamiltonian Mechanics,” *Annals of Physics*, vol. 376, pp. 17–39, 2017.
- [7] F. M. Ciaglia, H. Cruz, and G. Marmo, “Contact manifolds and dissipation, classical and quantum,” *Annals of Physics*, vol. 398, pp. 159–179, Nov. 2018.
- [8] V. Arnol'd, “Contact Geometry: The Geometrical Method of Gibbs's Thermodynamics,” in *Proceedings of the Gibbs Symposium: Yale University, May 15-17*, New Haven, CT, 1989.
- [9] G. J. L. Kruimer, “An Engineering Approach to Macroeconomic Scenario Modelling,” MSc Thesis, Delft University of Technology, 2021.
- [10] X. A. Van Ardenne, “Business Valuation in the Frequency Domain - A Dynamical Systems Approach,” MSc Thesis, Delft University of Technology, 2020.
- [11] N. Manders, “The Thermodynamics of Economic Engineering with Applications to Economic Growth,” MSc Thesis, Delft University of Technology, 2019.

- [12] T. Russell, “Symplectic geometry: The natural geometry of economics?” *Economics Letters*, vol. 112, no. 3, pp. 236–238, 2011.
- [13] R. Swierstra, “Foundations of Economic Geometry,” *SSRN Electronic Journal*, pp. 1–8, 2014.
- [14] V. Arnol’d, *Mathematical Methods of Classical Mechanics*, J. Ewing, F. Gehring, and P. Halmos, Eds. New York: Springer-Verlag, 1989.
- [15] D. Jeltsema and J. M. Scherpen, “Multidomain Modeling of Nonlinear Networks and Systems: Energy- and power-based perspectives,” *IEEE Control Systems*, vol. 29, no. 4, pp. 28–59, 2009.
- [16] B. N. M. Krabbenborg, “Duration Matching in the Frequency Domain - An Economic Engineering Approach to Asset and Liability Management,” MSc Thesis, Delft University of Technology, 2021.
- [17] J. F. Cariñena, “Theory of Singular Lagrangians,” *Fortschritte der Physik*, vol. 38, no. 9, p. 693, 1990.
- [18] Varian, Hal R, *Microeconomic Analysis*, 3rd ed. New York, NY: W. W. Norton & Company, 1992.
- [19] R. Abraham and J. E. Marsden, *Foundations of Mechanics*. Addison-Wesley Publishing Company, 1978.
- [20] J. E. Marsden and T. S. Ratiu, *Introduction to Mechanics and Symmetry*. New York, NY: Springer, 1998.
- [21] L. E. Blume, “Duality,” London, UK, 2020.
- [22] A. Bravetti, C. S. Lopez-Monsalvo, and F. Nettel, “Contact symmetries and Hamiltonian thermodynamics,” *Annals of Physics*, vol. 361, pp. 377–400, 2015.
- [23] A. Cannas da Silva, *Lectures on Symplectic Geometry*, 1, Ed. Berlin, Heidelberg: Springer, 2001.
- [24] P. Libermann and C.-M. Marle, *Symplectic Geometry and Analytical Mechanics*. Dordrecht, Holland: D. Reidel Publishing Company, 1987.
- [25] H. Geiges, *An Introduction to Contact Topology*. Cambridge, UK: Cambridge University Press, 2008.
- [26] V. I. Arnol’d, “Contact Geometry and Wave Propagation,” Geneva, 1989.
- [27] C. Godbillon, *Géométrie Différentielle et Mécanique Analytique*. Paris: Collection Méthodes Hermann, 1969.
- [28] V. Arnol’d, *Singularities of Caustics and Wave Fronts*. Dordrecht: Springer Science+Business Media, 1990, vol. 62.
- [29] P. Bamberg and S. Sternberg, *A Course in Mathematics for Students of Physics*. Cambridge, UK: Cambridge University Press, 1990, vol. 2.

- [30] W. L. Burke, *Applied Differential Geometry*. Cambridge: Cambridge University Press, 1985.
- [31] R. Hermann, *Geometry, Physics and Systems*. New York, NY: Marcel Dekker, 1973.
- [32] J. W. Gibbs, “Graphical Methods in the Thermodynamics of Fluids,” *Transactions of the Connecticut Academy*, vol. II, pp. 309–342, 1873.
- [33] A. S. Wightman and R. B. Israel, “Convexity and The Notion of Equilibrium State in Thermodynamics and Statistical Mechanics,” in *Convexity in the Theory of Lattice Gases*. Princeton, NJ: Princeton University Press, 1979.
- [34] R. Mrugała, J. D. Nulton, J. Christian Schön, and P. Salamon, “Contact structure in thermodynamic theory,” *Reports on Mathematical Physics*, vol. 29, no. 1, pp. 109–121, 1991.
- [35] R. Mrugała, “On contact and metric structures on thermodynamic spaces,” *RIMS Kokyuroku*, vol. 1142, pp. 167–181, 2000.
- [36] ———, “On equivalence of two metrics in classical thermodynamics,” *Physica A: Statistical Mechanics and its Applications*, vol. 125, no. 2-3, pp. 631–639, 1984.
- [37] ———, “Submanifolds in the Thermodynamic Phase Space,” *Reports on Mathematical Physics*, vol. 21, no. 2, pp. 197–203, 1985.
- [38] ———, “Continuous contact transformations in thermodynamics,” *Reports on Mathematical Physics*, vol. 33, no. 1-2, pp. 149–154, 1993.
- [39] ———, “On a Riemannian metric on contact thermodynamic spaces,” *Reports on Mathematical Physics*, vol. 38, no. 3, pp. 339–348, 1996.
- [40] R. Balian and P. Valentin, “Hamiltonian structure of thermodynamics with gauge,” *European Physical Journal B*, vol. 21, no. 2, pp. 269–282, 2001.
- [41] A. van der Schaft, “Liouville geometry of classical thermodynamics,” *Journal of Geometry and Physics*, vol. 170, p. 104365, 2021.
- [42] A. van der Schaft and B. Maschke, “Homogeneous Hamiltonian Control Systems Part I: Geometric Formulation,” *IFAC-PapersOnLine*, vol. 51, no. 3, pp. 1–6, 2018.
- [43] B. Maschke and A. van der Schaft, “Homogeneous Hamiltonian Control Systems Part II: Application to thermodynamic systems,” *IFAC-PapersOnLine*, vol. 51, no. 3, pp. 7–12, 2018.
- [44] A. A. Simoes, M. De León, M. L. Valcázar, and D. M. De Diego, “Contact geometry for simple thermodynamical systems with friction: Contact geometry for thermodynamics,” *Proceedings of the Royal Society A: Mathematical, Physical and Engineering Sciences*, vol. 476, no. 2241, pp. 1–21, 2020.
- [45] T. Frankel, *The Geometry of Physics*. Cambridge, UK: Cambridge University Press, 2012.

- [46] P. A. Dirac, “Generalized Hamiltonian Dynamics,” *Canadian Journal of Mathematics*, vol. 2, pp. 129–148, 1950.
- [47] E. Fermi, *Thermodynamics*. New York, NY: Dover Publications, 1956.
- [48] F. P. Schuller, “The Geometric Anatomy of Theoretical Physics,” Friedrich-Alexander Universität Erlangen-Nürnberg - Institut für Theoretische Physik II, Tech. Rep., 2014.
- [49] R. Hermann, *Topics in the Geometric Theory of Linear Systems*. Brookline, MA: Math Sci Press, 1984.
- [50] M. Verhaegen and V. Verdult, *Filtering and System Identification: A Least-Squares Approach*. Cambridge, UK: Cambridge University Press, 2007, vol. 9780521875.
- [51] M. Tokieda and S. Endo, “Equivalence of Dissipative and Dissipationless Dynamics of Interacting Quantum Systems With Its Application to the Unitary Fermi Gas,” *Frontiers in Physics*, vol. 9, no. September, pp. 1–9, 2021.
- [52] D. Schuch, “Nonunitary connection between explicitly time-dependent and nonlinear approaches for the description of dissipative quantum systems,” *Physical Review A - Atomic, Molecular, and Optical Physics*, vol. 55, no. 2, pp. 935–940, 1997.
- [53] W. Borutzky, *Bond Graph Methodology: Development and Analysis of Multidisciplinary Dynamic System Models*. Springer, 2010, vol. 44.
- [54] C.-M. Marle, “On Jacobi Manifolds and Jacobi Bundles,” in *Symplectic Geometry, Groupoids, and Integrable Systems*, ser. Mathematical Sciences Research Institute Publications, P. Dazord and A. Weinstein, Eds. New York, NY: Springer US, 1991, pp. 227–246.
- [55] A. Einstein and V. Bargmann, “Bivector Fields,” *Annals of Mathematics*, vol. 45, no. 1, pp. 1–14, 1944.
- [56] A. Lichnerowicz, “Les variétés de Poisson et leurs algèbres de Lie associées,” *Journal of Differential Geometry*, vol. 12, no. 2, pp. 253–300, Jan. 1977.
- [57] P. Dazord, A. Lichnerowicz, and C. Marle, “Structure locale des variétés de Jacobi,” *undefined*, 1991.
- [58] F. Mahmood, “Jacobi Structures And Differential Forms On Contact Quotients,” Ph.D. dissertation, Cornell University, Aug. 2012.
- [59] A. Van Der Schaft, “Port-Hamiltonian systems: An introductory survey,” *International Congress of Mathematicians, ICM 2006*, vol. 3, pp. 1339–1365, 2006.
- [60] J. Stillwell, *Naive Lie Theory*. New York: Springer Science+Business Media, 2008.
- [61] D. S. Dummit and R. M. Foote, *Abstract Algebra*. Hoboken, N.J.: John Wiley and Sons, 2004.
- [62] M. Jafari and Y. Yayli, “Matrix Theory over the Split Quaternions,” *International Journal of Geometry*, vol. 3, no. 2, pp. 57–69, 2014.

- [63] C. W. Misner, K. S. Thorne, and J. A. Wheeler, *Gravitation*. San Francisco, CA: W. H. Freeman and Company, 1970.
- [64] L. D. Landau and E. M. Lifshitz, *The Classical Theory of Fields*. Oxford: Pergamon Press, 1971, vol. 2.
- [65] S. Lang, *Algebra*. New York, NY: Springer-Verlag, 2002.
- [66] N. Bourbaki, *Lie Groups and Lie Algebras (Chapters 1-3)*. Reading, MA: Addison-Wesley Publishing Company, 1975, vol. 1.
- [67] H. K. Khalil, *Nonlinear Control*. Harlow: Pearson Education, 2015.
- [68] C. H. Edwards, D. E. Penney, and D. T. Calvis, *Differential Equation & Linear Algebra*. Pearson Education, 2018.
- [69] B. C. Hall, *Lie Groups, Lie Algebras, and Representations*. Cham, Switzerland: Springer International Publishing, 2013.
- [70] A. E. Motter and M. A. F. Rosa, “Hyperbolic Calculus,” *Advances in Applied Clifford Algebras*, vol. 8, no. 1, pp. 109–128, 1998.
- [71] A. A. Harkin and J. B. Harkin, “Geometry of Generalized Complex Numbers,” *Mathematics Magazine*, vol. 77, no. 2, pp. 118–129, 2004.
- [72] V. Arnold, *Ordinary Differential Equations*. Berlin: Springer-Verlag, 1984.
- [73] H. Dekker, “Classical and Quantum Mechanics of the Damped Harmonic Oscillator,” Physics Laboratory, TNO, Den Haag, Tech. Rep., 1981.
- [74] R. H. Rapp, “Geometric Geodesy, pt. 1,” Ohio State University - Department of Geodetic Science and Surveying, Columbus, OH, Tech. Rep., 1991.
- [75] W. P. Thurston, *Three-Dimensional Geometry and Topology*, S. Levy, Ed. Princeton, NJ: Princeton University Press, 1997, vol. 1.
- [76] T. Needham, *Visual Complex Analysis*. New York: Oxford University Press, 1997.
- [77] ——, *Visual Differential Geometry and Forms: A Mathematical Drama in Five Acts*. Princeton, NJ: Princeton University Press, 2021.
- [78] N. L. Balazs and A. Voros, “Chaos on the Pseudosphere,” *Physics Reports*, vol. 143, no. 3, pp. 109–240, 1986.
- [79] J. P. Joule and M. Faraday, “III. On the mechanical equivalent of heat,” *Philosophical Transactions of the Royal Society of London*, vol. 140, pp. 61–82, Jan. 1850.
- [80] M. de León and M. Lainz, “A Review on Contact Hamiltonian and Lagrangian Systems,” Instituto de Ciencias Matemáticas, Madrid, Spain, Tech. Rep., 2020.

Glossary

The entries in this glossary are separated in two sections. The first section contains the notation of Chapters 2 and 3, being mainly concerned with differential geometry. The second section pertains to Chapter 4, since some symbols have a different or more specific meaning in the context of split-quaternions.

Chapters 2 and 3

α	Contact 1-form
Ψ_α	Hamiltonian isomorphism for the contact form α
β	Work 1-form
A	Bivector (Jacobi structure)
ξ	Contact hyperplane distribution
ω	Symplectic form
ω_L	Lagrange 2-form
η	Heat 1-form
ϑ	Liouville 1-form
ϑ_L	Lagrange 1-form
E	Mechanical energy
\mathcal{F}	Fiber derivative
H	(Symplectic) Hamiltonian
\mathcal{H}	Homogeneous (Liouville) Hamiltonian
K	Contact / Jacobi Hamiltonian
L	Lagrangian
M	Phase space
Q	Configuration manifold
Q_e	Extended configuration manifold

R_α	Reeb vector field of the contact form α
U	Internal / dissipated energy
X_H	Hamiltonian vector field with respect to H
\mathcal{A}	Action functional
\mathbf{v}	Vector (bold notation)
p_i	Generalized momentum / price
\dot{q}^i	Generalized velocity / flow of goods
q^i	Generalized position / stock level
\mathbb{PR}	Projective real line
\mathbb{R}_\times	Real multiplicative group / real numbers without zero
$\mathfrak{X}(c)M$	Vector fields on the manifold M
$\mathfrak{X}_c(M)$	Contact Hamiltonian vector fields / inf. contactomorphisms on M
\oplus	Whitney sum
$\Gamma(M)$	Smooth sections of the bundle M
$\mathbb{P}\mathrm{T}^*M$	Projectivized cotangent bundle to M
$\dot{\mathrm{T}}^*M$	Cotangent bundle to M with zero section removed
$\blacktriangleleft G$	Group action of the group G
\sim	Equivalence relation
M/\sim	Quotient set of M with respect to \sim
$[,]$	Lie bracket
\llbracket , \rrbracket	Schouten bracket
∇	Function gradient
$M \xrightarrow{\pi} B$	Bundle with total space M , projection π and base B
$\{ , \}$	Poisson / Jacobi bracket
$C^\infty(M)$	Smooth functions on the manifold M
$\mathfrak{L}_X\eta$	Lie derivative of η with respect to X
d	Exterior derivative
\wedge	Exterior (wedge) product
\circ	Function composition
\otimes	Tensor product
\lrcorner	Interior product
$\mathrm{T}_x M$	Tangent space to the manifold M at the point x
$\mathrm{T}_x^* M$	Cotangent space of the manifold M at the point x
$\mathrm{T}M$	Tangent bundle of the manifold M
T^*M	Cotangent bundle of the manifold M

ϕ^*	Pullback of the map ϕ
ϕ_*	Pushforward of the map ϕ
ω^\flat	Flat mapping to the cotangent bundle based on ω
ω^\sharp	Sharp mapping to the tangent bundle based on ω

Chapter 4

ε	Idempotent unit
ζ	Damping ratio
$1, \hat{\mathbf{i}}, \hat{\mathbf{j}}, \hat{\mathbf{k}}$	Split-quaternion basis-elements
$X_1, X_{\hat{\mathbf{i}}}, X_{\hat{\mathbf{j}}}, X_{\hat{\mathbf{k}}}$	Vector fields associated with $1, \hat{\mathbf{i}}, \hat{\mathbf{j}}, \hat{\mathbf{k}}$
a^*	Split-quaternion conjugate of a
i	Imaginary unit
j	Hyperbolic unit
$sca(a)$	Scalar part of the split-quaternion a
a_0	Shorthand notation for $sca(a)$
$vec(a)$	Vector part of the split-quaternion a
\mathbf{a}	Shorthand notation for $vec(a)$
$\hat{\mathbf{a}}$	Unit vector (part)
a	General split-quaternion
D_n	Dihedral group; symmetry group of an n -polygon
$GL(n, \mathbb{R})$	General linear group over \mathbb{R}^n
$GL(n, \mathbb{R})$	Lie algebra of the general linear group over \mathbb{R}^n
$SL(n, \mathbb{R})$	Special linear group over \mathbb{R}^n
$SL(n, \mathbb{R})$	Lie algebra of the special linear group over \mathbb{R}^n
$Sp(n)$	Symplectic group group over \mathbb{R}^n
$\mathfrak{sp}(n)$	Lie algebra of the symplectic group group over \mathbb{R}^n
$N(a)$	Squared total norm of a
$\ a\ $	Total norm of a
$N(\mathbf{a})$	Squared vector norm of a
$\ \mathbf{a}\ $	Vector norm of a
\langle , \rangle_L	Lorentzian inner product
\times_L	Lorentzian cross product
\langle , \rangle	Euclidean inner product
ϕ	Ring / algebra isomorphism between real (2×2) -matrices and split-quaternions

\Re	Real part (complex number)
\Im	Imaginary part (complex number)
$[,]$	Lie bracket